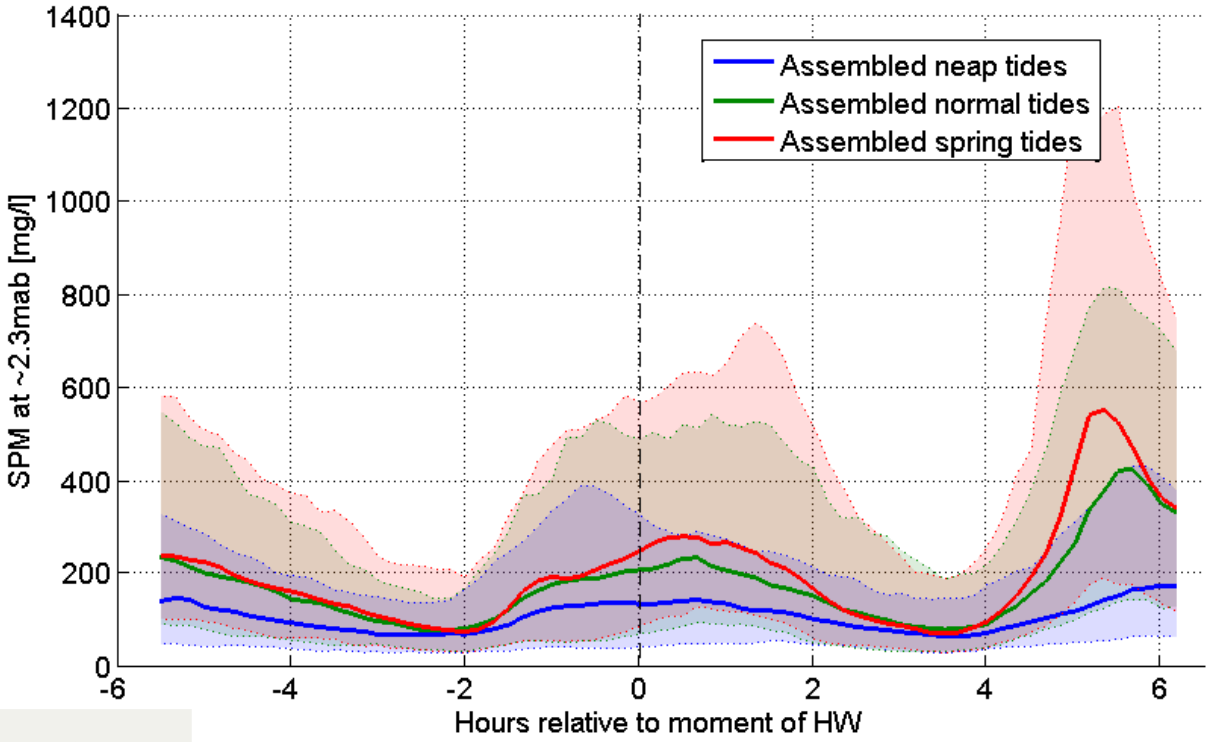

Flanders
State of the Art

00_067_2
FHR reports

Sediment Transport Model for the Port of Zeebrugge

Sub report 2
Analysis of the OD Nature Tripod measurements

DEPARTMENT
MOBILITY &
PUBLIC
WORKS

www.flandershydraulicsresearch.be

Sediment Transport Model for the Port of Zeebrugge

Sub report 2 – Analysis of the OD Nature Tripod measurements

De Maerschalck, B.; Nguyen, D.; Vanlede, J.; Mostaert, F.

Flanders Hydraulics Research
Flanders State of the Art

Cover figure © The Government of Flanders, Department of Mobility and Public Works, Flanders Hydraulics Research

Legal notice

Copyright and citation

This publication should be cited as follows:

De Maerschalck, B.; Nguyen, D.; Vanlede, J.; Mostaert, F. (2020). Sediment Transport Model for the Port of Zeebrugge: Sub report 2 – Analysis of the OD Nature Tripod measurements. Version 3.0. FHR Reports, 00_067_2. Flanders Hydraulics Research & Antea Group: Antwerp.

4245913004/TDN

Document identification

Customer:	Afdeling Maritieme Toegang (aMT)	Ref.:	WL2020R00_067_2
Keywords (3-5):	Sediment transport, suspended sediment, Zeebrugge		
Knowledge domains	Hydraulics and sediment > Sediment > Cohesive sediment > In-situ measurements		
Text (p.):	53	Appendices (p.):	28
Confidentiality:	☒ Yes	Released as from:	01/01/2025
		Exception:	☒ The Government of Flanders

Author(s):	De Maerschalck, B.; Nguyen , D.

Control

	Name	Signature
Reviser(s):	Vanlede, J.	Getekend door:Joris Vanlede (Signature) Getekend op:2021-01-22 10:25:22 +01:0 Reden:Ik keur dit document goed Joris Vanlede
Project leader:	Vanlede, J.	Getekend door:Joris Vanlede (Signature) Getekend op:2021-01-22 10:26:06 +01:0 Reden:Ik keur dit document goed Joris Vanlede

Approval

Head of Division:	Mostaert, F.	Getekend door:Frank Mostaert (Signature Getekend op:2021-01-22 11:41:53 +01:0 Reden:Ik keur dit document goed Frank Mostaert

Abstract

In project 00_067, Flanders Hydraulics Research (FHR) aims at the development of a detailed mud transport model for the Port of Zeebrugge and its environment.

In preparation of the calibration and validation phase of the model development, this report analyses the data of OD Nature tripod deployments at MOW1, Blankenberge and WZbuoy during the period 2005-2013. These tripods are equipped with several instruments and are able to measure continuously and weather independent for a period of several days to two months. In this analysis the velocity data from a SonTek 3 MHz ADP Acoustic Doppler Profiler and a SonTek 5 MHz ADVOcean Acoustic Doppler Velocimeter, and sediment concentrations derived from two OBS sensors are analysed. All good data are assembled according to tidal range in order to derive ensembles of neap, normal and spring tide.

Contents

List of tables

List of figures

1 Introduction

With the initiation of project 00_067, Flanders Hydraulics Research (FHR) aims at the development of a detailed mud transport model for the Port of Zeebrugge and its environment. In the preparation of the calibration and validation phase of the model development, FHR collected the available flow and sediment data of recent measurement campaigns inside and around the port of Zeebrugge (see De Maerschalck & Vanlede, 2011 and De Maerschalck et al., 2020).

One of the important data sources in terms of suspended sediment measurements and current velocities along the Belgian coastal zone are the OD Nature[1] tripod measurements within the framework of the MOMO[2] project (Fettweis et al., 2011, 2015). The most frequent measurement locations for the tripod are Blankenberge, MOW1 and WZbuoy. Limited datasets are also available at FHR for the locations MOW0, Blighbank and Gootebank. The measurements of the last two locations were carried out by OD Nature for a third party, and therefore the use and publication of this data is restricted. The raw data of all the tripod measurements available at FHR is visualized in a factual data report (De Maerschalck et al., 2020).

The tripod deployments at the locations Blighbank and Gootebank were carried out by OD Nature in the framework of BELWIND. This data is confidential and cannot be used nor distributed without the permission of OD Nature.

This report gives an in-depth analysis of the available data. The focus of the analysis is on the Blankenberge, MOW1 and WZbuoy data. For these locations the most data is available and they are closest to the port of Zeebrugge, for which a numerical sediment transport model is under development. For the other locations the available data is limited in time or incomplete: for MOW0 no sediment data nor ADV measurement is available at FHR and for Blighbank and Gootebank the ADP data is missing and the available sediment data is limited for statistical analysis. Furthermore, the Blighbank is outside the model domain.

In this report two types of statistical analysis are discussed: the first one is an analysis of the tidal harmonics of the measured velocities. For the second analysis all measured sediment concentrations and current velocities are filtered and assembled according to neap, normal and spring tides. The assembled velocities and sediment concentrations are then analyzed.

[1] OD Nature: Operational Directorate Natural Environment, Royal Belgian Institute of Natural Sciences (previously known as MUMM - Management Unit of the North Sea Mathematical Models and the Scheldt Estuary).
[2] MOMO: Monitoring and Measuring fine sediment transport and the evaluation of the effects of dredging and dumping on the marine ecosystem.

2 OD Nature tripod measurements

2.1 Measurement devices

In order to be able to measure continuously for at least one complete spring-neap tidal cycle, close to the bottom and weather independent, OD Nature disposes of two tripod measurement devices. In general the tripods are equipped with a LISST-100x, a SonTek 3 MHz ADP Acoustic Doppler Profiler, a SonTek 5 MHz ADVOcean Acoustic Doppler Velocimeter, a Sea-Bird SBE37 CT measurement system and two OBS sensors. Two SonTek Hydra systems are used for data acquisition and battery power. Figure 1 shows the fully equipped tripod.

Figure 1 - Lowering of the tripod from the RV Belgica (left), equipment of the tripod (right)

The SonTek ADVOcean, also referred as ADV, is mounted at about 40cm above the bottom and measures the velocity at the height of about 20cm above the bottom. Two OBS sensors are coupled to the ADV: one at about 30cm above the bottom and one at about 2.3m. The SonTek ADP is mounted on top of the tripod and looks downwards. It measures the velocity profile from the bottom till the sensor height.

The signals of the OBS sensors are logged by the data logger of the ADV. Afterwards this OBS signal is processed to turbidity levels, expressed in FTU. The calibration is based on laboratory tests. Finally the turbidity levels are converted by OD Nature to volume sediment concentrations in mg/l. The correlation is based on in-situ water samples taken with a Niskin Carrousel as shown in Figure 2. The samples are taken during at most one tidal cycle at the beginning or end of the deployment. Based on these available samples a correlation coefficient between turbidity and sediment concentrations is determined. Depending on the type of the deployed OBS sensors, the measurement range (converted to volume sediment concentrations) is between about 0-780 mg/l, 0-1550 mg/l or 0-3200 mg/l (see also Fettweis et al., 2015). Therefore, OBS will underestimate the sediment concentration values that are beyond the limits of the instrument.

Figure 2 - Niskin Carrousel (left) and SonTek ADVOcean sensor (middle) and SonTek ADP (right)

2.2 Available data

Frequent anchor positions of the tripod are MOW1, Blankenberge and WZbuoy and few measurement campaigns have been conducted at MOW0, Blighbank and Gootebank (see Figure 3 for the location). Table 1 to Table 6 (Appendix A) give an overview of the data of the OBS, ADP and ADV for Blankenberge, MOW1, WZbuoy, MOW0, Blighbank and Gootebank during the period 2005-2013 (see also De Maerschalck & Vanlede, 2011 and De Maerschalck et al. 2020). It is noted that the exact height of the sensors may vary between the campaigns (see Appendix A for the reported sensor heights). For two deployments near Blankenberge in 2008, the exact sensor positions were not documented. It is assumed that the sensor positions are the same as those for another deployment in the same year. The received data sets for the years 2010, 2011, 2012 and 2013 are in text format and stored according to year which contain data from multiple deployments. For the evaluation of the data quality per deployment, the yearly data sets are split into individual deployment data. The suspicious data is then easily eliminated.

The number of measurement days presented in Table 1 to Table 6 are the total number of deployment days. However, not all data is valid for further analyses due to different reasons (e.g. the sensor is tilted due to ship collision, or overgrown by algae…). All bad or doubtful data (noisy, suspicious time shift,..) is eliminated from further analysis. For deployments which the vertical sensor position deviates strongly from the common position the data is also ignored. Remarks on the quality of the data can be found in the tables. The total number of valid tidal cycles used for the analyses is added at the bottom of each table.

Figure 4 shows the numbers of valid tidal cycles for the different locations and sensors for the different seasons. The largest amount of data is for MOW1 with 1596, 1998 and 2314 valid tidal cycles for the OBS, ADP and ADV data, spreading over four seasons. Blankenberge and WZbuoy are ranked in the second and third place but no data is available during summer for Blankenberge and in winter for WZbuoy. Less data is available for Blighbank and Gootebank and there is no ADP data available for these two locations. The available data for MOW0 is restricted to one deployment during which the ADVOcean was heavily damaged. Therefore no ADV nor OBS data could be recuperated. The data is available at Flanders Hydraulics Research in a Matlab® data format.

Figure 3 - Location of the OD Nature tripod deployments (orange dots) and Meetnet Vlaamse Banken (MVB) measurement pylons (yellow markers). Upper: all locations; lower: zoom to locations close to the Zeebrugge port.
The white grid is the flow grid of the Zeebrugge model

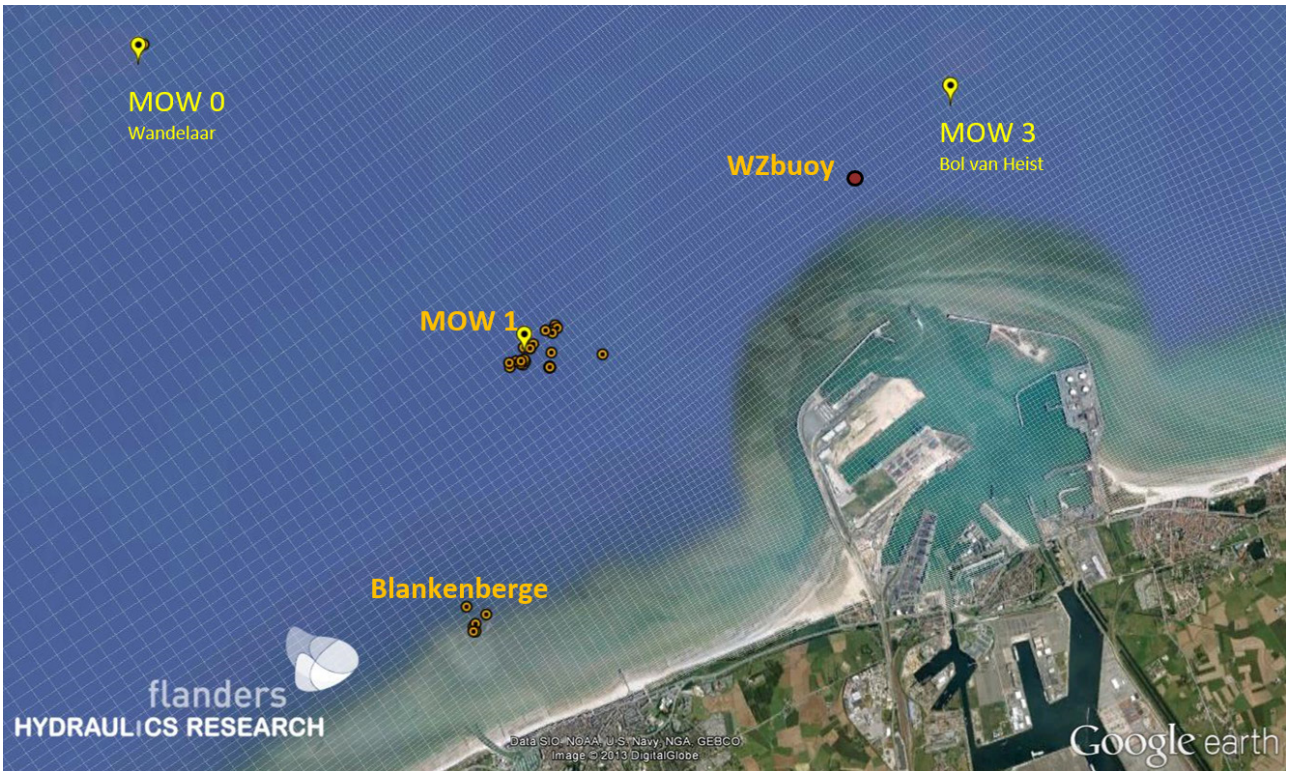

Figure 4 - OD Nature tripod deployments: valid OBS, ADP and ADV data.
Total # of valid tidal cycles is shown in brackets

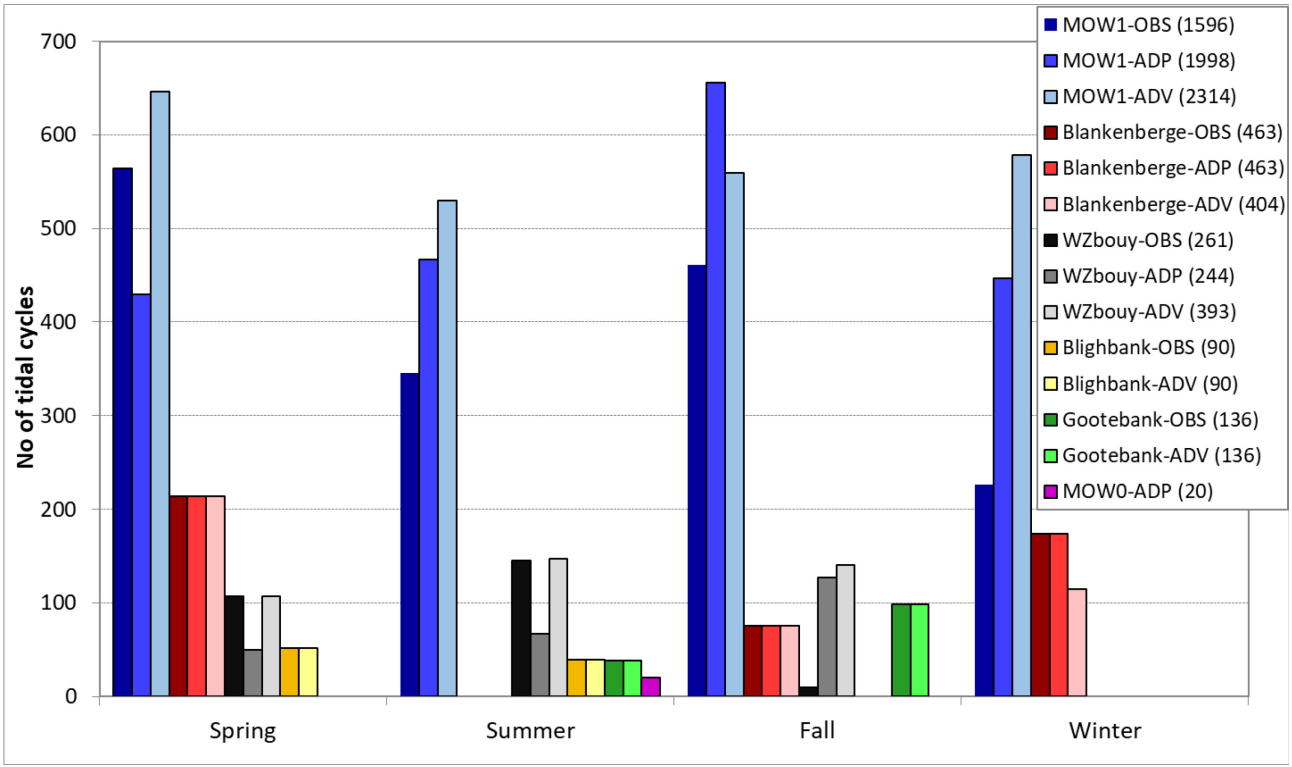

The analysis in this report is done using the valid data of OBS sediment concentrations at ~0.3mab and ~2.3mab, ADV current velocities at ~0.2mab. For ADP data, the profile-averaged velocities (averaged over the heights from the bottom to ~2mab) are used. In addition, the ADP velocities at the highest bin (positioned at ~1.9mab) are also employed to study the relation of the current velocities and sediment concentrations at the two nearest available vertical levels (velocities at ~1.9mab and sediment concentrations at ~2.3mab).

3 Analysis of the measured currents

3.1 Major directions

In the factual data report (De Maerschalck et al., 2020) it has been demonstrated that the major axis inclination might differ significantly from one tripod deployment to another.

Figure 5 to Figure 10 show the results of the bootstrapping analysis of the ADP and ADVOcean velocity measurements for the different locations, see De Maerschalck et al. (2020) for a description of the method. The red line in the graphs is the weighted sum of the normal distributions computed for each deployment individually. The weights are based on the length of the deployment. For the ADP data, the profile-averaged current velocity (positioned at ~1.2mab) is used and ADVOcean velocity is at ~0.2mab. The observed distinct peaks reveal the variation in the mean major direction during one or more tripod deployments at the same location. This is also seen in Appendix B.2 with the deviation in the estimated major directions among the deployments. One would expect that the major direction of the tidal ellipse, mostly dominated by the M2 component, would not differ for the different deployments at the same place. For the nearshore locations (Blankenberge, MOW1, MOW0 and WZbuoy), the major direction is expected to be parallel to the coast: 65°. This can be observed for the measurements at MOW1, Blankenberge (Figure 5 and Figure 6) with strong peaks around 65°, however the spread is significant. For WZbuoy the peaks around 65° can also be observed in the ADV velocities but the ADP data shows more peaks, spreading from 49° to 80° (Figure 7). The ADP measurement at MOW0 shows a sharp peak around 65° (Figure 8). Note that for this location, there is only one deployment available. For the locations Blighbank and Gootebank only two deployments are available at FHR. For Blighbank, two distinct major directions of 23° and 55° are observed (Figure 9), indicating some problem in the data for this location.

The variance in the major direction at the same measurement location might be due to a number of factors, e.g. the influence of the frame and the measuring devices on the flow, variability of the exact location of the deployment, variability of the position of the sensors on the tripod, local bed forms, compass problems and other measurement errors,…

Figure 5 - Probability density of the major axis direction for the assembled ADP (left) and ADVOcean (right) data of the deployments at MOW1

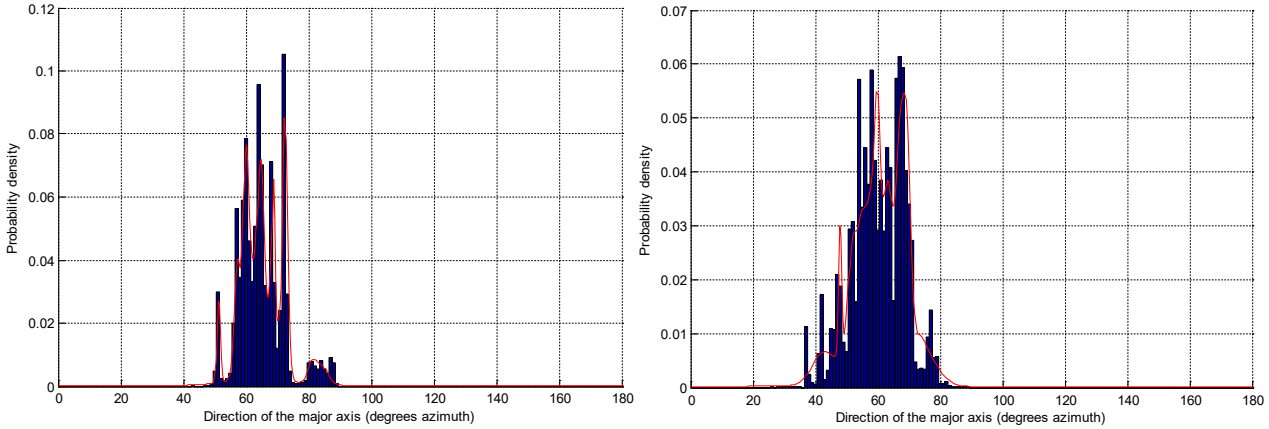

Figure 6 - Probability density of the major axis direction for the assembled ADP (left) and ADVOcean (right) data of the deployments at Blankenberge

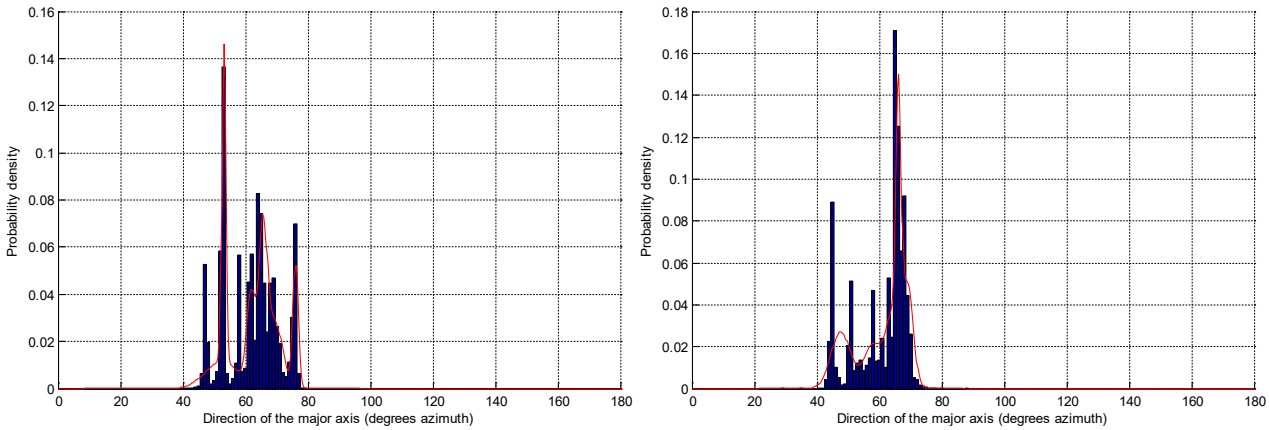

Figure 7 - Probability density of the major axis direction for the assembled ADP (left) and ADVOcean (right) data of the deployments at WZbuoy

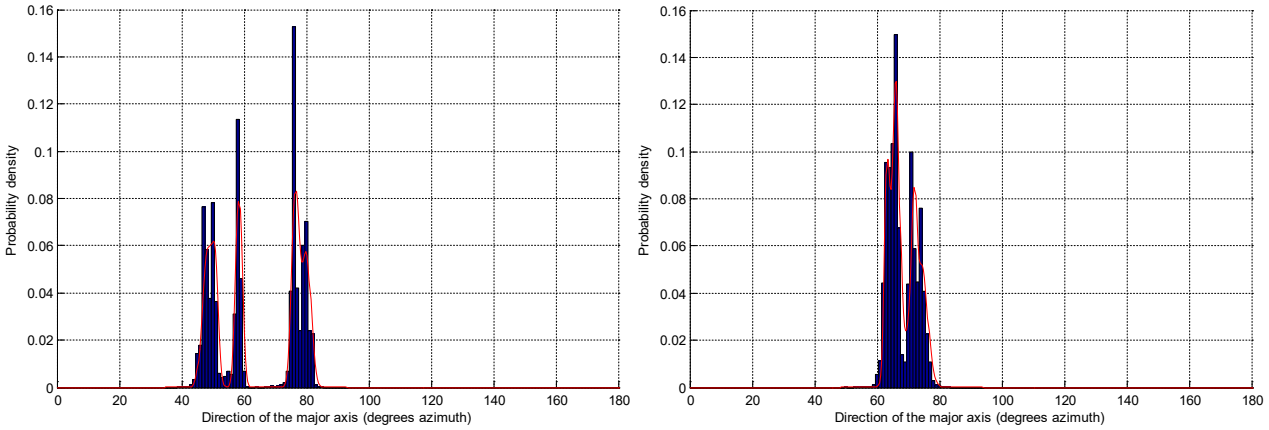

Figure 8 - Probability density of the major axis direction for the assembled ADP at MOW0

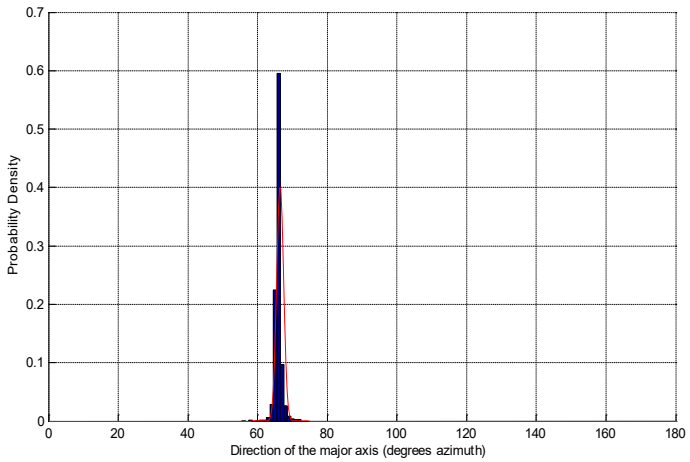

Figure 9 - Probability density of the major axis direction for the assembled ADVOcean data of the deployments at Blighbank

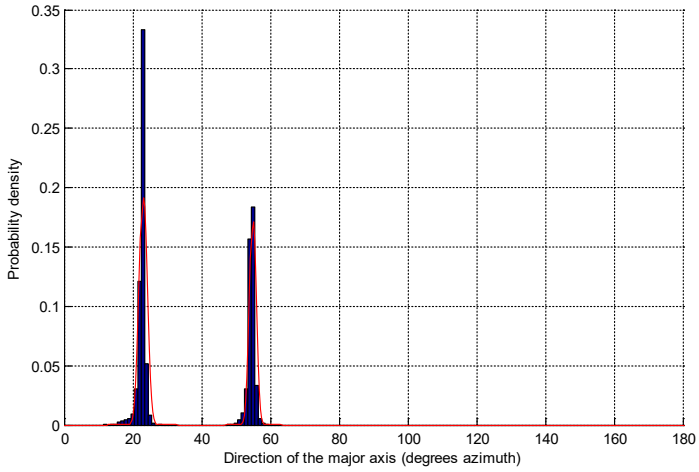

Figure 10 - Probability density of the major axis direction for the assembled ADVOcean data of the deployments at Gootebank

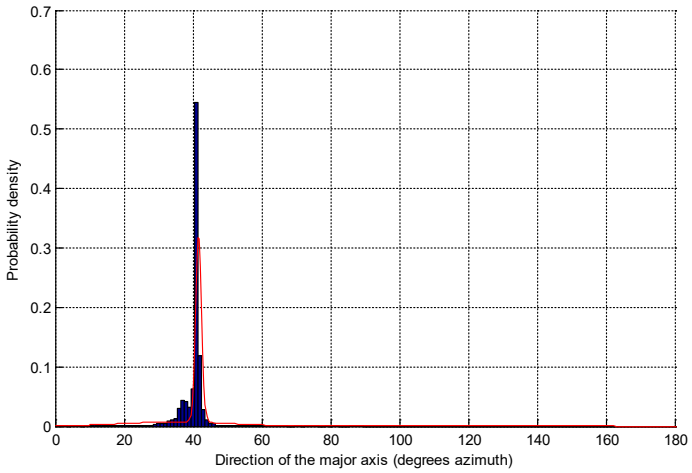

3.2 Tidal amplitudes, phase and direction of the M2, M4 and S2 constituents

In classical harmonic analysis a tidal signal can be modelled by a finite sum of harmonic functions with specific frequencies related to astronomical parameters. T_TIDE is a set of algorithms written in Matlab® that allow for tidal analysis of the measurement data (Pawlowicz et al., 2002). For current measurements the horizontal velocity vector is projected into the complex plane:

(1)

with and the west and north component of the horizontal velocity vector and the imaginary unit. When analyzing this complex time series using T_TIDE, for each tidal constituent the inclination of the major and minor direction is returned together with the tidal amplitudes and phases of the velocity components along these major and minor axes.

A characteristic of tidal currents is the predominance of the semidiurnal lunar M2 and solar S2 constituents with periods of 12.42 and 12 hours, respectively. The small difference in their periods produces the 15-day spring-neap tidal cycle. Together with the M4 component (6.21 hours) these are most dominant regarding sediment transport in a semi-diurnal tidal regime (Prandle, 1997). The contribution of each constituent to the current is defined by the major and minor amplitudes and phases, and the inclination of the major axis, also called the tidal ellipse orientation.

The tidal analysis is done on the individual deployments. Theoretically one would expect that the harmonic analysis of the currents would give similar amplitudes, phase angles and ellipse orientation for the different deployments at the same location if the measurement period is long enough to capture the constituent frequencies. This is definitely not the case for the major axis direction of the M2 component as seen in Appendix B.2. Neither is this the case for the other harmonic parameters of the tidal constituents. Section 3.1 lists possible reasons for this variance.

The weighted mean and standard deviation of the major and minor amplitude, ellipse orientation and phase are computed for each deployment location and for each sensor. The weights are the durations of the individual deployments. The mean and standard deviation for different measurement locations are presented in Figure 11 to Figure 18 below and Table 13 in Appendix B.2. Notice that for location MOW0 the data of only one deployment is available, therefore no standard deviation could be calculated. In addition, the deployment is too short for T_TIDE to be able to differentiate the M2 from the S2 constituent. For Blighbank and Gootebank only two deployments are available.

The M2 amplitudes for MOW1, Blankenberge and WZbuoy are comparable as shown in Figure 11. As expected, the M2 and S2 amplitude of the ADVOcean at ~0.2mab is lower (about 30%) than that of the ADP profile-averaged velocity (positioned at ~1.2mab).

It is clear from Figure 12 and Figure 13 that closer to the coast the minor amplitude becomes smaller and thus the eccentricity of the tidal ellipse increases as expected.

The mean directions of the M2 and S2 ellipse for the locations close to the coast Blankenberge, MOW1, WZbuoy and MOM0 are in the range of 60°-68°Az. (Figure 14) which is more or less parallel to the coast (65°Az.).

The large spread in the major direction of the tidal ellipse for ADP measurements at WZbuoy (Figure 7) and ADV measurements at Blighbank (Figure 9) is also evident in the larger standard deviation of the M2 major direction in Figure 14. At the moment it is unclear what exactly causes the difference among different deployments at the same location. One has to keep in mind that the exact location of the deployment is not always the same. If there is dune formation the flow just above the bottom might be deflected.

Figure 11 - Mean and standard deviation of the major amplitude of M2, S2 and M4 at the different measurement locations (ADVOcean: ≈ 0.2mab, ADP measurements: profile-average between 0 and ≈2mab)

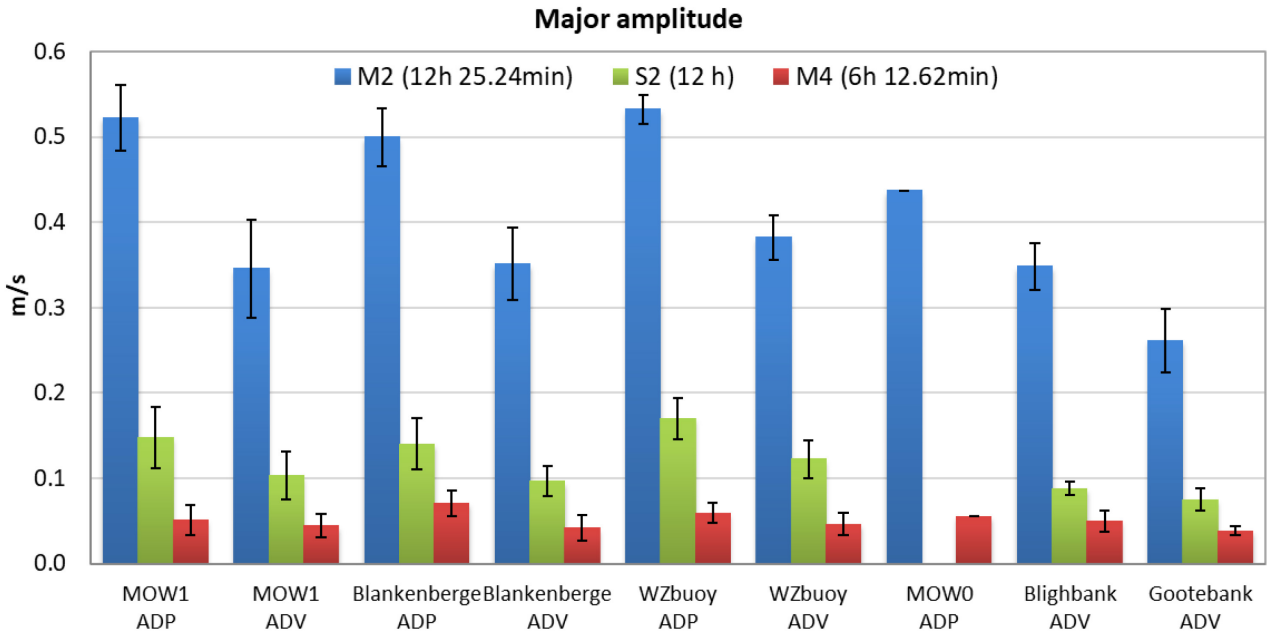

Figure 12 - Mean and standard deviation of the minor amplitude of M2, S2 and M4 at the different measurement locations (ADVOcean: ≈ 0.2mab, ADP measurements: profile-average between 0 and ≈2mab)

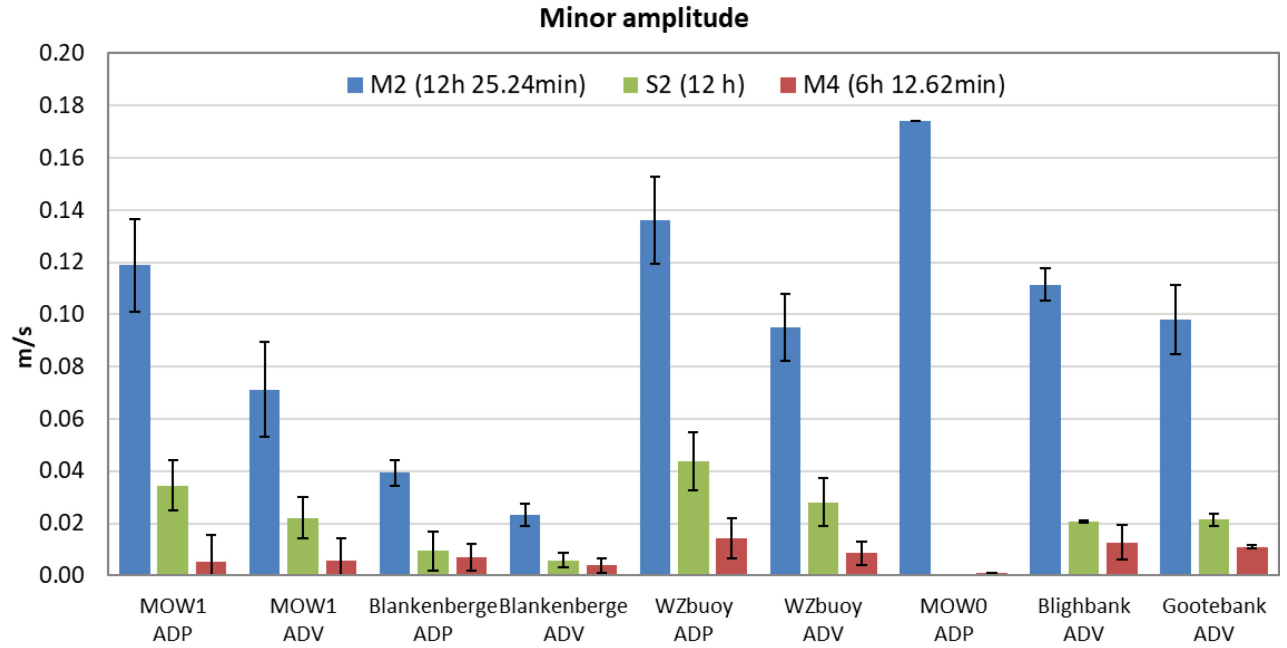

Figure 13 - Mean and standard deviation of the eccentricity of the tidal ellipses of M2 and S2 at the different measurement locations (ADVOcean: ≈ 0.2mab, ADP measurements: profile-average between 0 and ≈2mab)

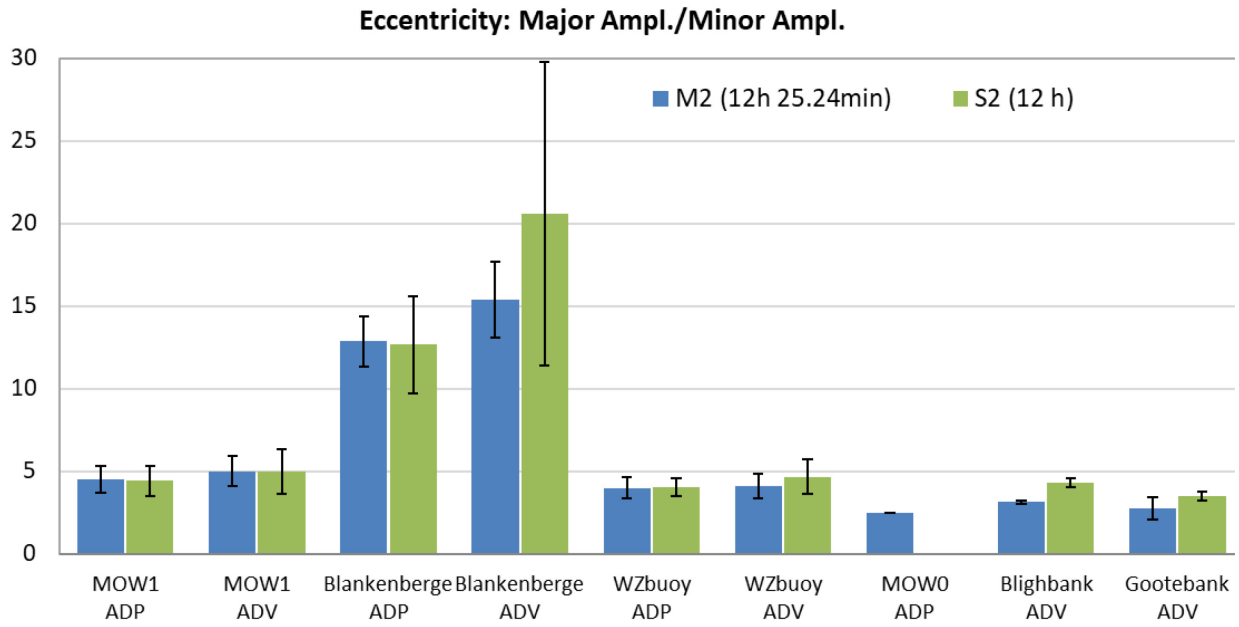

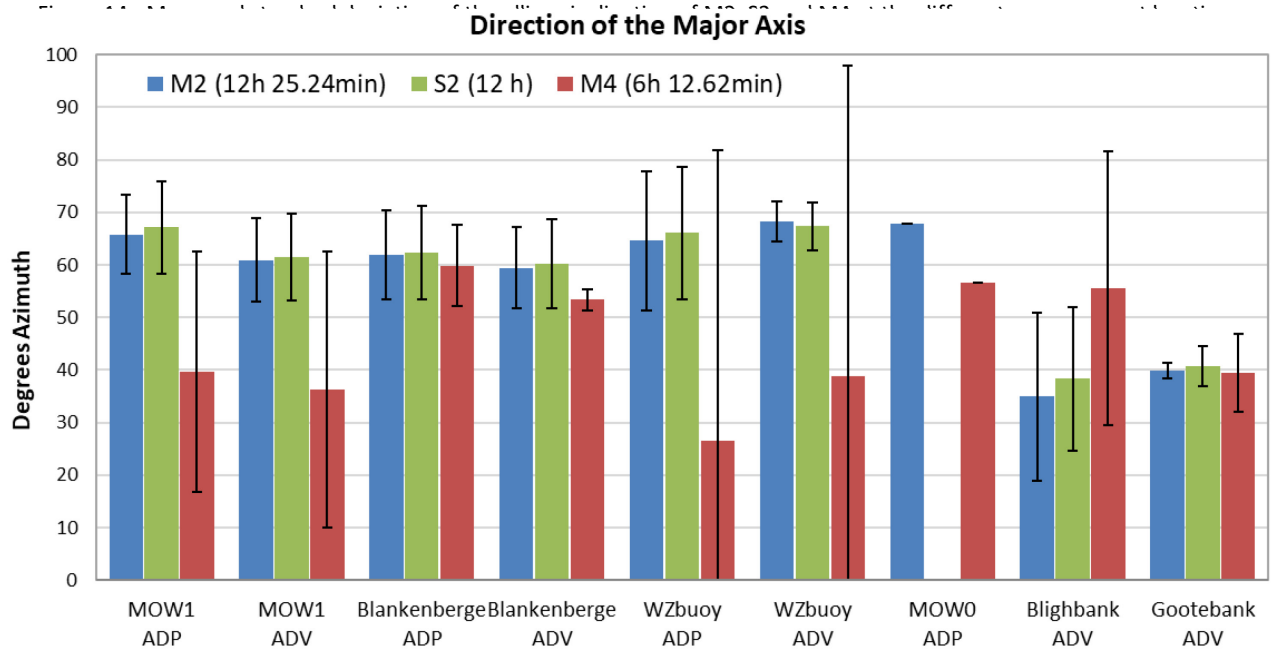

Figure 15 - Mean and standard deviation of the phases of M2, S2 and M4 at the different measurement locations (ADVOcean: ≈ 0.2mab, ADP measurements: profile-averaged between 0 and ≈2mab)

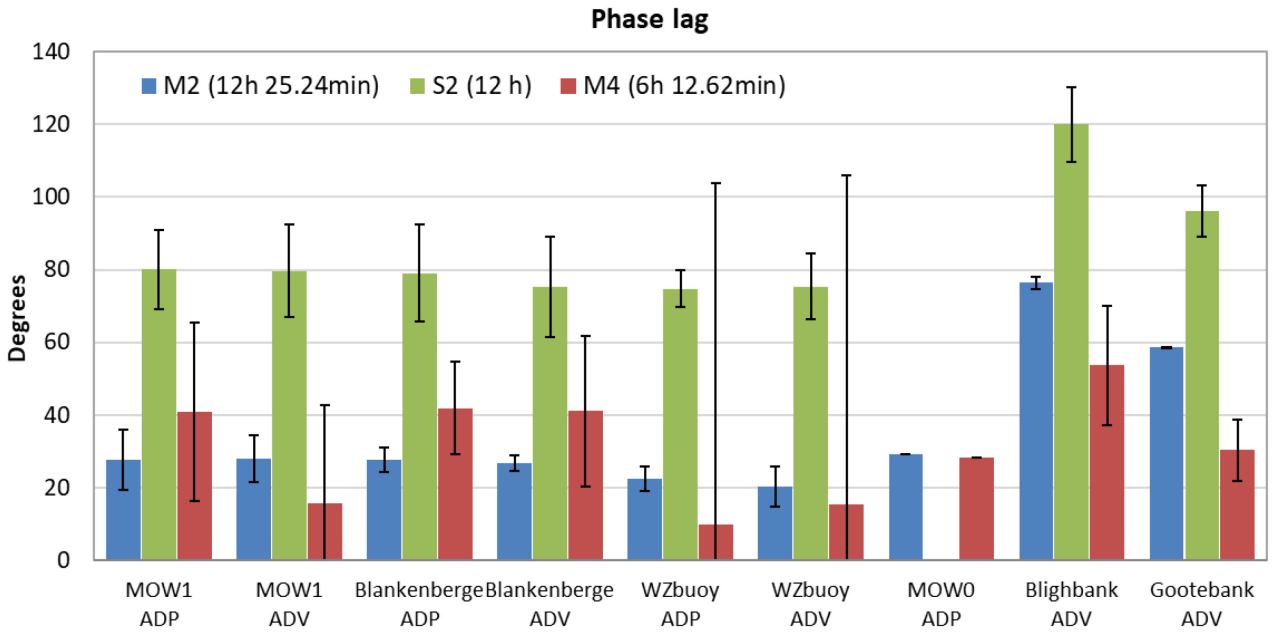

Figure 16 shows the residual of the velocity components. This is a component of the velocity which cannot be explained by harmonic analysis. The large standard deviation makes it hard to interpret these numbers.

The tidal excursion length is the maximum horizontal distance a suspended particle can travel in the direction of the major and minor axes direction when it is purely advected by the tidal current. This can be computed for each tidal constituent as:

(2)

with the major (minor) tidal amplitude and the period of the tidal constituent. The tidal excursion lengths for the M2, S2 and M4 are shown in Figure 17 and Figure 18.

Figure 16 - Mean and standard deviation of the residual velocity at the different measurement location (ADVOcean: ≈ 0.2mab, ADP measurements: profile-averaged between 0 and ≈2mab)

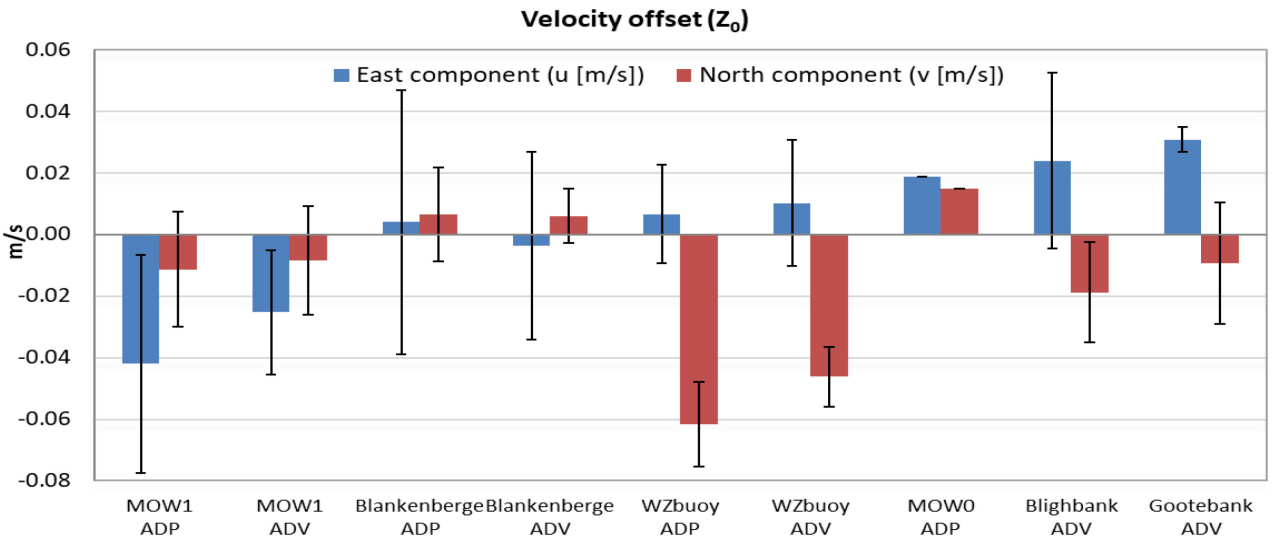

Figure 17 - Mean and standard deviation of the tidal excursion lengths in major axis direction of M2, S2 and M4 at different measurement locations (ADVOcean: ≈ 0.2mab, ADP measurements: profile-averaged between 0 and ≈2mab)

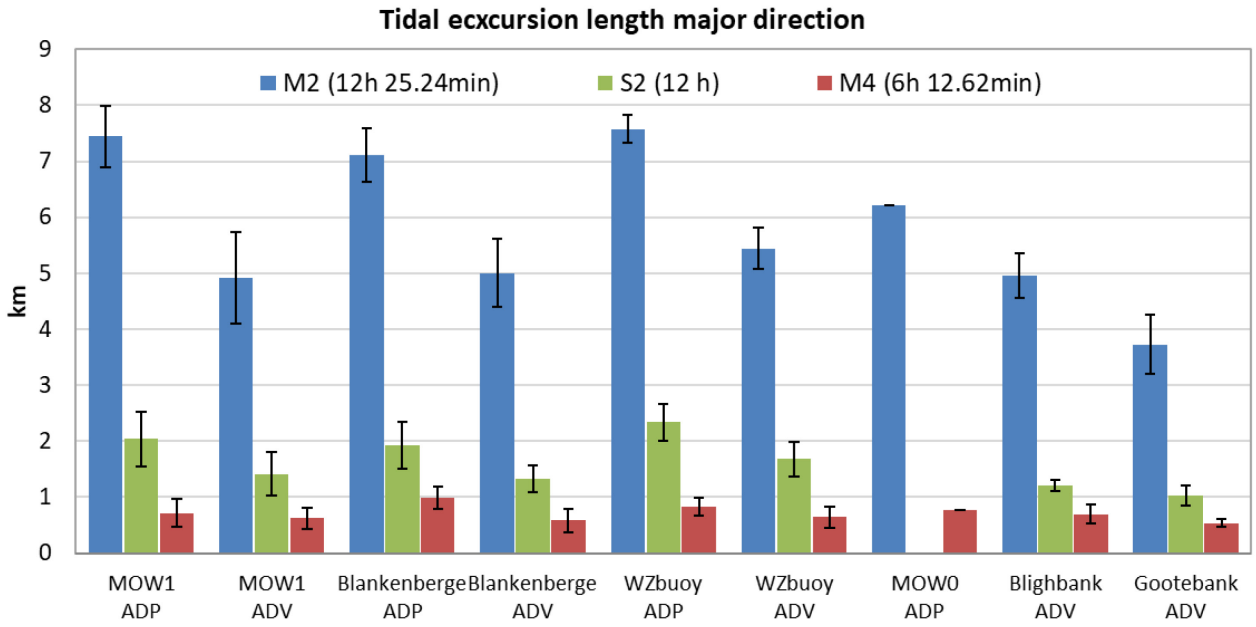

Figure 18 - Mean and standard deviation of the tidal excursion lengths in minor axis direction of M2, S2 and M4 at different measurement locations (ADVOcean: ≈ 0.2mab, ADP measurements: profile-averaged between 0 and ≈2mab)

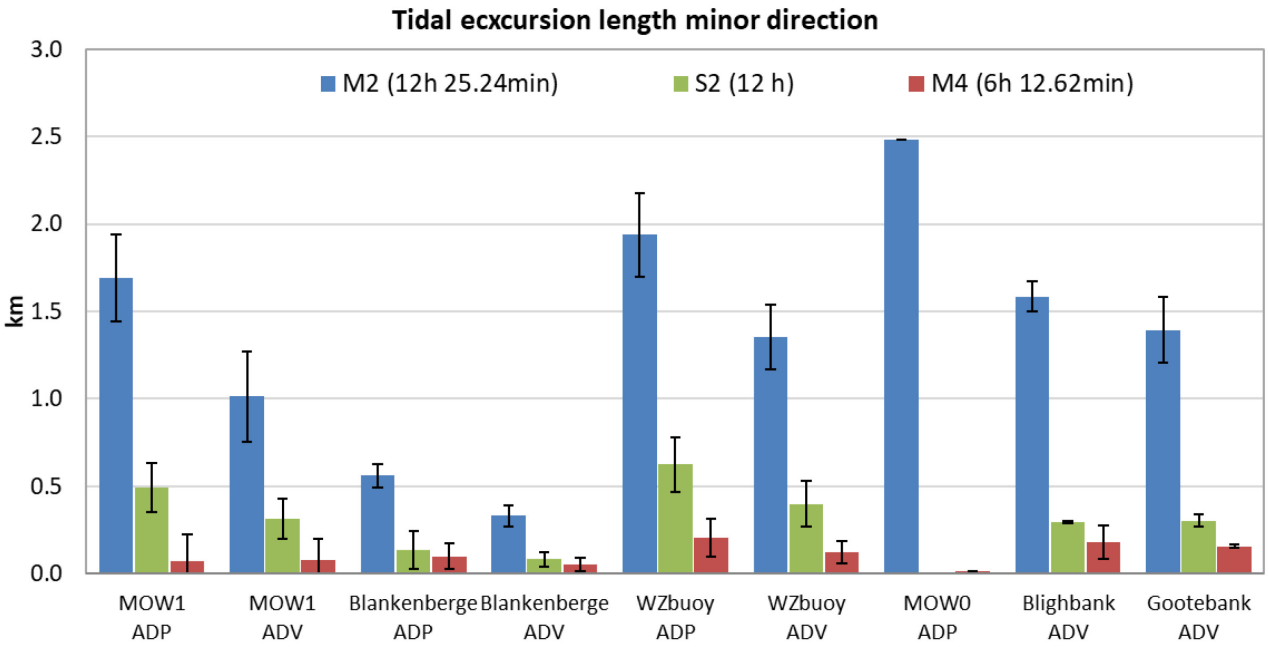

3.3 Tidal variability of current velocities

This section discusses the tidal variability of the assembled neap, normal and spring tides. The signal of the pressure sensor mounted on the tripod (≈ the local water depth) is used to split the time series into discrete tidal cycles which are defined as the time span between two consecutive low water moments. Each tidal cycle is then classified as neap, normal or spring tide depending on the corresponding tidal range at Vlissingen (source: Hydro Meteo Centrum Zeeland, www.hmcz.nl). Then all neap, normal and spring tides are assembled together to construct an ensemble average for the neap, normal and spring tides.

The neap, normal or spring tidal classification is determined using the 33rd and 66th percentiles of the tidal range at Vlissingen based on the water level measurements over the 10-year period (2004-2013):

- Neap tide: tidal range ≤ 3.54 m (P33)
- Normal tide: 3.54m (P33) < tidal range ≤ 4.11m (P66)
- Spring tide: tidal range > 4.11m (P66)

Since the local pressure (or water depth) signal is used to determine the high/low water moments for the construction the ensembles, only the velocity data from the tripod deployments for which pressure/depth data is available could be used to construct the ensembles. All bad and doubtful data is excluded from the ensemble analysis. Table 1, Table 2 and Table 3 in Appendix A indicate whether or not each of the individual deployments is included in the combined ensembles for Blankenberge, MOW1 and WZbuoy.

The wind climate for the periods in which the velocity data is used in the construction of the ensembles for Blankenberge, MOW1, WZbuoy, Blighbank and Gootebank is presented in Figure 19. For all measurement stations the same meteorological station Vlakte van de Raan (source HMCZ) is used. As a reference the 15-year wind climate is shown in Figure 19 (bottom, right).

For the three locations Blankenberge, MOW1 and WZbuoy the wind climate during ADP measurements is comparable with that during ADV measurements. Those wind roses also show some resemblance to the 15

year-wind data with the most dominant wind from the south-west, followed by the north-east and the north-west wind.

For Blighbank and Gootebank, only ADV velocity data from two deployments is available. The wind climate for these two deployment timeframes does not represent the average meteorological conditions.

Figure 19 - Wind roses at Vlakte van de Raan: during tripod deployments used in the ensemble analysis of ADP and ADV measurements at Blankenberge, MOW1, WZbuoy, Blighbank & Gootebank and 15 years (1999-2013)

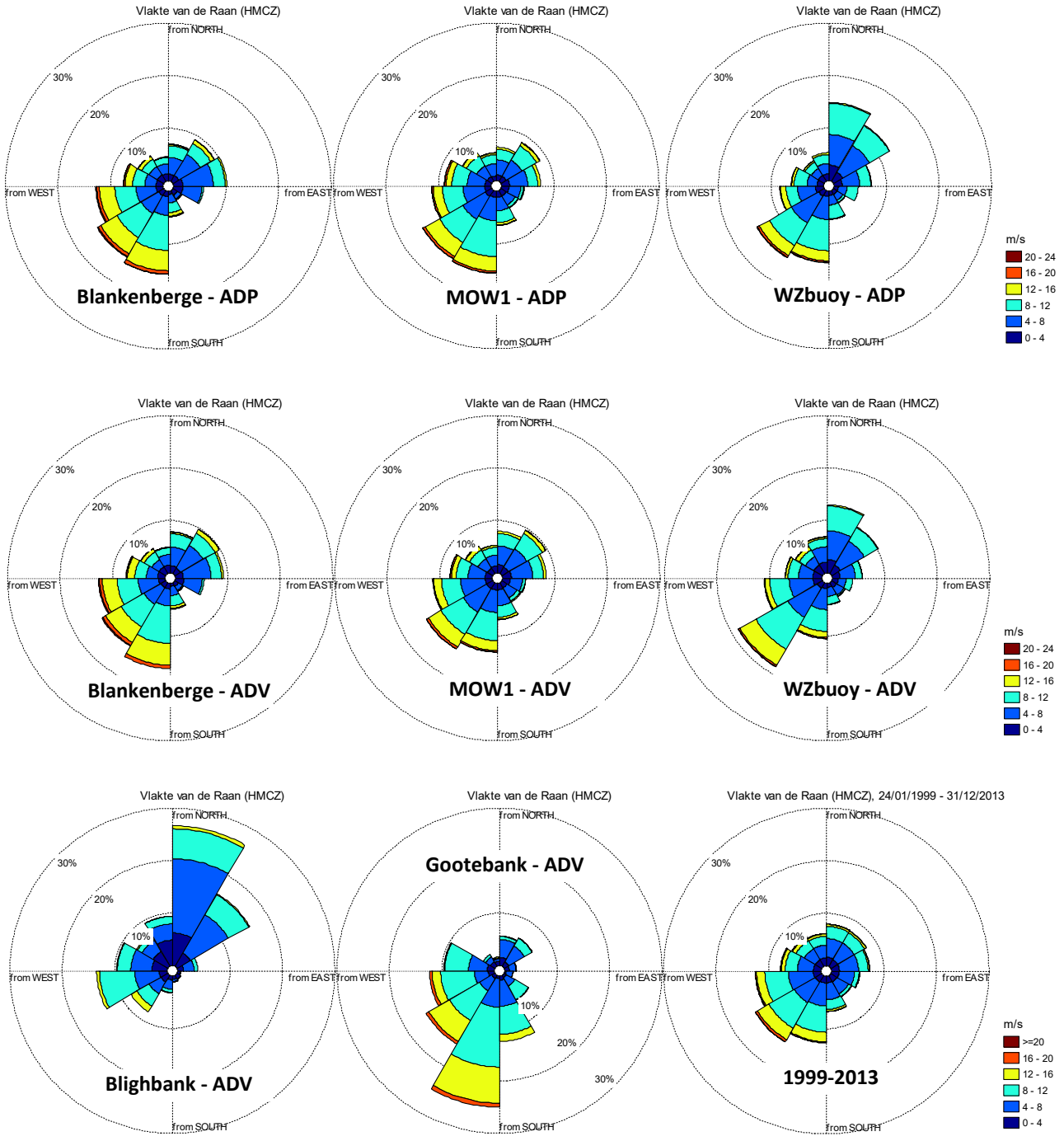

Figure 20 to Figure 32 below show the mean current magnitude and direction assembled according neap, normal and spring tides of all valid data for each measurement location. The error bands for the velocity magnitude and direction represent the standard deviations. The plots of all assembled tides with data points are shown in Appendix C.

For MOW0 there is only one deployment available. During this deployment, the tripod came into collision with a vessel during which the Sontek ADVOcean was heavily damaged. Therefore, there is no pressure data for this deployment and it is not possible to construct the tidal ensembles.

3.3.1 Current velocity at Blankenberge, MOW1 and WZbuoy - ADP measurements ~1.9mab

Since the distance between the deployment locations at Blankenberge, MOW1 and WZbuoy is within about 8km, it is not surprising that the mean current for these three sites are similar (see Figure 20 - Figure 22 for ADP velocity at each location and Figure 23 for velocity magnitude all three sites).

It is clear that the maximum flood is higher than the maximum ebb for all locations and for all tidal classes. The largest difference between maximum flood and maximum ebb flow (a measure for tidal asymmetry) is found for the Blankenberge site, while MOW1 shows the smallest asymmetry. The peak flood velocity at Blankenberge is up to about 15cm/s higher than at MOW1, while the peak ebb flow is up to about 15cm/s lower for the Blankenberge site. The larger tidal asymmetry in velocity at the Blankenberge site can be due to the presence of the port of Zeebrugge. During ebb flow Blankenberge is located in the wake of the outer port. In addition, the difference in wind climate during the deployment periods might influence the ensemble averages, as will be discussed in the next section.

For all sites maximum flood occurs about 1h before high water and varies between 0.5 and 1m/s. Slack water occurs between 2 and 3 hours before high water (or ~3-4h after low water - LW slack), and between 2.5 and 3.5 hours after high water (HW slack). During slack water the mean currents are between 0.1 and 0.3 m/s with slightly higher velocity during LW slack than during HW slack. Since the flow varies over a tidal ellipse, velocities never become truly zero, as they might in a straight channel.

The tidal ellipses in Figure 24, Figure 25 and Figure 26 for Blankenberge, MOW1 and WZbuoy are obtained by plotting the mean east-component of the assembled tides against the mean north-component. The colour scale of the scatter plots refers to the velocity magnitude. The figures confirm that for Blankenberge, although the current magnitude differs not that much from MOW1 and WZbuoy, the eccentricity of the tidal ellipses is much higher.

Figure 20 - Mean and standard deviation of the assembled ADP current velocity magnitude (left) and directions (right) at Blankenberge ~1.9mab, 145 tidal cycles from 6 deployments

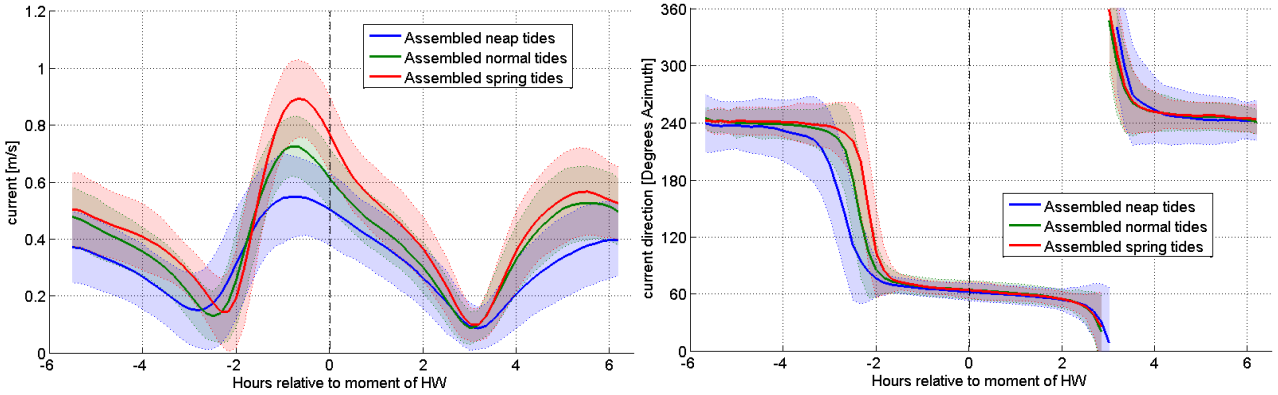

Figure 21 - Mean and standard deviation of the assembled ADP current velocity magnitude (left) and directions (right) at MOW1 ~1.90mab, 390 tidal cycles from 17 deployments

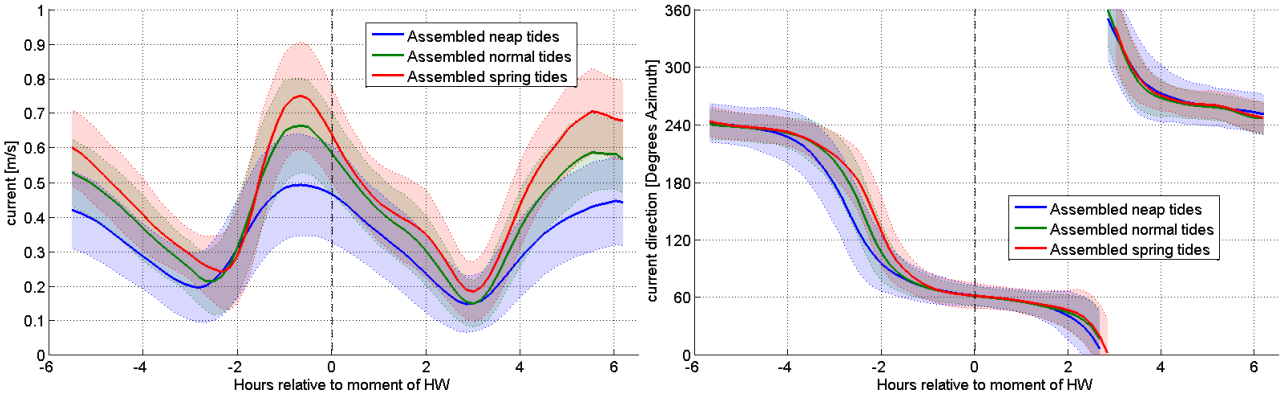

Figure 22 - Mean and standard deviation of the assembled ADP current velocity magnitude (left) and directions (right) at WZbuoy ~1.9mab, 92 tidal cycles from 5 deployments

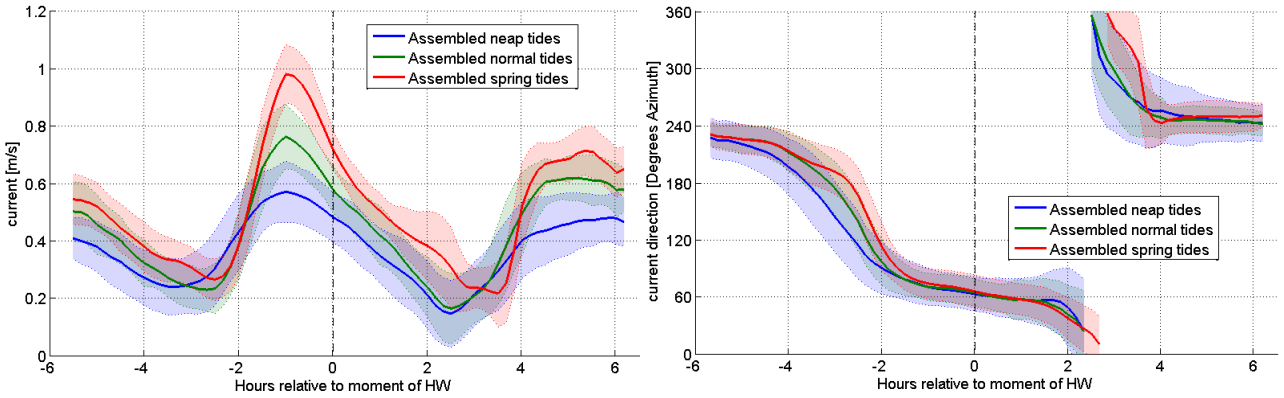

Figure 23 - Mean and standard deviation of the assembled ADP current velocity magnitude at MOW1, Blankenberge and WZbuoy ~1.9mab. Left: neap tides, middle: normal tides, right: spring tides

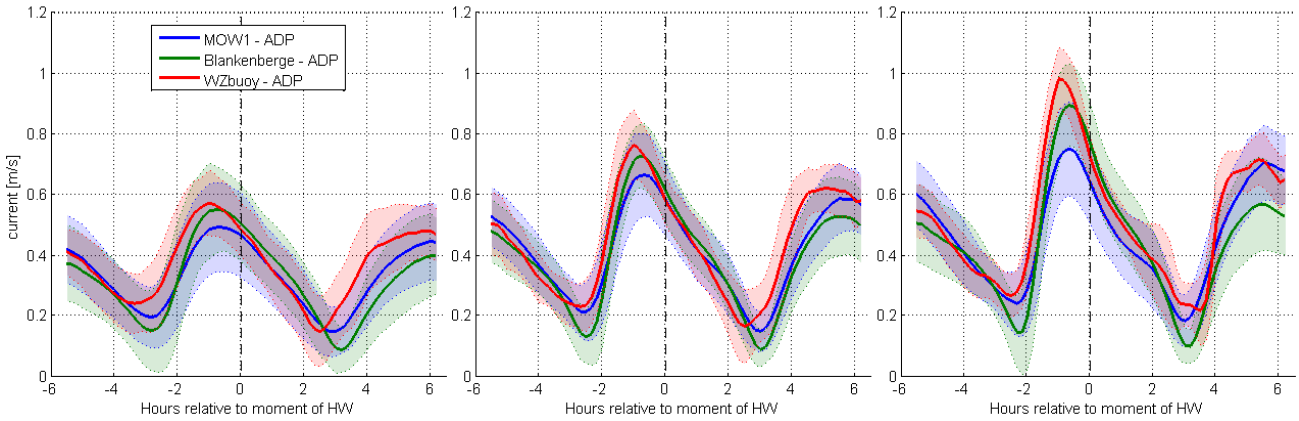

Figure 24 - Tidal ellipse with ADP current velocity colour scale, Blankenberge ~1.9mab.
Left: neap tides, middle: normal tides, right: spring tides

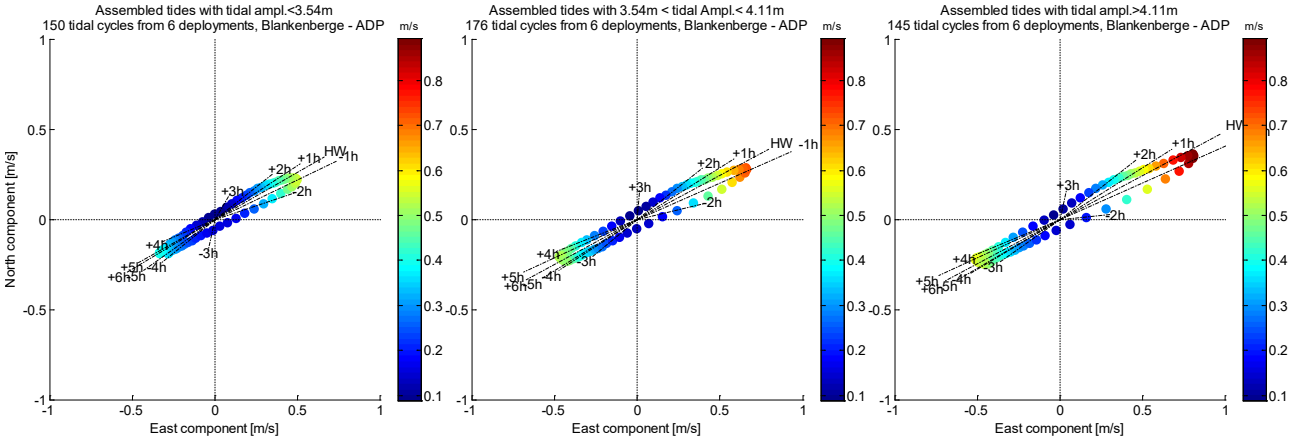

Figure 25 - Tidal ellipse with ADP current velocity colour scale, MOW1 ~1.9mab.
Left: neap tides, middle: normal tides, right: spring tides

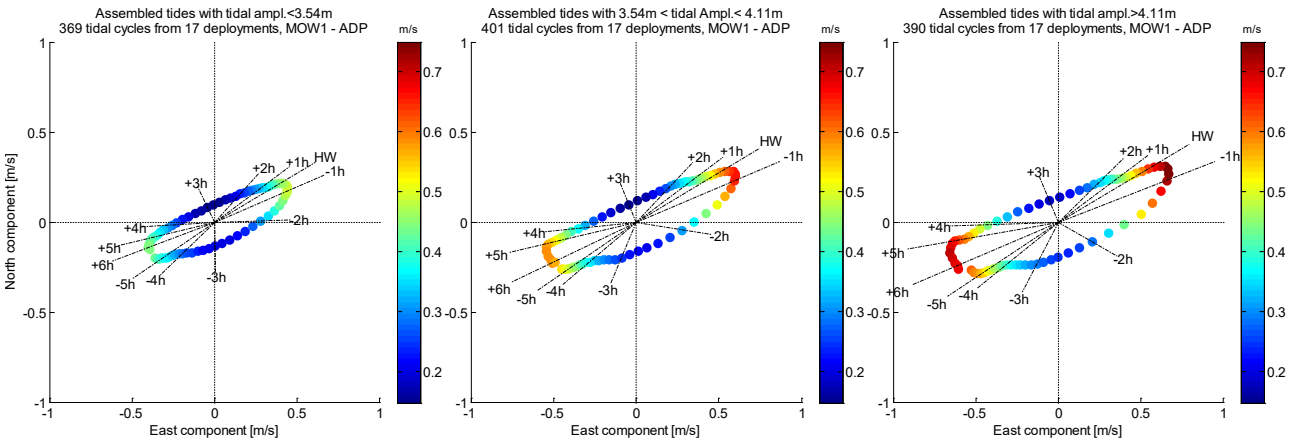

Figure 26 - Tidal ellipse with ADP current velocity colour scale, WZbuoy ~1.9mab.
Left: neap tides, middle: normal tides, right: spring tides

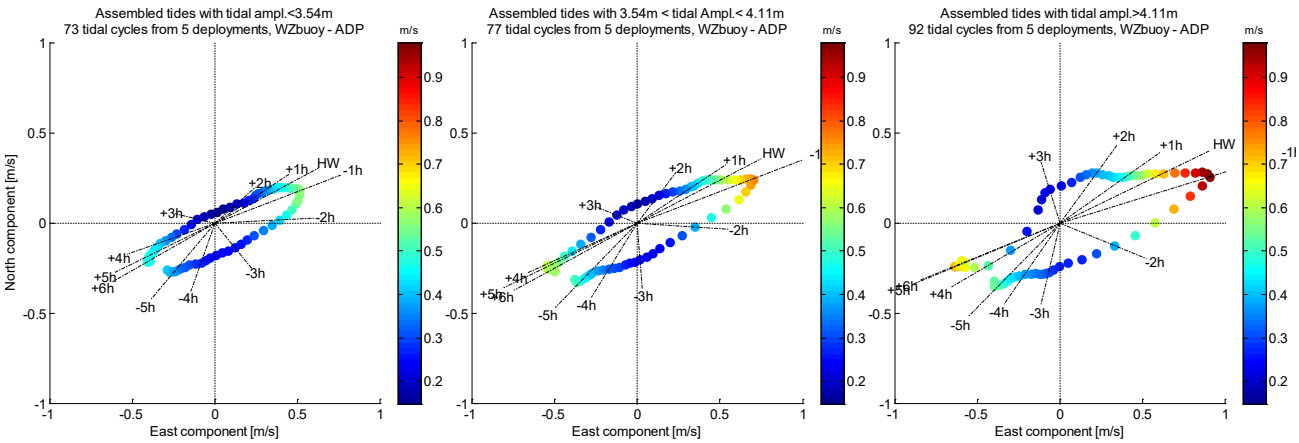

3.3.2 Current velocity at Blankenberge, MOW1 and WZbuoy - ADVOcean measurements ~0.2mab

Figure 27 illustrates for location MOW1 that the ADV measurements at ~0.2mab have a tidal variation similar to the ADP data at ~1.9mab, albeit with a lower velocity.

In Figure 28, Figure 29 and Figure 30, the ensembles of the ADV current velocities at ~0.2mab are presented for Blankenberge, MOW1 and WZbuoy. The mean maximum flood flow of the ADV measurement is in the range of 0.35-0.55 m/s, 0.3-0.52 m/s, and 0.4-0.65 m/s for Blankenberge, MOW1 and WZbuoy, respectively while the maximum ebb reaches up to 0.4 m/s, 0.42 m/s and 0.48 m/s for Blankenberge, MOW1 and WZbuoy. During slack water the flow velocity is around 0.05-0.2 m/s.

Figure 27 - Mean and standard deviation of the assembled current velocities at MOW1: ADP ~1.9mab (blue) and ADV ~0.2mab (red). Left: neap tides, middle: normal tides, right: spring tides

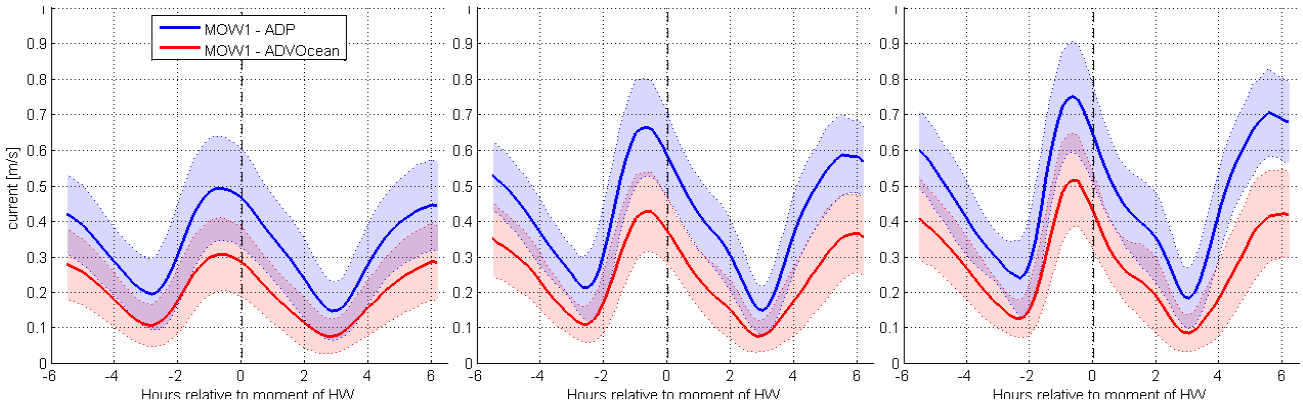

Figure 28 - Mean and standard deviation of the assembled ADV current velocity magnitude (left) and direction (right) ~0.2mab, Blankenberge, 124 tidal cycles from 5 deployments

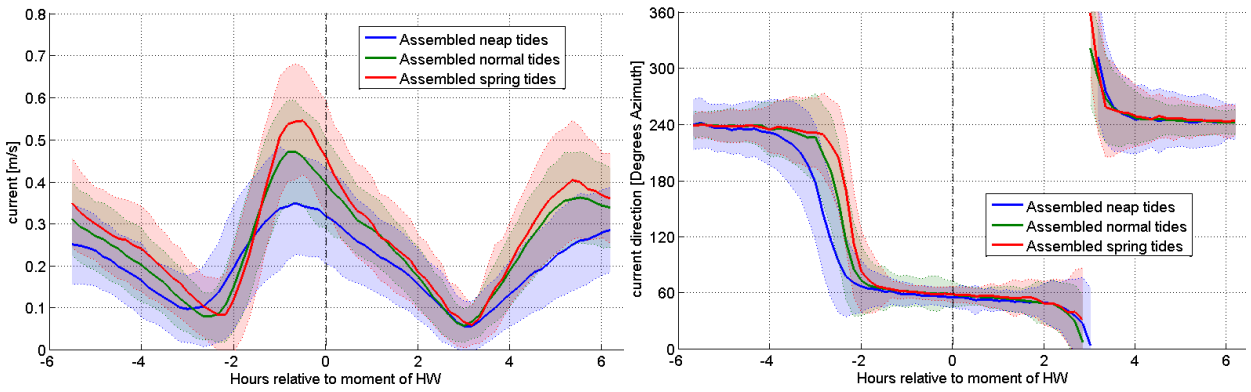

Figure 29 - Mean and standard deviation of the assembled ADV current velocity magnitude (left) and direction (right) ~0.2mab, MOW1, 622 tidal cycles from 29 deployments

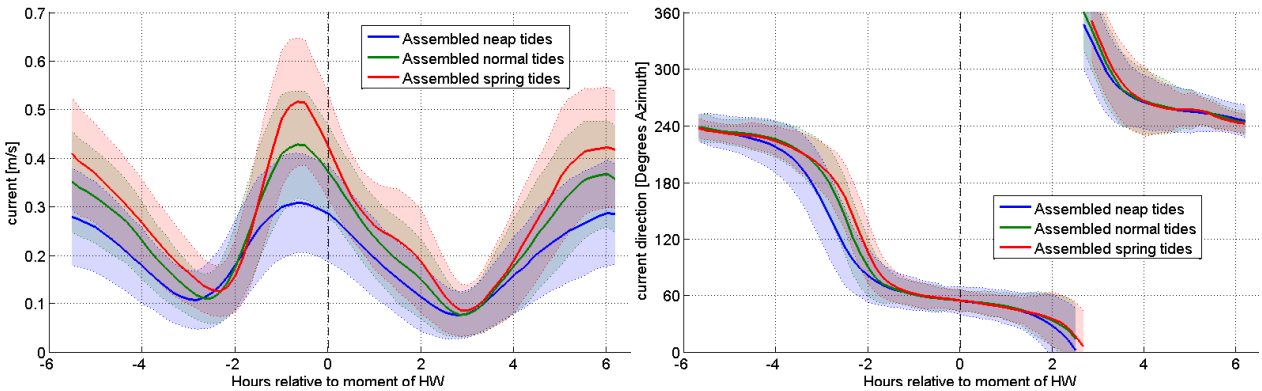

Figure 30 - Mean and standard deviation of the assembled ADV current velocity magnitude (left) and direction (right) ~0.2mab, WZbuoy, 158 tidal cycles from 10 deployments

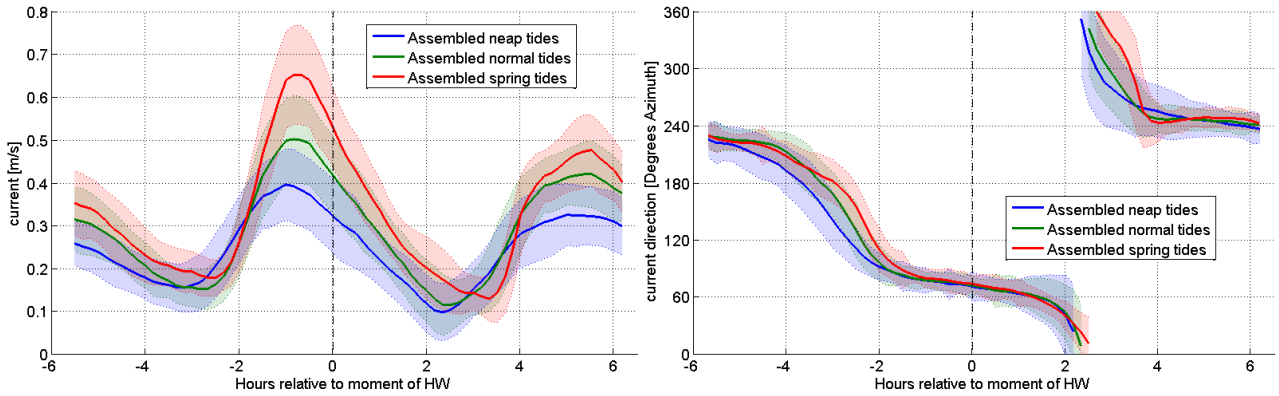

3.3.3 Current velocity at Blighbank and Gootebank - ADVOcean measurements ~0.2mab

The measurement sites Blighbank and Gootebank are at a distance of 48km and 21km from the coast, while Blankenberge, MOW1 and WZbuoy are relatively close to the coast (< 5km). Therefore the mean tidal current differs substantially from the ones discussed above. For these two locations only the ADVOcean measurements at 0.2mab are available at FHR.

Figure 31 - Mean and standard deviation of the assembled ADV current velocity magnitude (left) and direction (right) ~0.2mab, Blighbank, 27 tidal cycles from 2 deployments

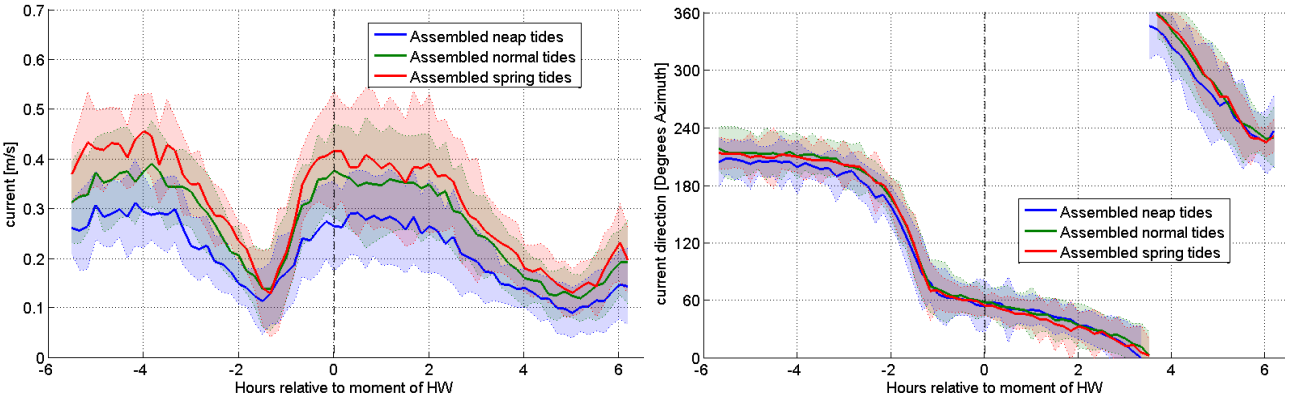

Figure 32 - Mean and standard deviation of the assembled ADV current velocity magnitude (left) and direction (right) ~0.2mab, Gootebank, 36 tidal cycles from 2 deployments

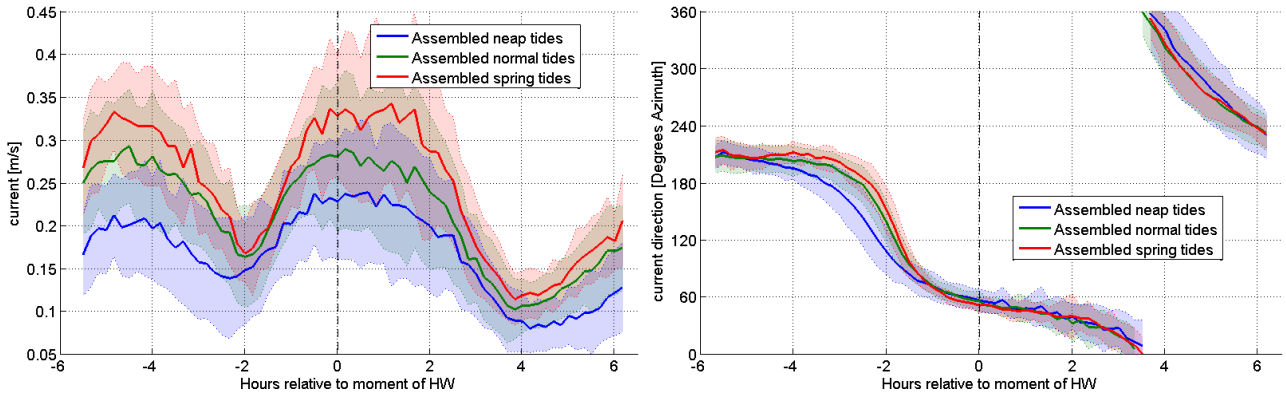

3.4 Wind effects

In Baeye et al. (2011), the relationship between subtidal alongshore flow and the alongshore wind component was studied for Blankenberge. The current and wind velocity vectors were decomposed into a cross-shore and an alongshore component. The alongshore axis is parallel to the coast, 65° Az. North, and is positive in the northeast direction. Baeye et al. (2011) reported quite high correlation between subtidal alongshore flow and the alongshore wind component for Blankenberge. It is thus assumed that a wind from the northeast can cause a negative subtidal alongshore velocity component, i.e. a residual flow towards the southwest whereas a wind from the south-west can cause a positive alongshore flow and thus a northeastward driven residual flow.

In this report, the analysis is carried out for other two locations, MOW1 and WZbuoy using ADP velocity at 1.9mab . For the completeness, the analysis for Blankenberge is also included.

In Figure 33 the wind roses at Vlakte van de Raan during the periods of valid ADP velocity measurements at Blankenberge, MOW1 and WZbuoy are presented. The overall wind climate based on 15-year data for the selected meteorological station has been already given in Figure 19. Notice that for this analysis it is not necessary to assemble the tides, therefore there is no restriction on the availability of the pressure data recorded by the SonTek 5MHz ADVOcean. For MOW1, more deployments are available for this analysis than in Section 3.3: the deployments marked with no(l) in the column (14) in Table 2 (Appendix A) are also included in this analysis. This is shown up in Figure 19 (top, middle) and Figure 33 (middle) where the wind roses for this location are slightly different.

Figure 33 - Wind statistics at Vlakte van de Raan (HMCZ) during valid ADP measurements at Blankenberge (left), MOW1 (middle) and WZbuoy (right)

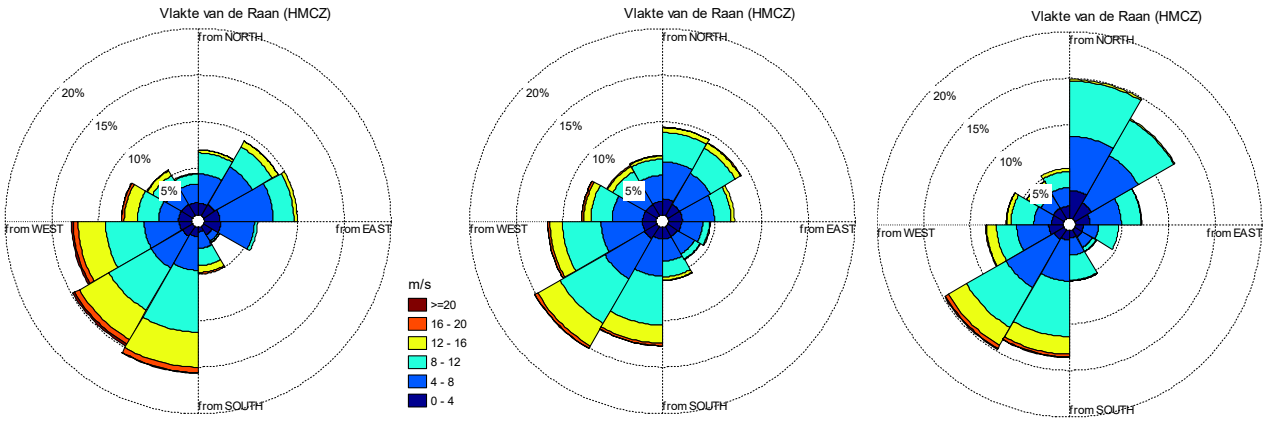

Figure 33 shows some resemblance of wind roses during Blankenberge, MOW1 and WZbuoy deployments with the most predominant wind coming from southwest and followed by the northeast direction. However, during the Blankenberge deployments strong wind coming from southwest occurred more often.

The similarities and differences in the wind climate during the deployments at the three sites are also noticeable in Figure 34 (left panel) which shows the probability density of the averaged alongshore wind component. For all measurement locations, about 60% of the time the alongshore wind component is from southwest direction (alongshore wind > 0). However, about 12% of the time the wind coming from SW and being higher than 10m/s is observed during the Blankenberge deployments, while only about half of that (~6%) is found during the MOW1 and WZbuoy deployments.

The probability density of the subtidal alongshore flow component (from SonTek ADP ~1.9mab) for the three measurement sites Blankenberge, MOW1 and WZbuoy is presented in Figure 34 (right panel). Although 60% of the time the wind blowing from the SW direction, the NE oriented subtidal alongshore flow accounts for

only about 30% of the time for Blankenberge. Other two locations, WZbuoy and MOW1 give smaller percentage (around 20%).

Figure 34 - Probability density distribution of the 12h25min-averaged alongshore wind component (Vlakte van de Raan, HMCZ) during ADP measurements (left panel) and subtidal alongshore current (ADP measurements ~1.9mab) (right panel). Top: Blankenberge, middle: MOW1 and bottom: WZbuoy

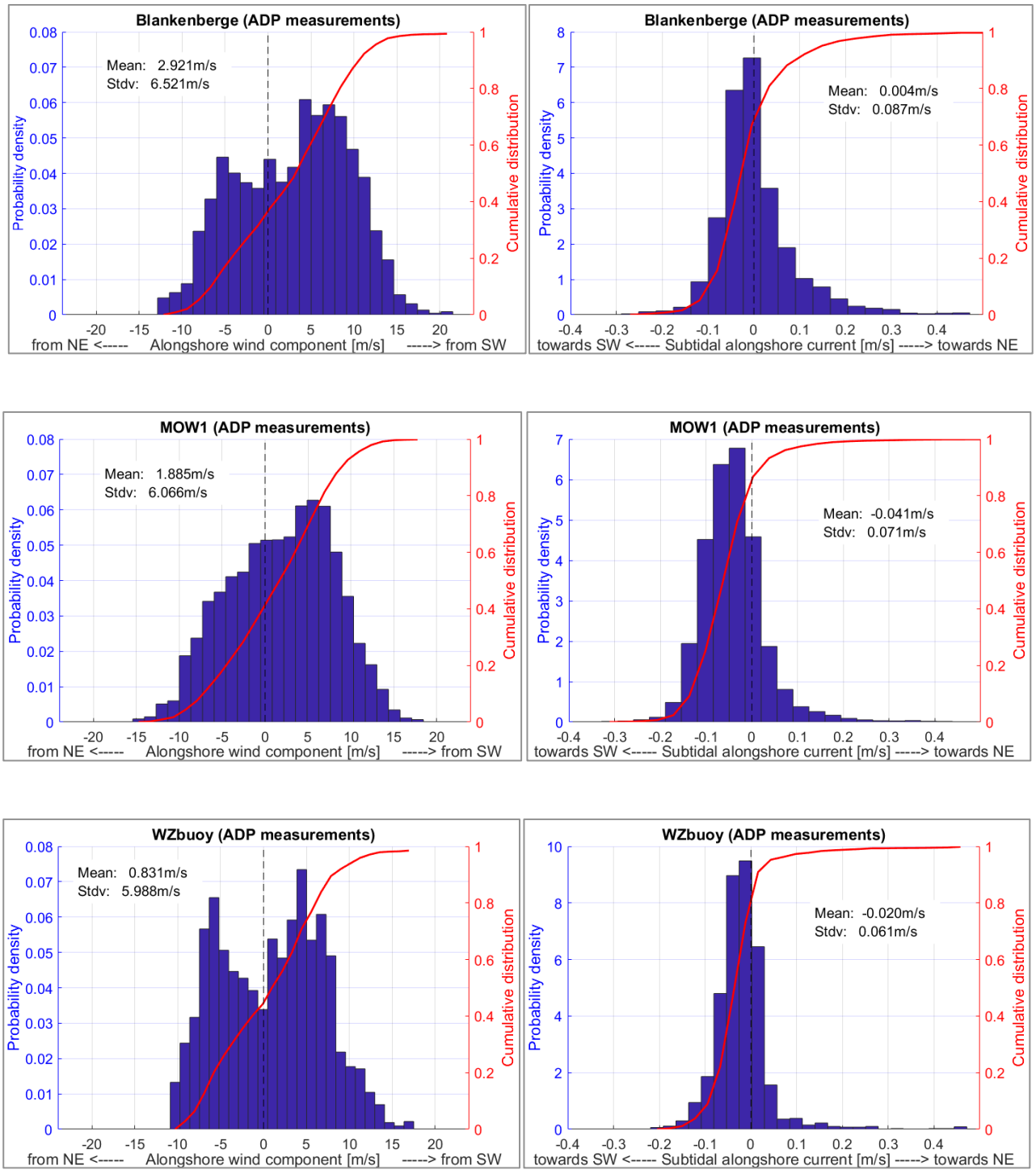

Figure 35 shows the correlation between the subtidal alongshore flow velocity component and the alongshore wind component for the measurement sites Blankenberge, MOW1 and WZbuoy. The subtidal alongshore flow component is determined by using a 12h25min moving average filter. The corresponding wind is obtained using the same averaging technique. The wind data is from the reference measurement station Vlakte Van De Raan.

There are some similarities in the relation of the subtidal alongshore flow velocity and the alongshore wind among the three locations. With little wind from SW or NE (-5m/s < alongshore wind < 5m/s) the flows are more tidally dominated and the subtidal currents are more directed to the SW. For wind blowing from the northeast (negative wind component), the dominant subtidal flow is towards the southwest (with negative alongshore current component). Stronger winds blowing from SW (>10m/s) cause more significant NE subtidal alongshore flow for all three locations.

This nonlinearity in the response of the subtidal alongshore current to the alongshore wind component is also apparent in the fact that a 3rd degree polynomial gives a demonstrably better fit than a linear relationship. The correlation between the alongshore flow velocity and alongshore wind component is also higher for station Blankenberge than for MOW1 and WZbuoy, which might due to the fact that Blankenberge is the shallowest measurement location. Therefore, the influence of the wind on the current at this location would be strongest. In addition, the higher proportion of the strong SW winds during its measurement periods presented above might also lead to this higher correlation.

Figure 35 - Correlation of (moving average 12h25min) subtidal alongshore flow (ADP measurements ~1.9mab) and alongshore wind component for the tripod deployments at Blankenberge (top), MOW1 (middle) and WZbuoy (bottom)

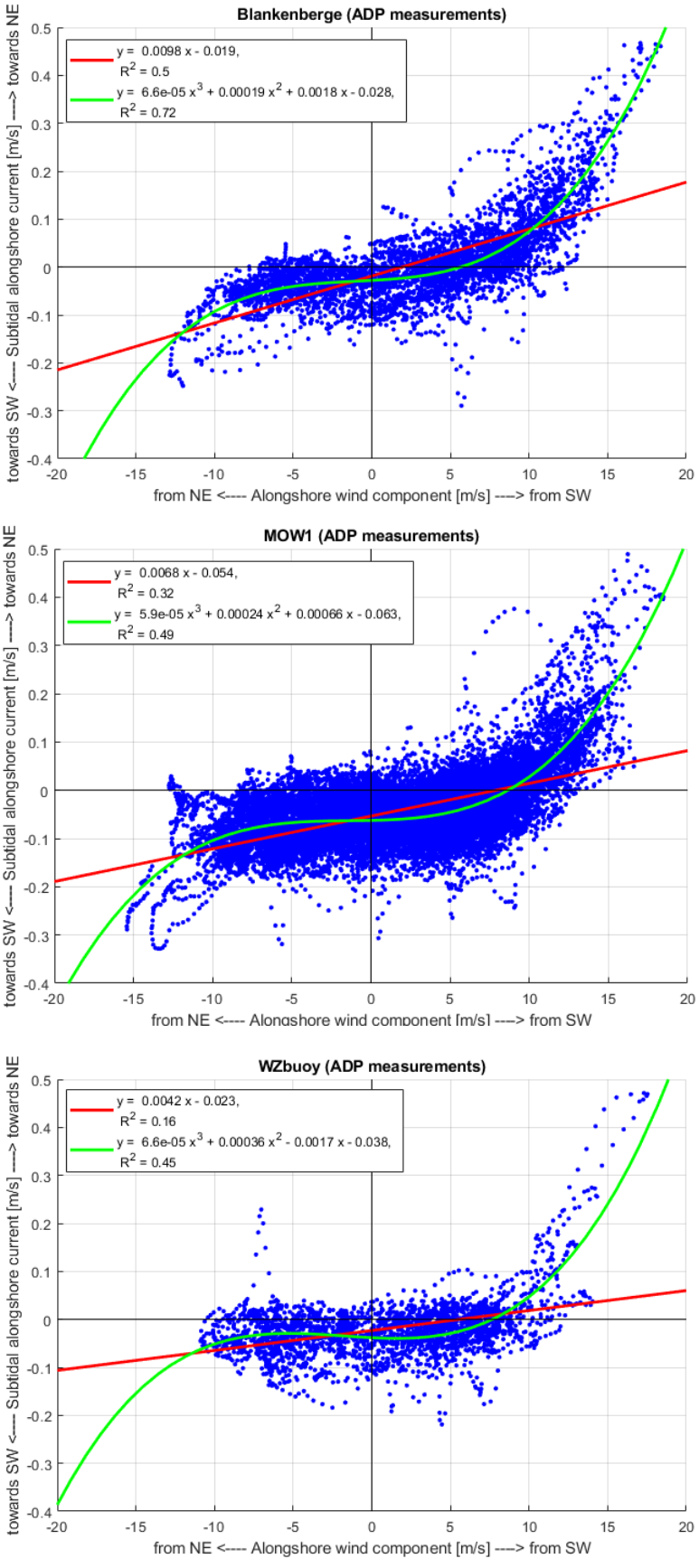

In the previous section it is observed that the tidal asymmetry in velocity is more pronounced for Blankenberge than for MOW1 and WZbuoy, with the strong maximum flood flow and the low maximum ebb, see Figure 23. It is suggested that near Blankenberge the currents will be influenced by the presence of the outer port of Zeebrugge. However, it is also noticed that higher percentages of strong southwest winds occurred during the tripod deployments at the Blankenberge site. As discussed above, these winds will result in a stronger flood flow and a weaker ebb flow.

In order to further investigate the influence of the wind on the alongshore flow, the alongshore wind component (moving average with window 1h) is used to filter the ensembles as shown in Figure 36, Figure 37 and Figure 38 for Blankenberge, MOW1 and WZbuoy, respectively. The blue lines represent the ensembles of the ADP velocity measurements when the low pass filtered alongshore winds are smaller than -5m/s (significant wind blowing from the northeast). The red lines is for the wind component larger than +5m/s, thus southwesterly winds.

For all locations, the effect of the wind on the flow is the most obvious for neap tides as the tidally influenced velocities are smallest, leading to the highest influence of the wind on the flow. The flood current is higher during the period with SW winds than with NE winds and an opposite trend is found for the ebb currents.

For MOW1 and WZbuoy, the effect of wind is quite comparable for flood and ebb current (Figure 37 and Figure 38). However, for the deployments at Blankenberge, the wind has very strong effect on the ebb flow for all tidal classes while limited effect on the flood flow (Figure 36). During periods with a strong southwesterly wind, the current at Blankenberge during maximum flood can be more than twice as strong as the maximum ebb (red line in Figure 36, right panel), whereas the flow could become nearly symmetric with the strong northeastern winds (blue line in Figure 36, left panel).

Figure 36 - Mean and standard deviation of the assembled ADP current velocity ~1.9mab at Blankenberge.
The ensembles are filtered for the alongshore wind components

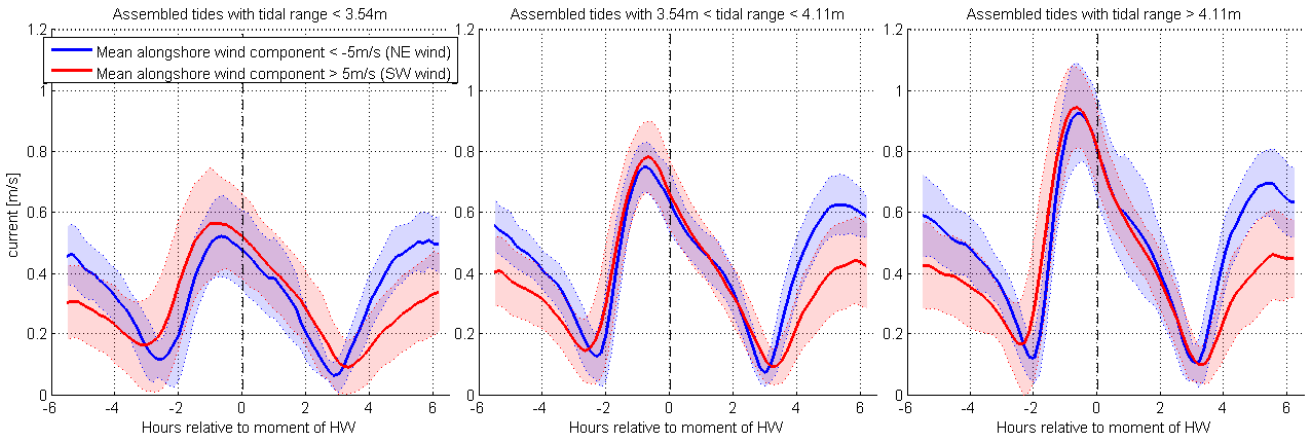

Figure 37 - Mean and standard deviation of the assembled ADP current velocity ~1.9mab at MOW1.
The ensembles are filtered for the alongshore wind components

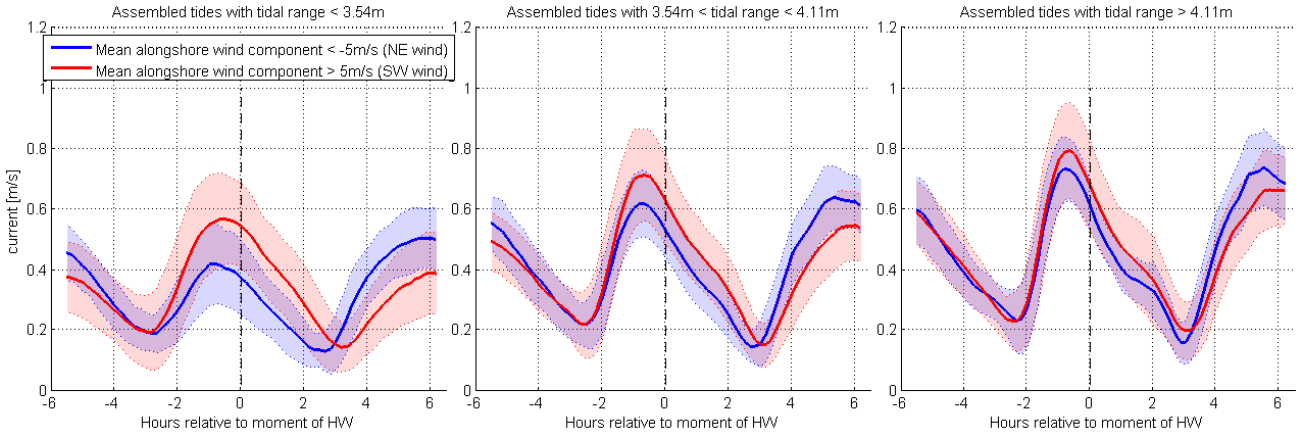

Figure 38 - Mean and standard deviation of the assembled ADP current velocity ~1.9mab at WZbuoy.
The ensembles are filtered for the alongshore wind components

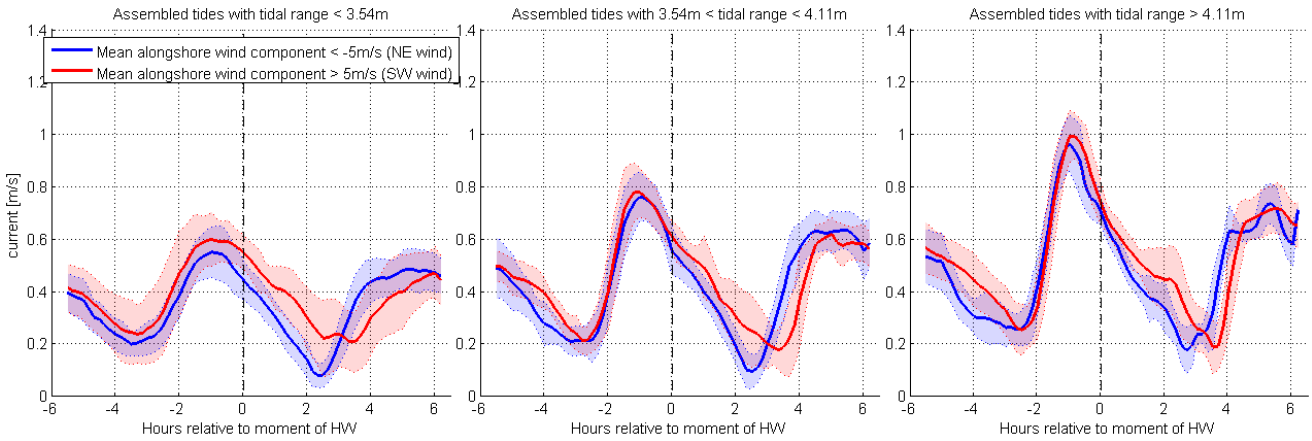

4 Analysis of suspended sediment concentrations

In this chapter, the analysis is performed for the available valid suspended sediment data, also referred as SPM[3]. This SPM data is assembled according to neap, normal and spring tides in the same way as for the velocity measurements in Section 3 but the median and 10^{th}-90^{th} percentile band are plotted instead of the mean and standard deviation. The deployment data selected for the construction of the combined ensembles of SPM is indicated in the columns (12) of Table 1, Table 2 and Table 3 (Appendix A). The plots of all assembled tides with SPM data points are shown in Appendix C.3, C.6, C.9 for Blankenberge, MOW1 and WZbuoy, respectively.

Figure 39 shows the wind climate during the OD Nature tripod deployments at Blankenberge, MOW1 and WZbuoy for which valid SPM and pressure (or depth) data is available. For station MOW1 and WZbuoy, the available valid SPM data is not exactly the same as the available deployments with valid current measurements (see the columns (12), (13), (14) of Table 1, Table 2 and Table 3 in Appendix A for the selection of deployments to construct combined ensembles). These differences in sampling periods explain why the wind roses below do not fully agree with those in Figure 19, although the differences are small.

Figure 39 - Wind statistics at Vlakte van de Raan (HMCZ) during OD Nature tripod deployments used for SPM data analyses near Blankenberge (left), MOW1 (middle) and WZbuoy (right)

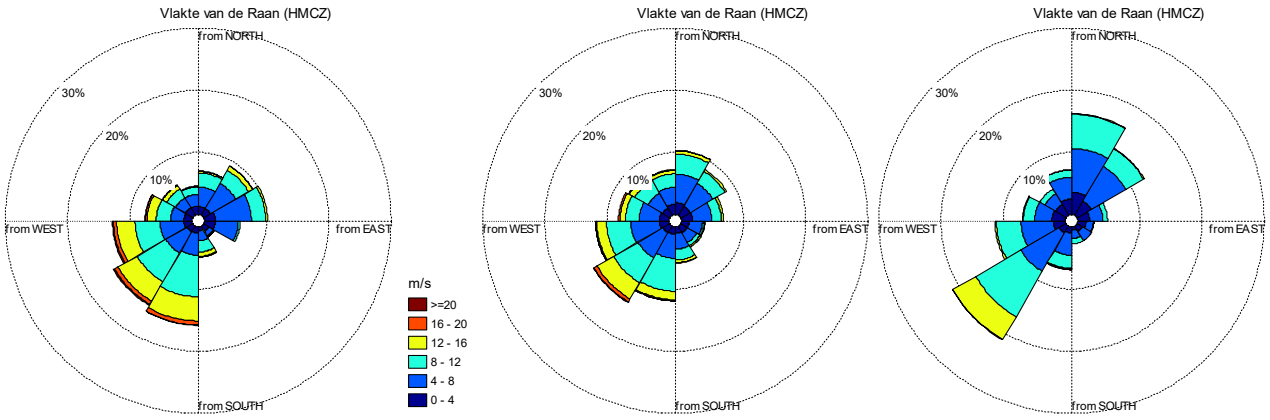

As presented in §2.1, the tripod is equipped with two optical backscatter sensors (OBS) at about 0.3mab and 2.3mab. In the text and the figures OBS_1 and SPM_1 refer to the lowest OBS sensor and OBS_2 and SPM_2 to the highest one. The exact position of the sensors might slightly differ between the deployments, see Table 1 to Table 6 in Appendix A. The deployments with the sensor positions outside the expected range are ignored in the analyses. For Blankenberge the exact height of the sensors was not reported for two deployments. It is assumed that these sensors were mounted at the same positions as the third deployment near Blankenberge in 2008.

[3] Suspended Particle Matter

4.1 Suspended sediment concentrations at Blankenberge, MOW1 and WZbuoy ~0.3mab.

Figure 40 shows the median and 10^{th}-90^{th} percentile band of suspended sediment concentrations at about 0.3mab for the locations Blankenberge, MOW1 and WZbuoy. As expected, the highest concentrations are generally obtained for spring tide and the lowest values for neap tide. The signal of tidal variation is observed in the ensemble plots with several concentration peaks and troughs.

The SPM concentration peaks are observed around 1.5h before high water and around low water (Figure 40) which are just before peak flood and peak ebb flow (see also the previous chapter). Another peak signal also appears at about 1 to 2hours after HW. This peak is evident for MOW1 for all tidal classes, whereas only obvious during spring tides for Blankenberge and spring/normal tides for WZbuoy. The peak around LW moments at MOW1 is much higher than other two peaks. Around the moments of slack tide (2-3h before and after HW), low suspended sediment concentrations are observed with the median value in the range of 100 to 300mg/l. It is noticed that very large P10 and P90 percentile band is calculated for all locations.

Although the tidal modulation of the concentrations is observed in the ensemble plots, it is much stronger in the time series plot in Figure 41 with high peaks and strong gradients. For an example tide in Figure 42, the concentration drops rapidly from 1400mg/l (about HW-1h) to less than 100mg/l as the tide falls. Also during rising phase of the tide, there is a dip of about 150mg/l around slack water. The rise and fall of the concentrations near the bottom are defined by a combination of bottom shear stresses for suspension, sedimentation speed and vertical turbulent mixture. The time series in Figure 41 and Figure 42 show that the processes of suspension and sedimentation can occur suddenly and quickly. One can assume that there is not only a natural variability in the amount of sediment that comes into suspension, but also a natural variability in the moment during the tidal cycle at which the most sediment comes into suspension or settles down again. This would explain why the OBS measurements show much stronger temporal variability in the time series plot (Figure 41, Figure 42) than in the ensemble plots (Figure 40).

In Appendix C all the ensembles are plotted together. From Figure 68, Figure 71 and Figure 75, it is observed that the median (P50) curve is much closer to the P10 curve than the P90 one. To estimate the frequency of appearance of the concentrations, the probability density functions of the SPM measurements are constructed. This is done for Blankenberge, MOW1 and WZbuoy as shown in Figure 43. It is noticed that very large proportion of the higher limit sediment concentration (˜1000 mg/l) is observed for WZbuoy (Figure 43, bottom panel). This is due to the limitation of the OBS used at this location which could not capture the concentration value (converted from turbidity) higher than 1000mg/l. This is also observed for MOW1 at the value of 1500 mg/l, but less pronounced. The red lines are lognormal fits. The modulus, median and mean values are also calculated. The modulus and median are significantly lower than the mean value for all three locations. It indicates that most of the time the SPM concentrations are significantly lower than the mean values.

The probability density plots in Figure 43 are based on all the measurement data used to construct ensembles, disregarding the moment of the data points during the tidal cycle. Therefore, they do not give any information at which moments during the tidal cycle the lower and higher values can be expected. Based on the lognormal fit, the probability density distributions are constructed for every time step of the ensemble tide without filtering for the tidal range in Figure 44. The probability density plots for the assembled neap, normal and spring tides are presented in Appendix D. It is clear that during slack tide, i.e. at around 2h30 before and 3h after high water, it is very likely to measure significantly lower suspended sediment concentrations.

Figure 40 - Median and 10-90th percentile band of the assembled SPM at ~0.3mab:
Blankenberge (top), MOW1 (middle), WZbuoy (bottom)

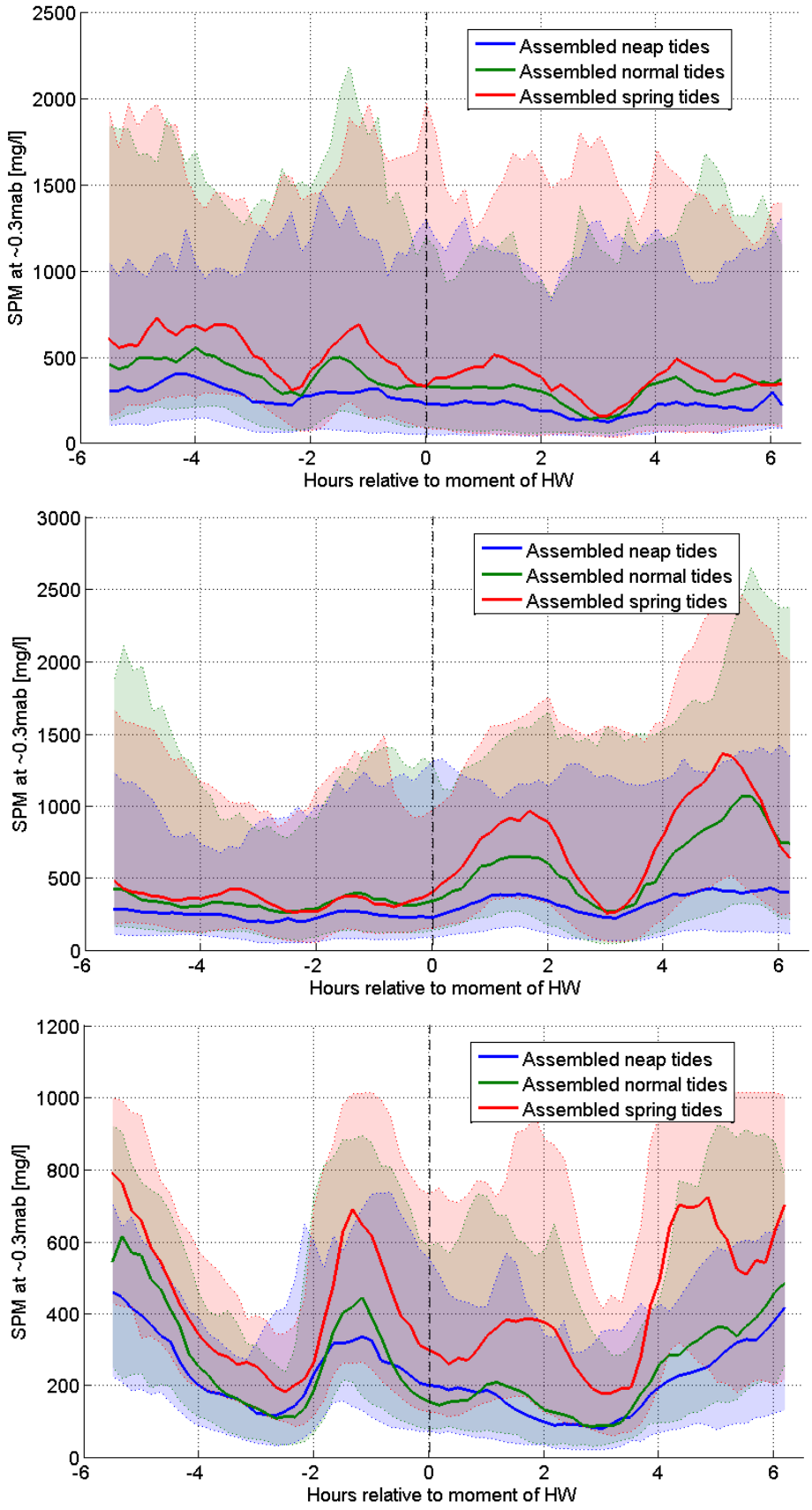

Figure 41 - OD Nature Tripod Deployment near Blankenberge January - February 2008.
Top: SPM concentrations at 0.3mab and 2.3mab [mg/l, bottom: pressure [dbar] (≈water depth in m)

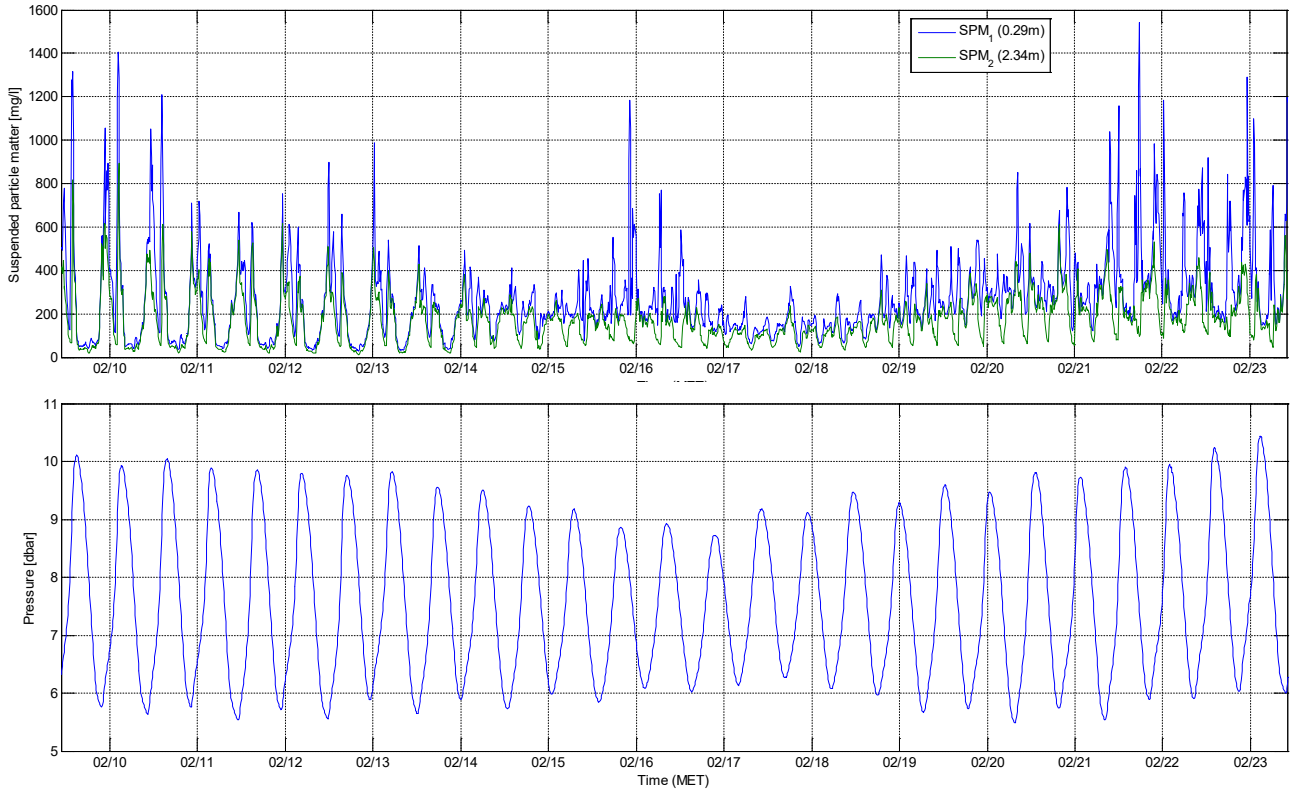

Figure 42 - Detailed zoom of one spring tide of Figure 41.
Left: SPM concentrations at 0.3mab and 2.3mab, right: water depth [m]

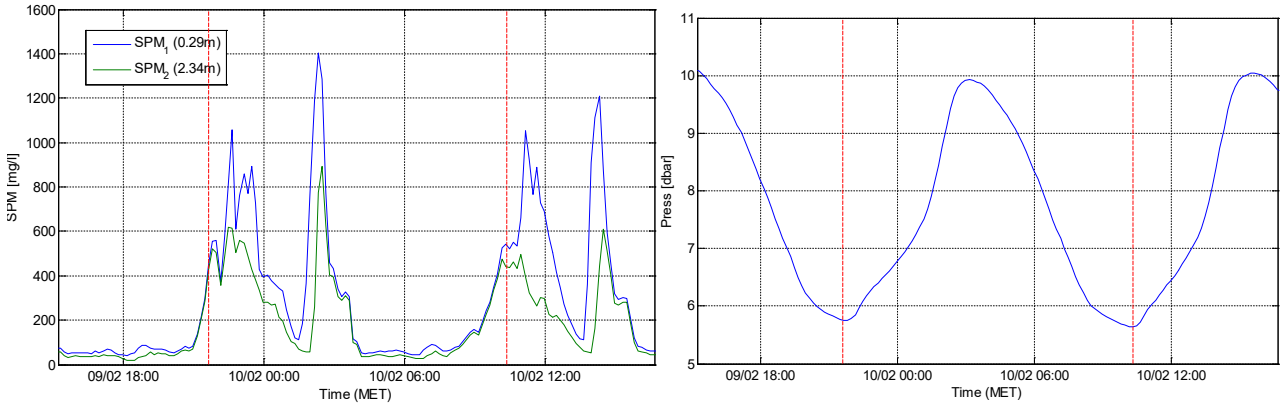

Figure 43 - Probability density of the assembled SPM concentrations [mg/l] at ~0.3mab:
Blankenberge (top), MOW1 (middle), WZbuoy (bottom)

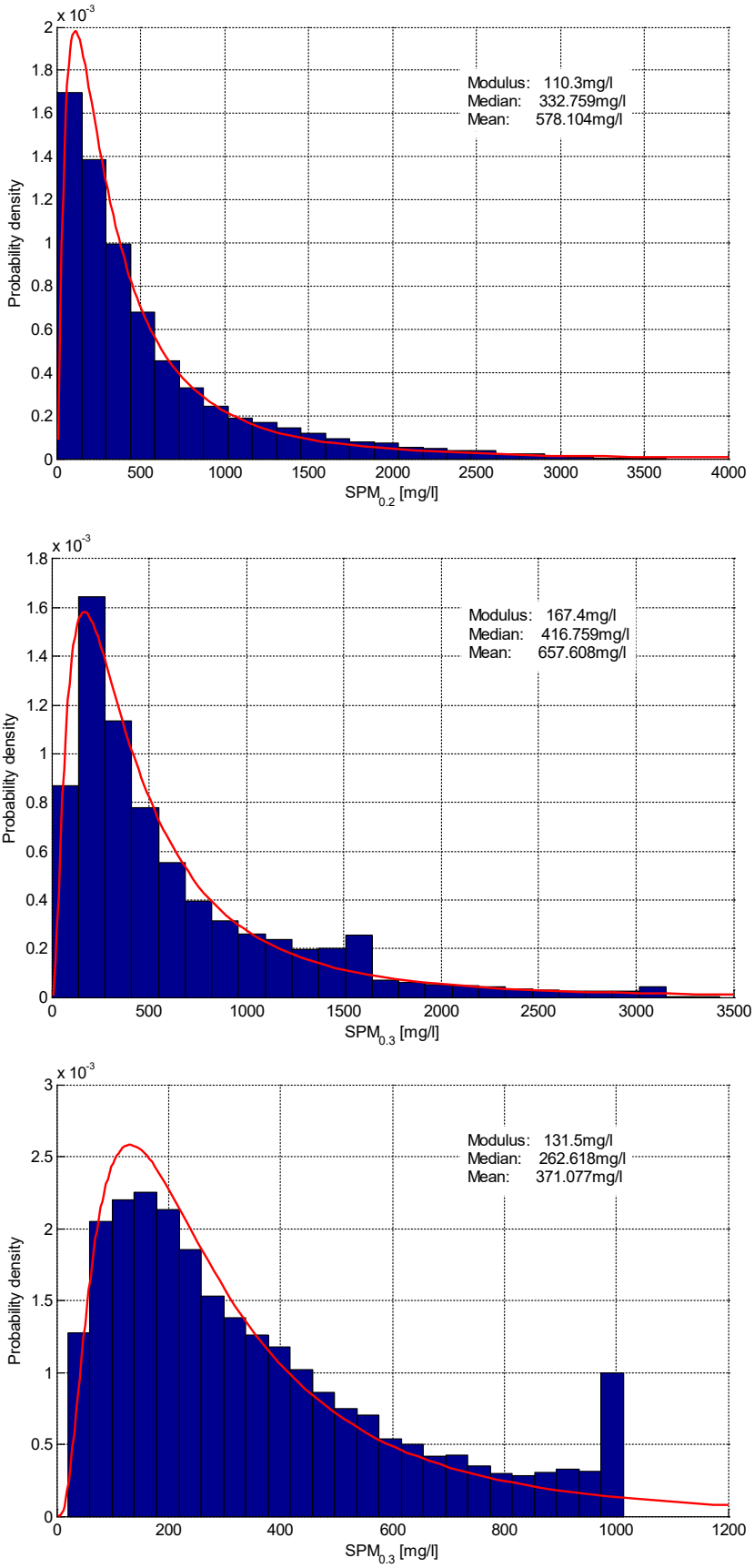

Figure 44 - Time dependent probability density of the assembled SPM [mg/l] at ~0.3mab:
Blankenberge (top), MOW1 (middle), WZbuoy (bottom)

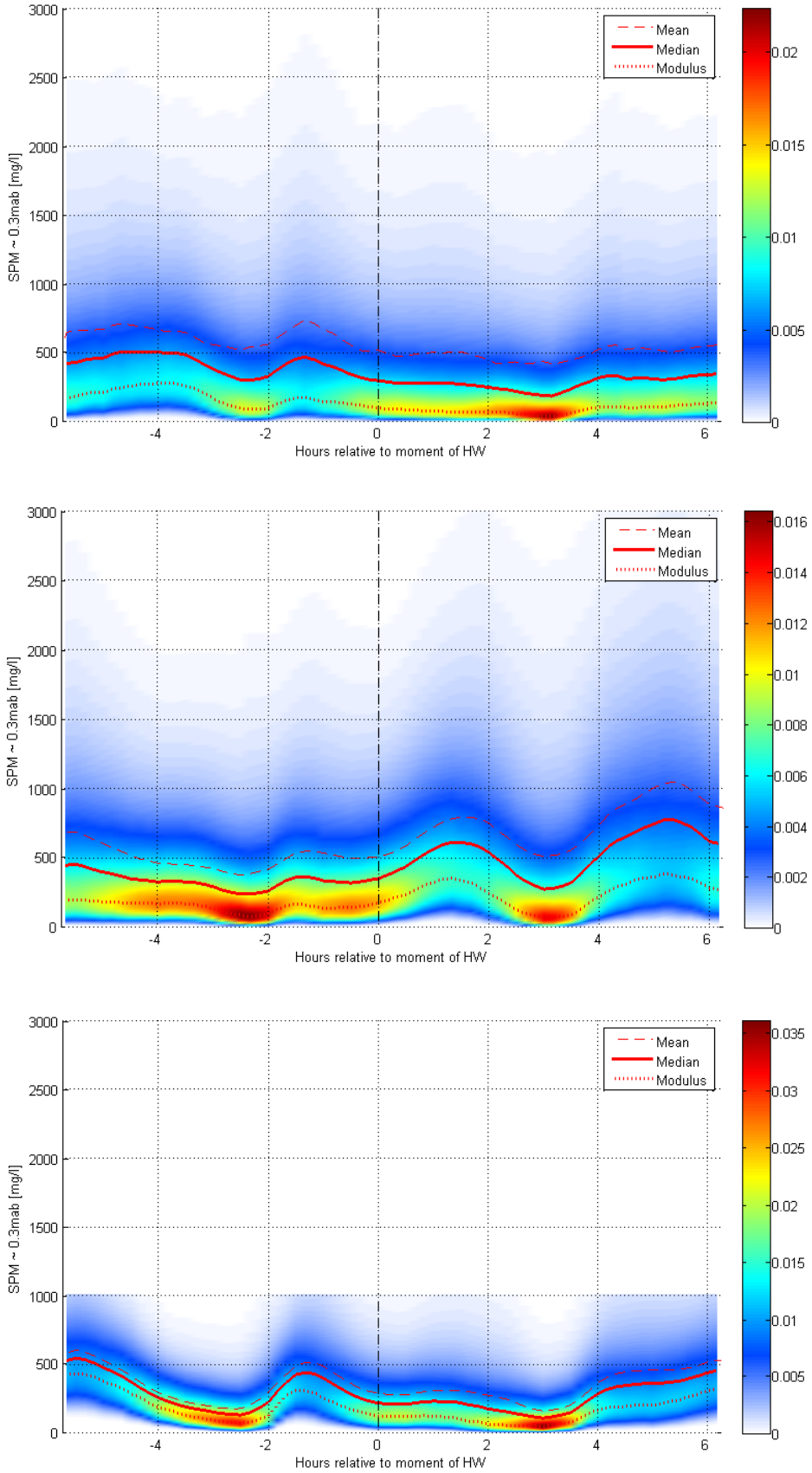

4.2 Suspended sediment concentrations at Blankenberge, MOW1 and WZbuoy ~2.3mab

Figure 45 presents the median and the P10-P90 percentile band of the suspended sediment concentrations at about 2.3mab during the assembled neap, normal and spring tides for the three locations Blankenberge, MOW1 and WZbuoy. The plots in Figure 45 are also combined in Figure 46 to make the comparison of SPM for the three locations easier. For Blankenberge the tidal variation is better observable at this height (i.e. 2.3mab) than at 0.3mab (Figure 40). Not only do the concentrations vary more strongly during the tidal cycle, but also the natural variability shows a clearer pattern (apparent in the percentile band around the median concentration).

The ensemble plot of SPM concentration at 2.3mab for Blankenberge (Figure 45 top panel) shows a quite similar pattern to that for WZbuoy (Figure 45 bottom panel), with concentration peaks during flood being slightly higher than or comparable to those during ebb. For Blankenberge the SPM concentration at 2.3mab peaks around 1h before high water and around low water (Figure 45 top panel) which are the moments of maximum flood and just after maximum ebb (see also the previous chapter). The concentration peaks during flood at WZbuoy occur about 0.5h earlier than at Blankenberge (Figure 46) which is mainly related to the earlier flood peak velocity for WZbuoy (Figure 23).

Although the distance between locations MOW1 and Blankenberge or WZbuoy is only 4-5km and the tidal currents at these sites are quite comparable (see Figure 23), the SPM concentration at MOW1 has a different tidal response than at Blankenberge or WZbuoy (Figure 45 and Figure 46). For the measurement site MOW1 the highest concentrations occur just before low water during maximum ebb. For normal and spring tides these concentration peaks are about 1.5 times higher than the corresponding peak concentrations near Blankenberge and WZbuoy. A second peak occurs at 0.5-1h after HW, which is about 1.5 hours after the maximum flood flow. Around the moment of the peak flood current, there are also peak signals in concentrations but not as pronounced.

The relation between the sediment concentration and the current velocity is more visible if plotting the mean tidal ellipse as in Figure 24, Figure 25 and Figure 26 but now with the colour scale for the mean sediment concentrations. This is done in Figure 47 for the all tidal classes. The mean tidal ellipses for the assembled spring, normal and neap tides are shown in Appendix E.

When comparing the tidal variation of the suspended sediment ~2.3mab in Figure 46 with the tidal currents ~1.9mab in Figure 23, we observe that at Blankenberge and WZbuoy, the maximum flood velocity is significantly higher than the maximum ebb flow, but the concentration peaks during flood are only slightly higher than those during ebb or even comparable. For MOW1, the maximum ebb flow is comparable to or slightly smaller than the maximum flood but the suspended sediment concentrations are significantly higher during ebb than during flood. These might partly due to the fact that at these three locations, the tidal range is large compared to the water depth. Therefore the relative difference in water levels is large between low and high water. Therefore the suspended sediment mixes in a smaller water column during low water, and thus the concentrations will be higher. In addition, Baeye et al. (2011) indicated that local resuspension of SPM is more important during flood whereas during ebb the sediment concentration is significantly influenced by advection. The advection of sediment from higher turbid region in the NE of the measurement sites and Scheldt estuary during ebb phase would lead to an increase of SPM concentration at the three locations.

Another reason might be related to the smaller current velocity at HW slack than at LW slack (see Figure 23), leading to longer time for sediment settling down around HW slack than around LW slack. As a result, more sediments are accumulated on the bed after HW slack, thus more sediments are available for being eroded during the ebb phase than flood phase (Fettweis pers. comm.). This hypothesis is true for MOW1 with a very high peak in the altimetry signal at about 3.5-4h before LW (i.e. around HW slack) (see Fettweis et al., 2015). However, the study of Baeye et al. (2011) shows for Blankenberge that the high peak in the altimetry signal occurs during LW slack most of the time. For WZbuoy, this is not obvious with more stable bed level during

tidal cycle and the accumulation of the sediment in the bed during HW slack and LW slack is comparable (Fettweis et al., 2015).

Even though the concentrations show different behaviour, the median concentrations around slack water (~2h before and 3h after high water) drop to more or less the same minimum value of 50-100mg/l for all locations. This has been also noted in the previous section for the concentrations at ~0.3mab. The probability density graphs in Figure 49 show that during slack water the natural variability for the three sites is low as well. One can assume that during slack water most suspended sediment settles down, except for some background concentration between 50 and 100mg/l which consists of the finest fraction that hardly settles.

Figure 45 - Median and 10-90th percentile band of the assembled SPM ~2.3mab:
Blankenberge (top), MOW1 (middle), WZbuoy (bottom)

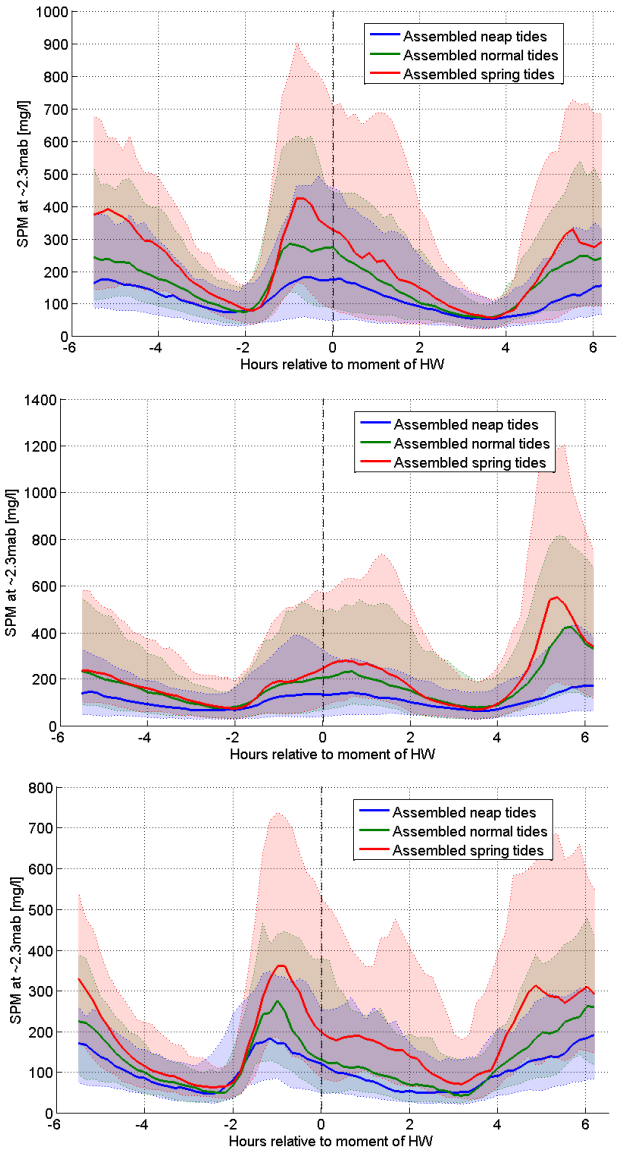

Figure 46 - Median and 10-90th percentile band of the assembled SPM at Blankenberge, MOW1 and WZbuoy ~2.3mab.
Left: neap tides, middle: normal tides, right: spring tides

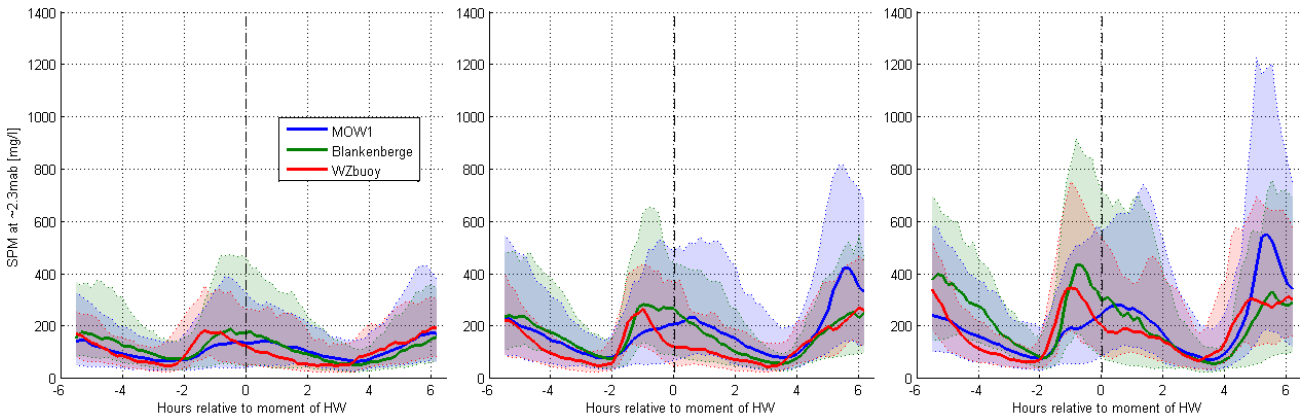

Figure 47 - Tidal ellipse with SPM colour scale, ADP velocity ~1.9mab, SPM ~2.3mab:
Blankenberge (top), MOW1 (middle), WZbuoy (bottom)

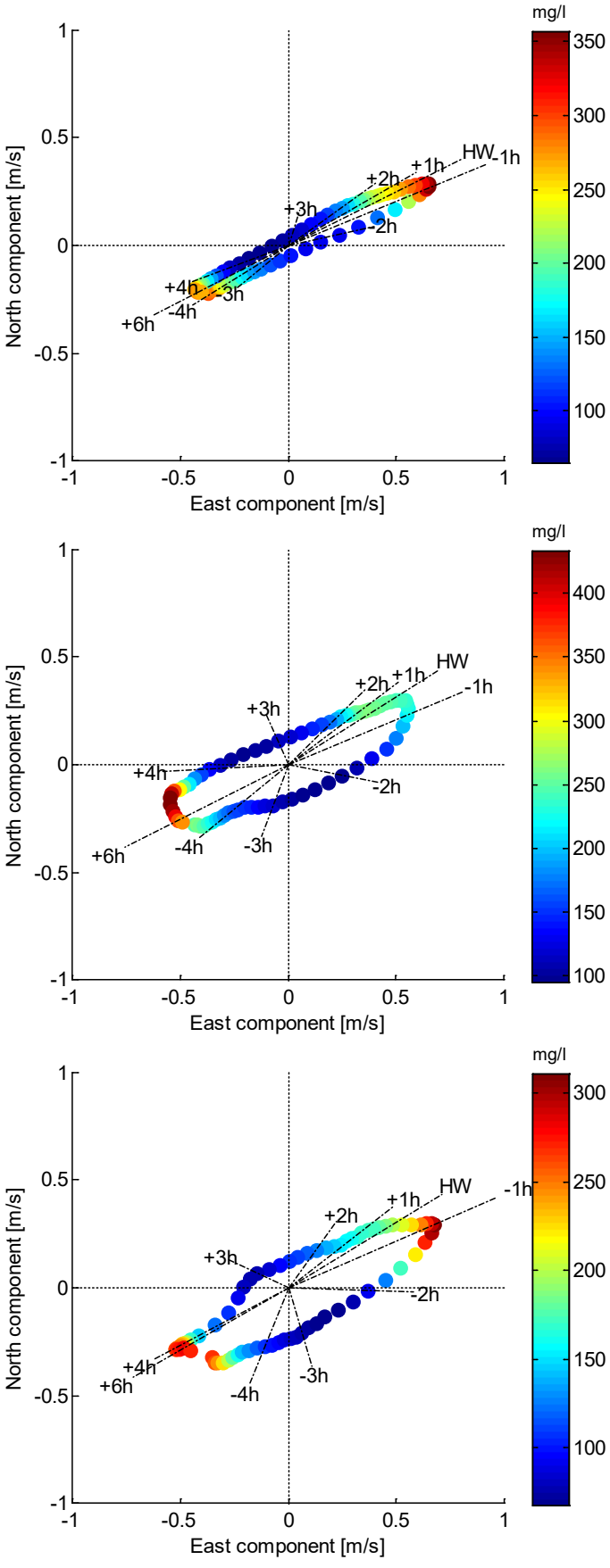

Figure 48 - Probability density of the assembled SPM concentrations at ~2.3mab:
Blankenberge (top), MOW1 (middle), WZbuoy (bottom)

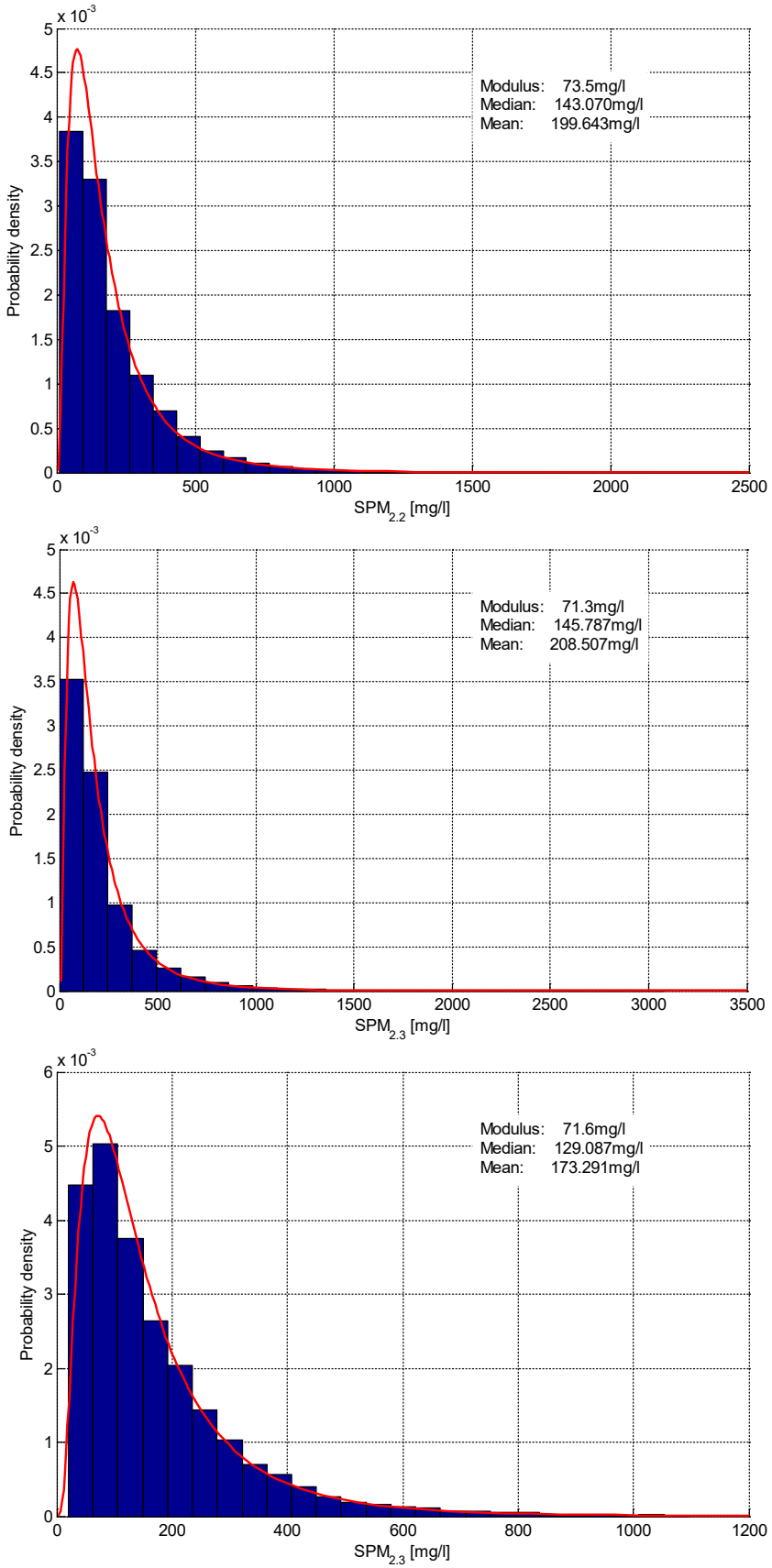

Figure 49 - Time dependent probability density of the assembled SPM [mg/l] at ~2.3mab:
Blankenberge (top), MOW1 (middle), WZbuoy (bottom)

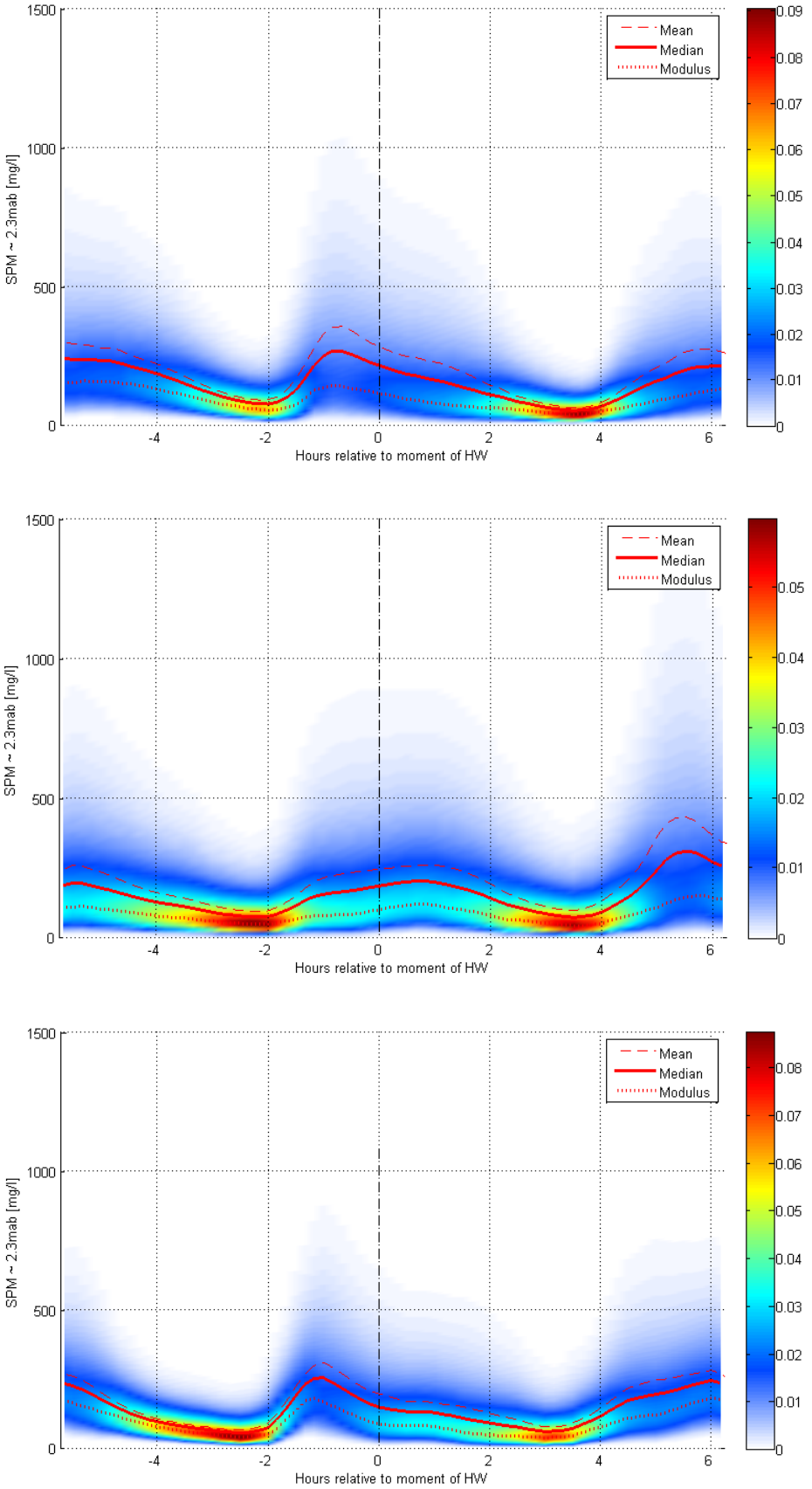

4.3 Concentration profile and sediment mixing condition

Under stationary flow and under the assumption of a constant settling velocity and a parabolic dispersion coefficient profile, the vertical suspended concentration profile can be described by the Rouse equation:

$$c_z = c_a \left(\frac{h - z}{z} . \frac{a}{h - a} \right)^{Ro} \tag{3}$$

$$Ro = \frac{w_s}{\beta \kappa u_*} \tag{4}$$

with: c_z: suspended concentration at a height z above the bed

c_a: reference concentration at the reference height a above the bed

h: water depth

Ro: Rouse number

w_s: settling velocity

β: coefficient relating mass and momentum transfer (β = 1 for fine sediments)

κ: von Karman's constant (κ = 0.4 for clear water)

u_*: shear velocity

The Rouse number is the ratio of the downward settling of the sediment to upward turbulence strength. It determines the shape of the concentration profile as seen in Figure 50. A high value of Ro leads to a high concentration gradient over the water column. In contrast, a smaller Ro corresponds a higher homogeneity of suspended sediment over the depth. The water column is perfectly mixed when Ro approaches zero. A negative Ro would imply an inverse. Therefore, Rouse number can be used to evaluate the mixing condition of sediment in the water column. Note that the Rouse profile theoretically predicts a zero concentration at the surface of the water column.

Figure 50 - Relative concentration vs. relative vertical distance from the bed for different values of Rouse number (after Bridge & Demicco, 2008)

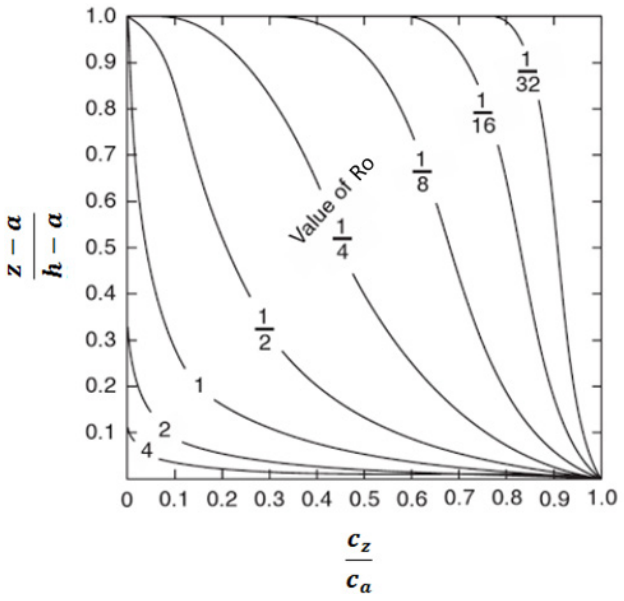

Having simultaneously measured data for suspended sediment concentration at two different heights, $z_2>z_1$, one has:

$$c_{z_1} = c_a\left(\frac{h - z_1}{z_1}.\frac{a}{h - a}\right)^{Ro} \quad (5)$$

$$\Rightarrow \quad \ln c_{z_1} = \ln c_a + Ro.\ln\left(\frac{h - z_1}{z_1}.\frac{a}{h - a}\right) \quad (6)$$

$$\Rightarrow \quad \ln c_{z_1} = \ln c_a + Ro.\ln\frac{h-z_1}{z_1} + Ro.\ln\frac{a}{h-a} \quad (7)$$

Similarity for the height z_2:

$$\ln c_{z_2} = \ln c_a + Ro.\ln\frac{h-z_2}{z_2} + Ro.\ln\frac{a}{h-a} \quad (8)$$

Subtract equation (7) to equation (8), one has:

$$\ln c_{z_1} - \ln c_{z_2} = Ro.\ln\frac{h - z_1}{z_1} - Ro.\ln\frac{h - z_2}{z_2} \quad (9)$$

$$\Rightarrow \quad \ln\frac{c_{z_1}}{c_{z_2}} = Ro.\ln\left(\frac{h - z_1}{h - z_2}.\frac{z_2}{z_1}\right) \quad (10)$$

$$\Rightarrow \quad Ro = \frac{\ln\frac{c_{z_1}}{c_{z_2}}}{\ln\left(\frac{h - z_1}{h - z_2}.\frac{z_2}{z_1}\right)} \quad (11)$$

Given water depth h, measured heights z_1, z_2 and concentration at two heights c_{z_1}, c_{z_2}, Rouse number Ro can be calculated following Equation (11) and mixing condition of sediment in the water column can be evaluated as above. Note that we're calculating the Rouse number merely as an indication of the vertical gradient strength.

Figure 51 presents for the assembled neap, normal and spring tides the variation of the median and P10-P90 percentile band of Rouse number for Blankenberge and MOW1. Due to the high proportion of the cut off of SPM concentrations (at the value of ~1000 mg/l) at the sensor 0.3mab for WZbuoy (see Figure 43), the Ro number for this location will be affected and therefore not shown here. The mean tidal ellipses with the Rouse number as colour scale are plotted Figure 52.

The Ro number for Blankenberge and MOW1 shows quite regular pattern as seen in Figure 51 and Figure 52. As expected, a lower Rouse number (i.e. water column is better mixed) is calculated during strong flow condition as the result of high turbulent mixing, while higher Rouse number (more stratified water column) around slack tide due to settling.

The mean Ro number for Blankenberge varies from 0.15 (i.e. well mixed) to 0.62 (strongly stratified). The range of about [0.3-0.75] is calculated for MOW1. Low values appear at strong flow moments around HW and LW and high values are at about 1.5-2h before HW and around 4h after HW which are right after LW-slack and HW-slack, respectively (see Figure 23 the velocity plot). For MOW1, the water column is more stratified (higher Rouse) during HW-slack than during LW-slack (Figure 51, right).

Figure 51 - Median and 10-90th percentile band of the assembled Rouse number for Blankenberge (left) and MOW1 (right)

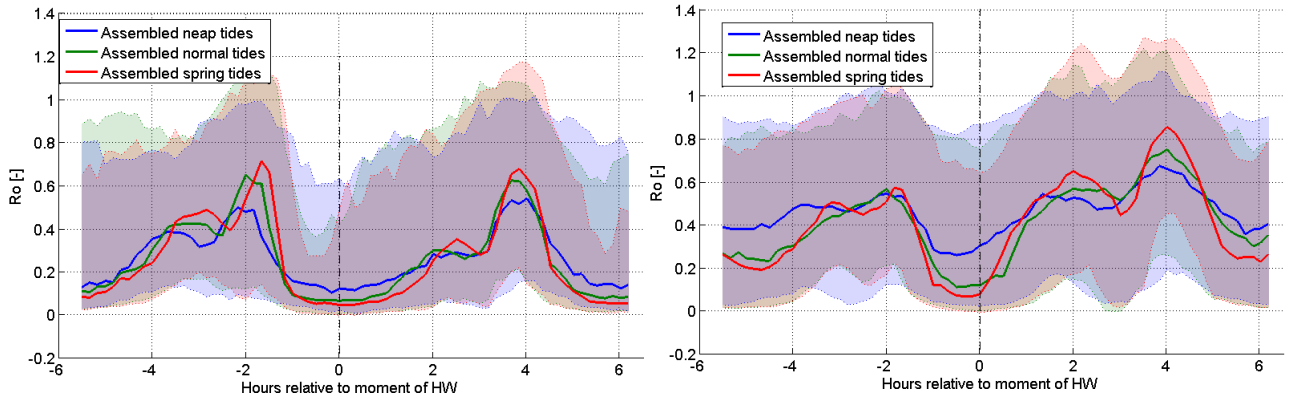

Figure 52 - Tidal ellipse with Rouse number colour scale, ADP velocity ~1.9mab for Blankenberge (left) and MOW1 (right)

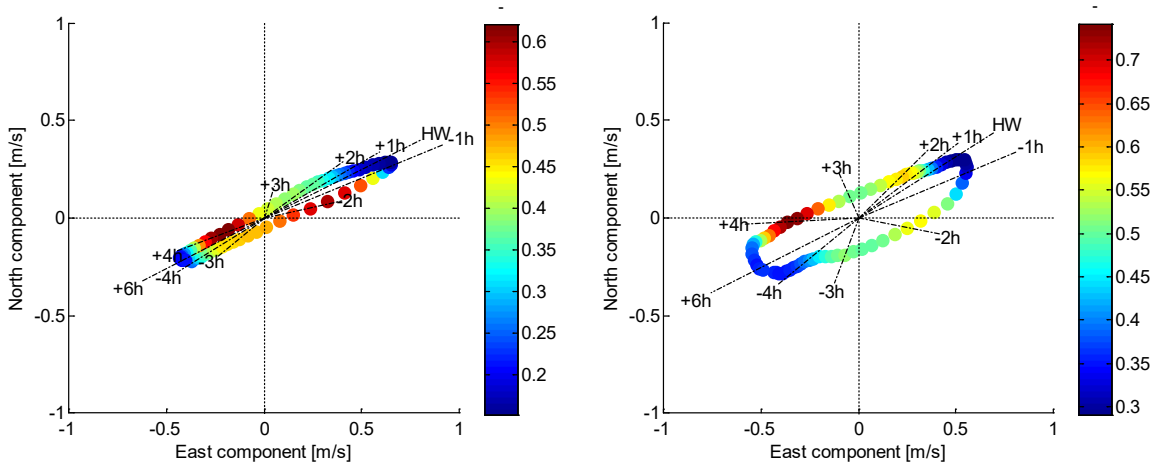

4.4 Correlation between the subtidal alongshore current and SSC

In Section 3.4 it has been already discussed how strong alongshore wind components can cause subtidal alongshore flows. The effects are stronger for the Blankenberge site than for the MOW1 and WZbuoy sites. In Baeye et al. (2011) it is argued that northeastward residual flows, i.e. driven by south-west winds, can transport water from the English Channel with lower sediment concentrations to the Belgian coast resulting in a lower coastal turbidity maximum. In this section, the subtidal alongshore flow component is used as a filter to assemble the tides.

Figure 53, Figure 54 and Figure 55 show the filtered ensembles for the SPM data according to subtidal alongshore currents (u_a) near Blankenberge, MOW1 and WZbuoy. The value u_a<-5cm/s represents the southwestward subtidal currents while the northeastern ones are the case with u_a>5cm/s.

For Blankenberge the southwestward subtidal currents (u_a<-5cm/s) generally result in significantly higher sediment concentrations than the northeastern ones (u_a>5cm/s) (Figure 53), which is in line with Baeye et al. (2011). However, the data retrieved from the OD Nature tripod deployments at WZbuoy and MOW1 does not seem to confirm this hypothesis as this is only true during the ebb phase (Figure 54 and Figure 55). During flood phase the northeastward residual flows (u_a>5cm/s) generally cause higher SPM concentration than southwestward currents do, although the effect is limited for MOW1. The observation for WZbuoy and MOW1 agrees with the conclusion in the study of Fettweis et al., (2015) for the data during the year 2013 at these two locations that the SPM concentrations are higher if the current is in the same direction as the

residual alongshore flow. Thus, during low tide, the higher sediment concentrations are observed for SW-directed subtidal currents while during high tide SPM is higher for NE-directed subtidal alongshore currents.

Figure 53 - Median and 10-90th percentile band of the assembled SPM ~2.3mab at Blankenberge filtered for subtidal alongshore currents for neap tides (left), normal tides (middle), spring tides (right)

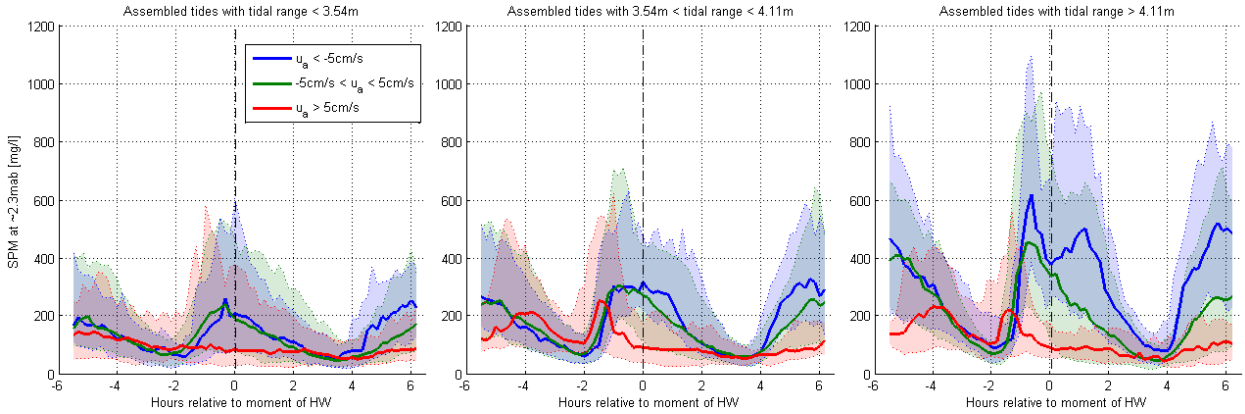

Figure 54 - Median and standard deviation of the assembled SPM ~2.3mab at MOW1 filtered for subtidal alongshore currents for neap tides (left), normal tides (middle), spring tides (right)

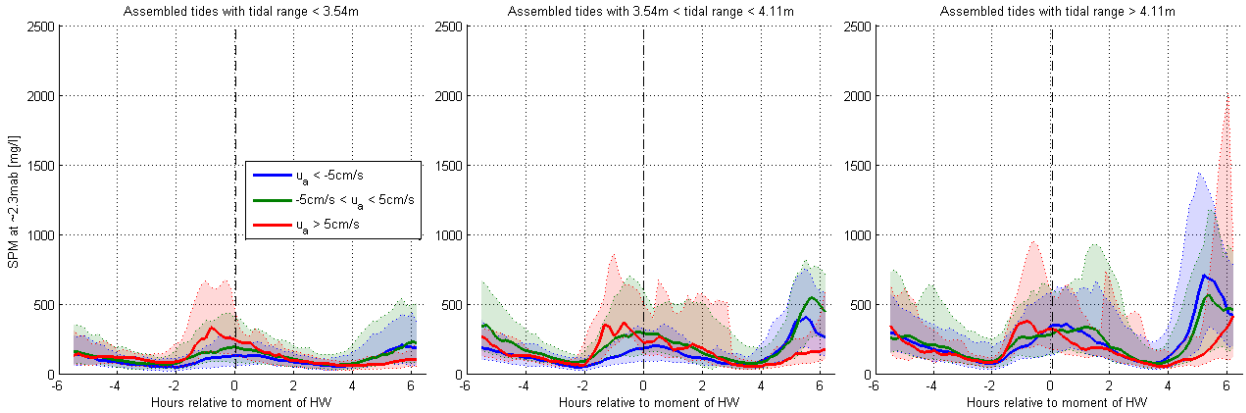

Figure 55 - Median and 10-90th percentile band of the assembled SPM ~2.3mab WZbuoy filtered for subtidal alongshore currents for neap tides (left), normal tides (middle), spring tides (right)

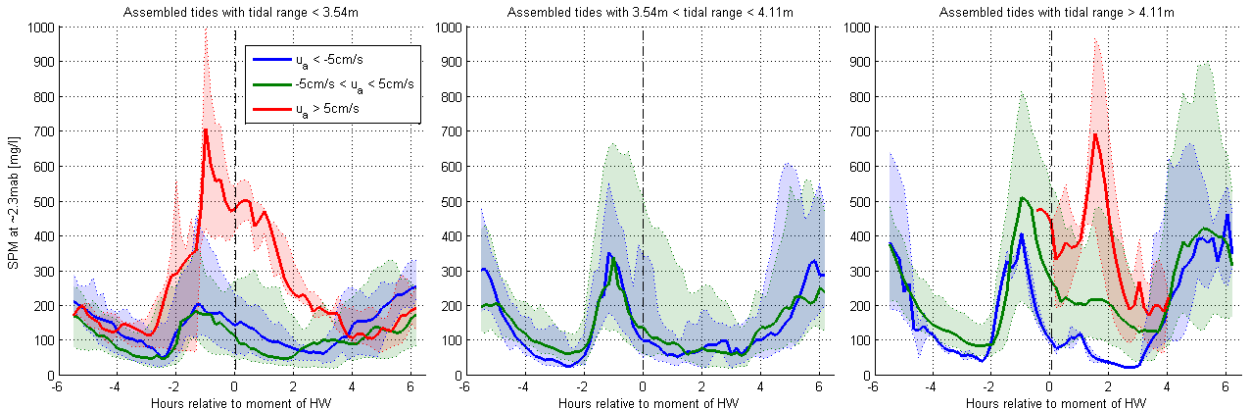

In Figure 56, Figure 57, and Figure 58 the hourly mean alongshore wind component is used to filter the ensembles for the three locations. For station MOW1 and WZbuoy, the sediment concentrations are only slightly affected by the alongshore wind component. Some clear effects are only noticed for spring tide for station Blankenberge.

Figure 56 - Median and 10-90th percentile band of the assembled SPM at 2.3mab (lower), Blankenberge filtered for the alongshore wind for neap tides (left), normal tides (middle), spring tides (right)

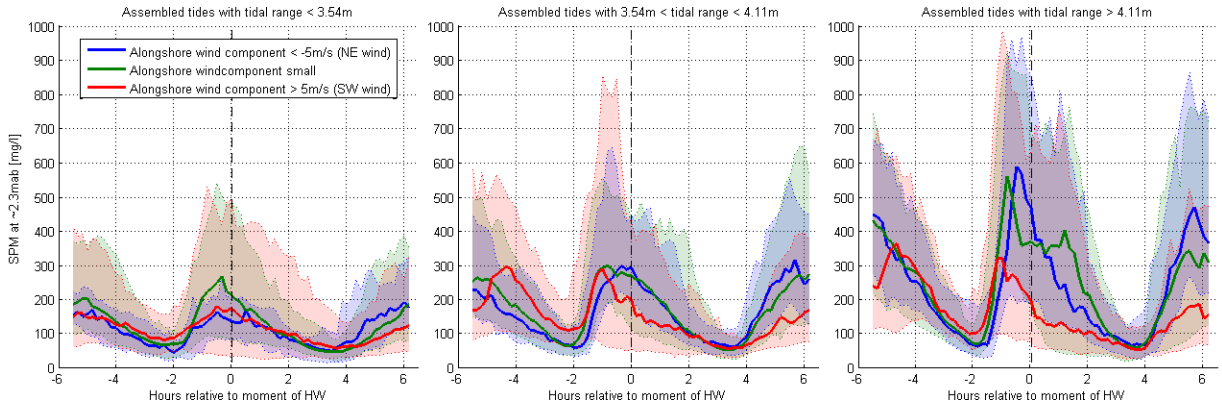

Figure 57 - Mean and standard deviation of the assembled SPM [mg/l] at 2.3mab (lower), MOW1 filtered for the alongshore wind for neap tides (left), normal tides (middle), spring tides (right)

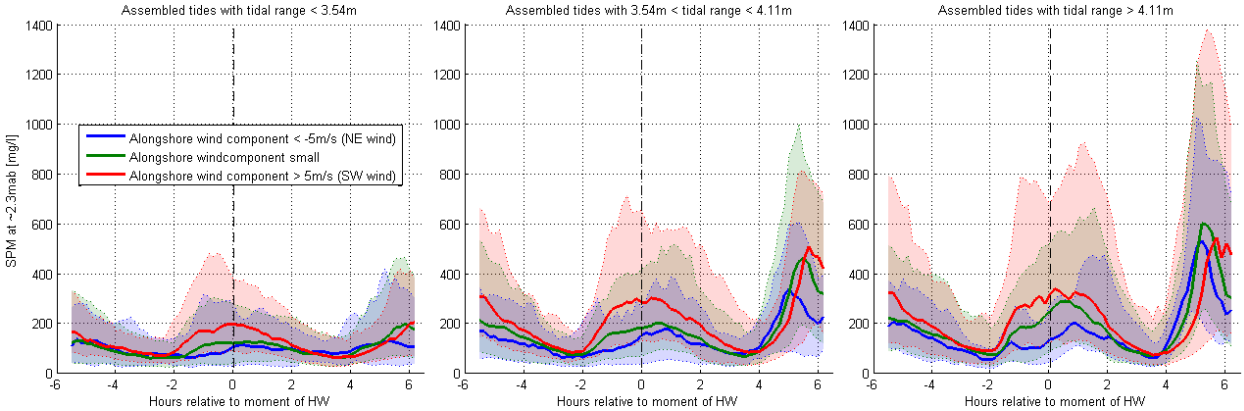

Figure 58 - Median and 10-90th percentile band of the assembled SPM [mg/l] at 2.3mab (lower), WZbuoy filtered for the alongshore wind for neap tides (left), normal tides (middle), spring tides (right)

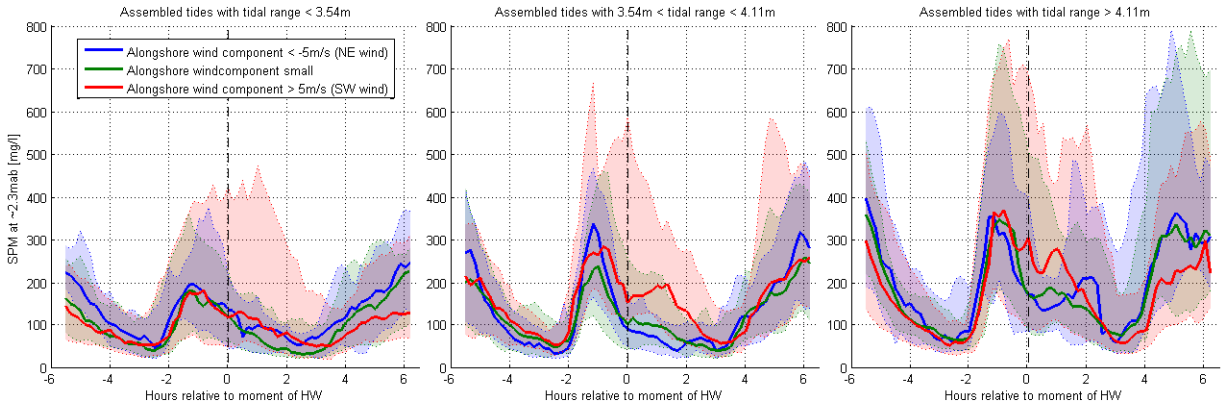

Notice that when comparing to Figure 36, Figure 37 and Figure 38 in Section 3.4 the variation in sediment concentrations cannot be explained by the direct wind effects on the currents. If the variation of the sediment concentrations due to wind effects would be related to wind induced large scale residual flows, one would expect that the deployment sites MOW1 and Blankenberge would show some similar response to the variation of the subtidal flow since they are only located less than 4km from each other. However, one would jump to conclusions saying that the hypothesis of the wind induced residual flows does not hold at all.

The Belgian near-shore area is characterized by a turbidity maximum ranging from Oostende till the mouth of the Watershed and with the port of Zeebrugge located in the center of it. Oostende is about 20km southeast of the measurement locations Blankenberge and MOW1 and the distance to the English Channel is about 100km. In the previous section it was demonstrated that positive residual flows only occur with sufficiently high alongshore wind speeds and residual flows of more than 10cm/s are quite rare. This means that in order to get some fresh water from the English Channel to the locations of the tripod deployments, the prevailing south-west wind must hold for multiple days. As an example the frequencies of the alongshore seven day mean wind velocities during the Blankenberge, MOW1 and WZbuoy deployments are presented in Figure 59. The higher values appear more frequently for the Blankenberge deployments. This might indicate more chance of fresh water from English Channel entering to the measurement sites during the deployments near Blankenberge than the other two. This is not related to the deployment locations but to the measurement periods. For all deployments the same meteorological station, Vlakte van de Raan (HMCZ), is used as a reference station. In the next section the seasonal variations will be discussed. Figure 63 shows that during the fall/winter deployment near Blankenberge the wind was nearly continuously blowing from the southwest.

One also has to keep in mind that for the Blankenberge site only 6 deployments are available at FHR, while 21 deployments are included in the ensemble analysis of SPM concentrations for MOW1.

Figure 59 - Frequencies of the seven day mean alongshore wind velocities (negative: NE wind; positive: SW wind) during the OD Nature tripod deployments at Blankenberge (top), MOW1 (middle) and WZbuoy (bottom)

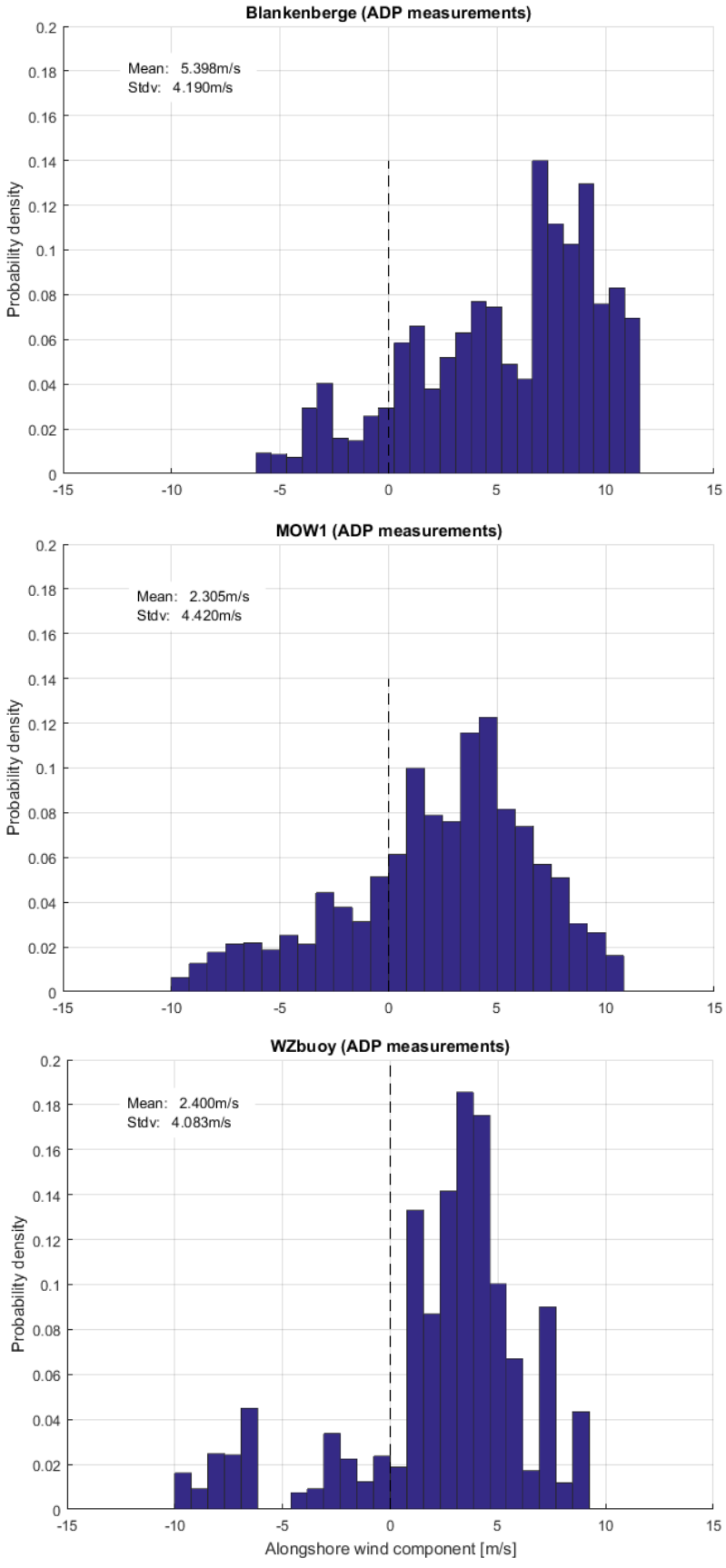

4.5 Seasonal variation

Generally one would expect higher SPM concentrations during winter due to higher waves, more storms and stronger winds. This is observed in Figure 60 which shows the depth averaged seasonal mean sediment concentrations derived from SeaWiFS satellite images (Van den Eynde et al., 2007; Fettweis et al., 2007).

Figure 60 - Depth averaged seasonal mean SPM concentrations derived from SeaWiFS satellite images (Van den Eynde et al., 2007; Fettweis et al., 2007). Top left: spring; top right: summer; bottom left: fall; bottom right: winter. The red lines mark the domain of the sediment transport model

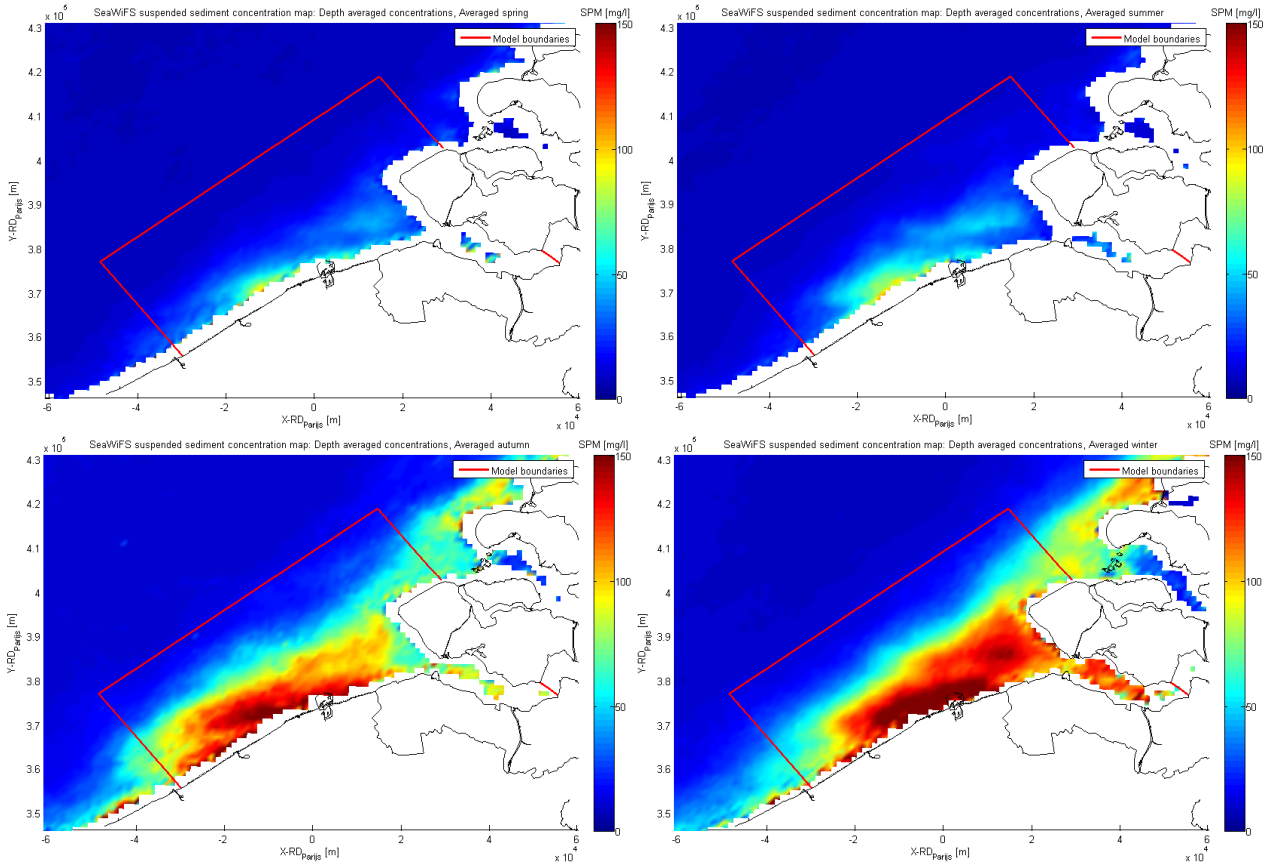

Figure 62 and Figure 61 compare the SPM concentrations during fall-winter and spring-summer for MOW1 and Blankenberge. The data of SPM concentrations at WZbuoy during the fall-winter season is limited and therefore is excluded from the analysis.

Figure 61 - Median and 10-90th percentile band of the assembled SPM concentrations ~2.3mab (upper) and ~0.3mab (lower) at MOW1 for fall-winter and spring-summer. Left: neap tides, middle: normal tides, right: spring tides

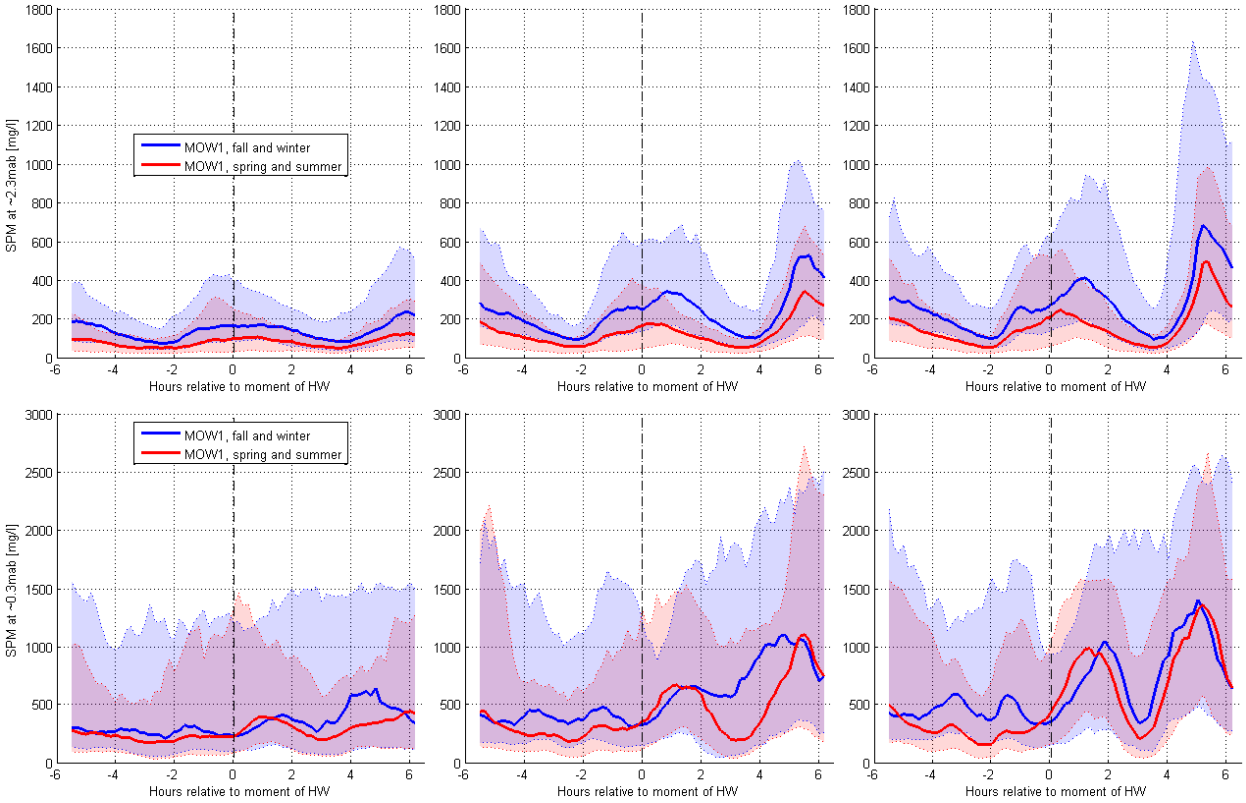

Figure 62 - Median and 10-90th percentile band of the assembled SPM concentrations ~2.3mab (upper) and ~0.3mab (lower) at Blankenberge for fall-winter and spring-summer. Left: neap tides, middle: normal tides, right: spring tides

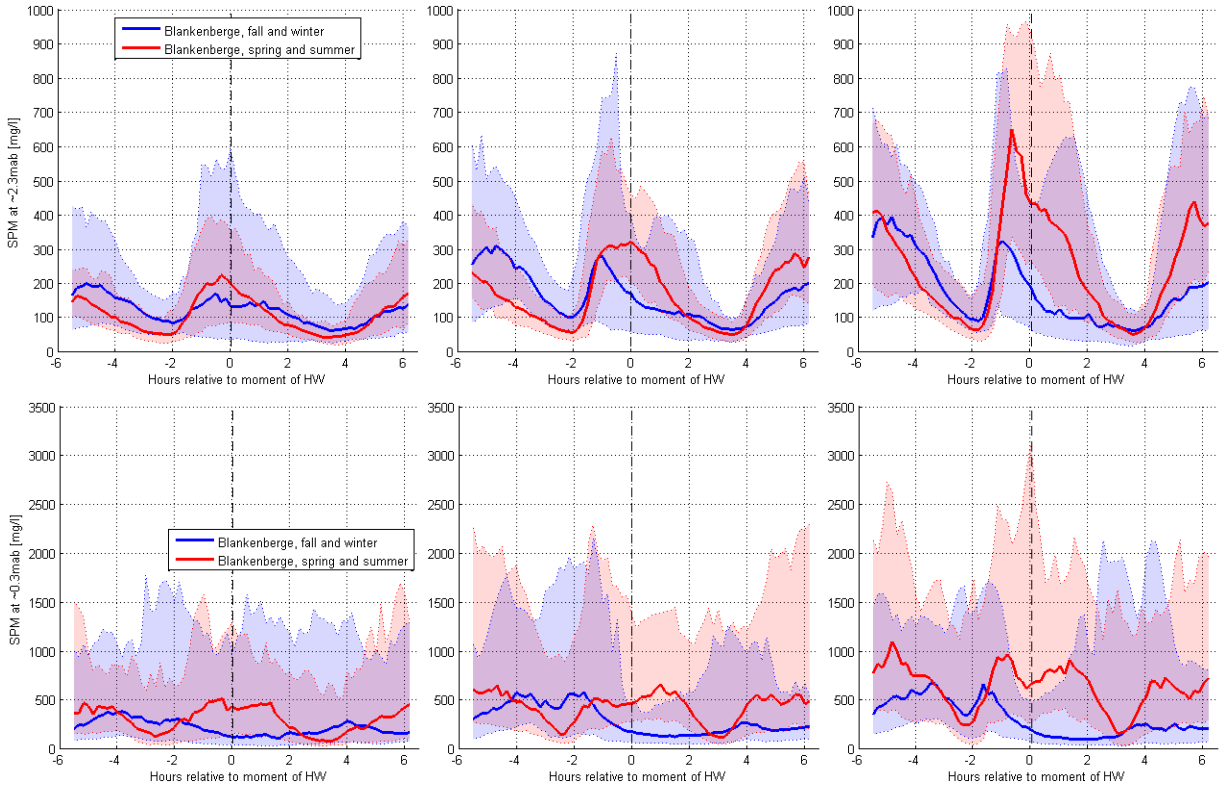

For MOW1, the general trend of higher SPM concentrations during fall-winter is obvious for the SPM data at higher sensor (~2.3mab) (Figure 61, upper panel). The seasonal variation trend of SPM at the lower sensor (~0.3mab) is less pronounced. The deployments near Blankenberge does not support the seasonal variation in the SPM concentrations (Figure 62). An opposite trend is even observed during flood and ebb flow with higher concentrations during spring-summer than during the fall-winter.

The opposite seasonal variation for Blankenberge might be partially explained by comparing the seasonal wind statistics during tripod deployments for Blankenberge with seasonal long-term wind climate and for MOW1 in Figure 63. It is clear for Blankenberge that the wind during the measurement periods is not representative for the seasons. During the fall-winter measurements the wind is almost continuously blowing from the south to southwest and strong southwest wind is more frequent compared to long-term fall/winter data. During the spring-summer deployments there is a prevailing north-east wind while averaged wind climate shows west-southwest dominant direction. In the previous section the sensitivity of the sediment concentrations near Blankenberge to the alongshore subtidal flow has been already discussed. Since during the fall and winter tripod deployments, the wind was nearly continuously blowing from the south to southwest, this can initiate a northeast oriented residual flow. It is assumed that if this subtidal flow holds on long enough it can transport water from the English Channel to the Belgian coast. This could possibly explain the lowered ensemble average SPM concentration during the fall and winter deployments near Blankenberge. Another striking point during the fall/winter deployment near Blankenberge is the absence of north to northeasterly winds as well. The wind during MOW1 deployments is resemble to the long-term data with the most predominant wind from south-southwest during fall-winter and from west-southwest during spring-summer.

In the study of Fettweis & Baeye (2015), the variation of the SPM concentrations, floc size and settling velocity were studied for summer and winter seasons using ADP- and OBS-derived SPM concentration data at MOW1. The study reported smaller flocs and thus smaller settling velocities in winter and larger flocs and settling velocities in summer. As the result, the SPM is better mixed throughout the water column in winter, whereas the SPM is more concentrated in the near-bed layer in summer. The study showed an increase in the near-bed ADP-SPM concentration at 0.5mab during spring-summer. These might be also applied to Blankenberge which contribute to higher near-bed SPM during spring-summer than fall-winter. Fettweis & Baeye (2015) also discussed that the higher near-bed SPM concentrations during slack in winter are due to the lower settling velocities and the higher SPM concentrations in the water column. This trend is also observed in the measurements at MOW1 and Blankenberge during slack tides around HW-2.5h and HW+3h (Figure 61 and Figure 62)

The assemble Rouse number for the sites Blankenberge and MOW1 for the different seasons is plotted in Figure 64. Both locations show a lower Rouse number for fall-winter than spring-summer, meaning that the water column is more mixed during fall-winter. This agrees well with the conclusion in Fettweis & Baeye (2015) presented above.

Figure 63 - Wind roses at Vlakte van de Raan for fall/winter and summer/spring during tripod deployments used in the ensemble analysis of SPM at Blankenberge, MOW1, WZbuoy and 15 years (1999-2013)

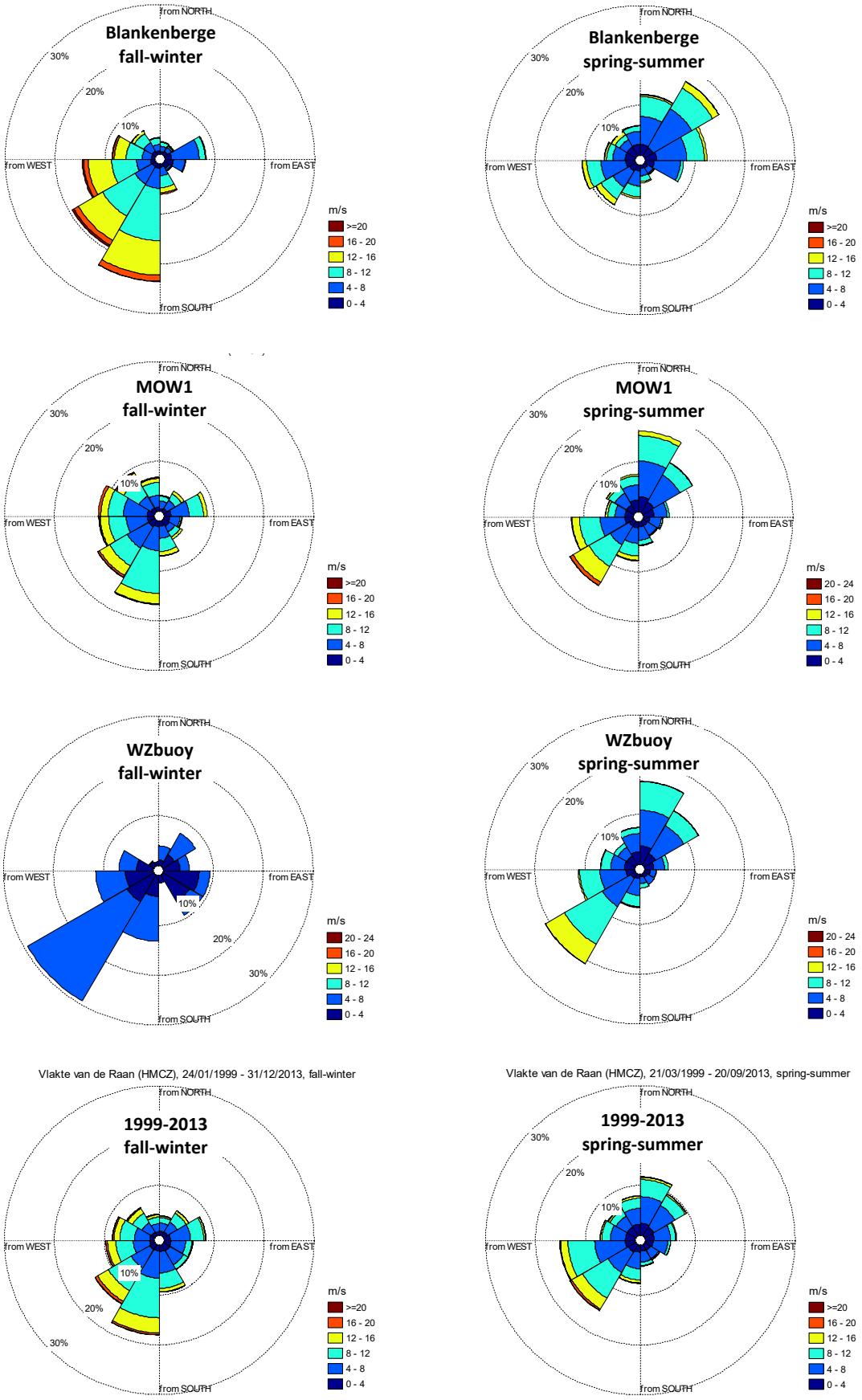

Figure 64 - Median and 10-90th percentile band of the assembled Ro during tripod deployments at Blankenberge (upper) and MOW1 (lower): spring-summer (red) and fall-winter (blue)

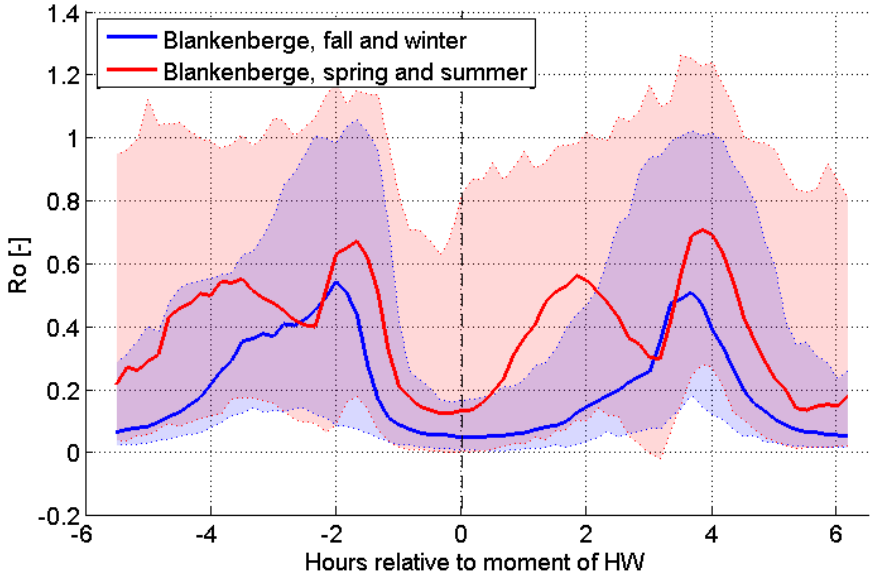

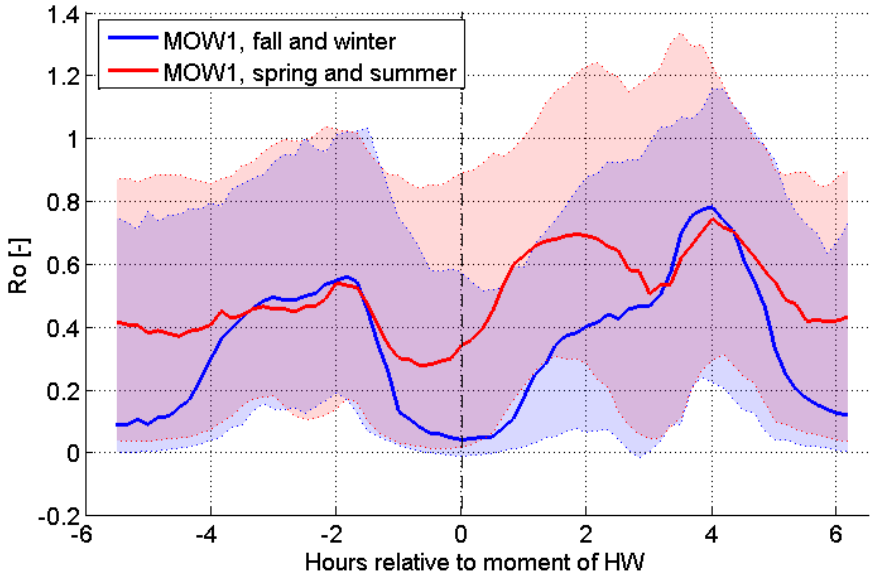

5 Conclusions

This document gives a detailed analysis of available velocity measurements (ADP and ADVOcean) and sediment concentrations from nine years of OD Nature tripod deployments. The focus of this document is on the measurement sites Blankenberge, MOW1 and WZbuoy. For these sites most data is available and they are closest to the port of Zeebrugge for which a sediment transport model is currently under development.

5.1 Currents

In Section 3 the measured velocities are analyzed. Through tidal analysis, the tidal components, i.e. major and minor axes and inclination of the tidal ellipse are estimated for the individual deployments. Although tidal analyses return M2, S2 and M4 components with a high confidence interval, the intercomparison between the different deployments for the same site show some deviations in the estimated major, minor amplitude and also the ellipse inclination.

The measured time series of the current velocities were binned into an average neap, normal and spring tide. The mean velocities are comparable for Blankenberge MOW1 and WZbuoy, although the tidal asymmetry for Blankenberge seems to be more pronounced with rather low maximum ebb flow compared to its maximum flood flow. Since during the measurement periods at the Blankenberge site the wind was blowing more often from the southwest than during the MOW1 measurements, this might explain the more pronounced tidal asymmetry of the mean flow near Blankenberge than near MOW1.

Stronger winds blowing from SW (>10m/s) cause more significant NE subtidal alongshore flow for all three locations.

5.2 Suspended sediment concentrations

Although the distance between the measurement locations Blankenberge, MOW1 and WZbuoy is less than 8 kilometers, some differences in the intratidal variation of sediment concentrations can still be observed. For the Blankenberge site during one tide, two peaks can be observed one during maximum flood flow and another shortly after maximum ebb flow. For the MOW1 site two main peaks are also observable. During flood the concentration gradually increases and reaches its maximum one hour after high water. During ebb the concentrations rise from its minimum to its maximum value within one to two hours with a maximum concentration during maximum ebb flow nearly twice as high as the peak during flood.

When considering the time series of the concentrations measured close to the bottom during one tide, concentrations jump in a short time from 50mg/l to more than 1000mg/l and back. However, after assembling the tides the ensemble concentrations does not show this behavior: the ensemble median shows much smoother variation of the SPM concentration over tidal cycles, but with a very large 10^{th}-90^{th} percentile band. Apparently there is not only a natural variability in the amount of sediment that comes into suspension during a tidal cycle, but also the moments the erosion and deposition start and end. This makes the peaks being smoothed out after assembling all individual tidal cycles. By plotting the probability density of the concentrations as a function of time, it is noticed for all three sites that during slack water, i.e. around 2h30 before and 3h after high water, the concentrations drop to low values (less than 100mg/l for the sensor at 2.3mab).

In Baeye et al. (2011), it is argued that northeastward residual flows, i.e. driven by south-western winds, can transport water from the English channel with lower sediment concentrations to the Belgian coast resulting in a lower coastal turbidity maximum. Using the subtidal alongshore flow component to filter the ensembles for all three locations, these effects could only be noticed for Blankenberge deployments. However, in the analysis of the flow it was concluded that the response of the residual flow to the alongshore wind component only occurs for sufficiently high velocities. Besides that, water from the English Channel can only reach the measurement sites if these strong southwesterly winds hold on for multiple days. Analysis of the wind characteristics showed that this condition occurred during the Blankenberge measurements while during the deployments near MOW1 and WZbuoy it happened rarely that a strong wind was blowing from the southwest continuously for multiple days.

The ensemble concentration during autumn-winter is higher during spring-summer for the higher sensor (2.3mab) at MOW1. This is in line with the analysis of SeaWiFS satellite images (Van den Eynde et al., 2007; Fettweis et al., 2007). From the data retrieved from the Blankenberge site, it was not possible to reproduce this seasonal trend. The concentrations are even higher during spring-summer than during fall-winter. When comparing the wind conditions during the Blankenberge measurements with the average wind climate, then one will notice that during the fall and winter deployments at the Blankenberge site the wind was mostly blowing from the south to southwest and strong south-west wind occurred more frequent. For the spring and summer deployments the prevailing wind direction was northeast while the west-southwest was the most dominant direction in the long-term wind data. Therefore, the wind conditions during the Blankenberge deployments were in general not representative for the time of the year. This might partly contribute to this opposite behavior. In addition, the study of Fettweis & Baeye (2015) related the seasional variation of the SPM concentrations and floc size and settling velocity. The study reported smaller flocs and thus smaller settling velocities in winter and larger flocs and settling velocities in summer. As the result, the SPM is more concentrated in the near-bed layer in summer, whereas in winter, the SPM is better mixed throughout the water column. This might be another reason for higher SPM concentration in the near-bed layer during spring-summer for Blankenberge.

6 References

Baeye, M.; Fettweis, M.; Voulgaris, G.; Van Lancker, V. (2011). Sediment mobility in response to tidal and wind-driven flows along the Belgian inner shelf, southern North Sea. *Ocean Dynamics* 61(5): 611-622

Bridge, J., & Demicco, R. (2008)**.** Earth Surface Processes, Landforms and Sediment Deposits. Cambridge: Cambridge University Press

De Maerschalck, B.; Vanlede, J. (2011). Memo: Metingen Sediment Concentraties. Versie 2.0. *WL Rekennota*, 753_17: Antwerpen, België

De Maerschalck, B.; Nguyen, D.; Vanlede, J.; Mostaert, F. (2020). Sediment Transport Model for the Port of Zeebrugge: Sub report 1- Factual Data Report OD Nature tripod measurements: SonTek ADP, ADVOcean and OBS data. Versie 0.1. FHR Report, 00_067_1. Flanders Hydraulics Research & Antea Group: Antwerp

Fettweis M., Baeye M. (2015)**.** Seasonal variation in concentration, size and settling velocity of muddy marine flocs in the benthic boundary layer. *Journal of Geophysical Research*, doi: 10.1002/2014JC010644

Fettweis, M.; Baeye, M.; Lee, B.J.; Van den Eynde, D.; Van Lancker, V.R.M. (2011). Monitoring en modellering van het cohesieve sedimenttransport en evaluatie van de effecten op het mariene ecosysteem ten gevolge van bagger- en stortoperatie (MOMO): activiteitsrapport (1 juli 2010 - 31 december 2010). BMM: Brussel

Fettweis, M.; Baeye, M.; Francken, F.; Van den Eynde, D. (2015). Monitoring en modellering van het cohesieve sedimenttransport en evaluatie van de effecten op het mariene ecosysteem ten gevolge van bagger- en stortoperatie (MOMO): activiteitsrapport (1 januari 2015 - 30 juni 2015). BMM: Brussel

Fettweis, M.; Nechad, B.; Van den Eynde, D. (2007). An estimate of the suspended particulate matter (SPM) transport in the southern North Sea using SeaWiFS images, in situ measurements and numerical model results. *Cont. Shelf Res.* 27(10-11): 1568-1583

Pawlowicz, R.; Beardsley, B.; Lentz, S. (2002). Classical tidal harmonic analysis including error estimates in MATLAB using T_TIDE. *Comput. Geosci.* 28(8): 929-937. DOI 10.1016/S0098-3004(02)00013-4

Prandle, D. (1997). Tidal characteristics of suspended sediment concentrations. *J. Hydraul. Eng.* 123341-350

Van den Eynde, D.; Nechad, B.; Fettweis, M.; Francken, F. (2007). Seasonal variability of suspended particulate matter observed from SeaWiFS images near the Belgian coast. *Estuarine and Coastal Fine Sediment Dynamics*

Appendix A OD Nature tripod deployment data at Flanders Hydraulics Research

Table 1 - OD Nature deployments at Blankenberge:
available data, valid data and data selected to construct combined ensembles

Tripod deployment			Data available [days]				Height of the sensors [cm]				Inclusion in combined ensemble?			
	Start	End	OBS	ADV	ADP	Depth Pressure	OBS1	OBS2	ADV	ADP	SPM (OBS)	Velocity (ADV)	Velocity (ADP)	
(1)	*(2)*	*(3)*	*(4)*	*(5)*	*(6)*	*(7)*	*(8)*	*(9)*	*10)*	*(11)*	*(12)*	*(13)*	*(14)*	*(15)*
Nov. 2006	08/11/2006	15/12/2006	36.7	36.7	36.7	36.7	202	17	20	233	yes	yes	yes	
Dec. 2006	18/12/2006	07/02/2007	51.1	51.1	51.1	51.1	26	216	20	228	yes	yes	yes	
Jan. 2008	28/01/2008	25/02/2008	26.8	~~26.8~~	26.9	26.8	29 (a)	234 (a)	-	224 (a)	yes	no(e)	yes	e
Mar. 2008	06/03/2008	10/04/2008	32.5	32.5	32.5	32.5	29 (a)	234 (a)	18 (a)	224 (a)	yes	yes	yes	b
Apr. 2008	15/04/2008	05/06/2008	51.0	50.9	51.0	51.0	29	234	18	224	yes	yes	yes	c
May 2009	04/05/2009	15/06/2009	41.9	41.8	41.9	41.9	26	216	20	228	yes	yes	yes	d
Total measurement days:			**240**	**240**	**240**									
Number of valid tidal cycles:			**463**	**404**	**463**									

Remarks: a - Exact heights of the sensors not reported, take the sensor heights of the deployment in the same year; b - Data on the last days eliminated due to tripod tilted; c – SPM data from 24/05/2008 on the lower sensor eliminated due to algae growth on the sensor; d - Dredging experiment Albert II dock; e - ADV measurements significantly lower than other deployments (sensor position?)

Table 2 - OD Nature deployments at MOW1: available data, valid data and data selected to construct combined ensembles

Tripod deployment			Data available [days]				Height of the sensors [cm]				Inclusion in combined ensemble?			Remarks
	Start	End	OBS	ADV	ADP	Depth/ Pressure	OBS_1	OBS_2	ADV	ADP	SPM (OBS)	Velocity (ADV)	Velocity (ADP)	
(1)	*(2)*	*(3)*	*(4)*	*(5)*	*(6)*	*(7)*	*(8)*	*(9)*	*10)*	*(11)*	*(12)*	*(13)*	*(14)*	*(15)*
Feb. 2005	07/02/2005	08/02/2005	0.8	0.8	-	0.8	27	202	43	218	yes	yes	-	
Apr. 2005	04/04/2005	15/04/2005	2.9	5.5	-	2.9	27	202	23	218	yes	yes	-	
Jun. 2005	22/06/2005	11/07/2005	5.5	5.5	-	5.5	27	202	43	218	yes	yes	-	
Nov. 2005	21/11/2005	05/12/2005	13.0	13.2	-	13.0	28	186	30	218	yes	yes	-	
Feb. 2006	13/02/2006	27/02/2006	14.0	13.9	14.0	14.0	25	224	28	233	yes	yes	no(j)	
Mar. 2006	27/03/2006	18/04/2006	~~21.9~~	-	-	21.9	65	95 (f)	-	-	no(f)	-	-	Tripod tilted during deployment; too low OBS sensors
May. 2006	15/05/2006	15/06/2006	31.0	~~30.9~~	31.0	31.0	20	202	17	233	yes	no(g)	no(j)	noisy ADV measurements in 06/2006
Jul. 2007	10/07/2007	19/07/2007	~~8.8~~	8.8	8.8	8.8	23	130 (f)	23	228	no(f)	yes	no(j)	too low OBS_2 sensor
Oct. 2007	23/10/2007	28/11/2007	35.9	35.9	35.9	35.9	26	236	15	226	yes	yes	no(j)	
Nov. 2008	17/11/2008	12/12/2008	24.7	-	24.8	16.6	26	220	18	223	yes	-	no(j)	
Feb. 2009	09/02/2009	19/03/2009	37.8	37.8	37.8	16.4	29	234	18	228	yes	yes	yes	
Mar. 2009	26/03/2009	29/04/2009	34.0	34.0	~~33.7~~	32.7	29	234	18	228	yes	yes	no(h)	Algae growth on the sensors; strange ADP ensemble
Sep. 2009	10/09/2009	21/10/2009	2.1	2.1	34.0	-	29	234	18	228	no(l)	no(l)	no(l)	
Nov. 2009	06/11/2009	08/12/2009	~~32.3~~	32.3	32.3	32.3	29	234	18	228	no(k)	yes	yes	SPM_1 (OBS_1) and/or SPM_2 (OBS_2) data: timeshift?
Dec. 2009	11/12/2009	25/01/2010	~~45.3~~	44.9	45.3	45.3	29	234	18	228	no(k)	yes	yes	SPM_1 and/or SPM_2 data: timeshift?; low SPM_1 (OBS_1)
Jan. 2010	25/01/2010	25/03/2010	~~58.8~~	58.8	58.8	58.8	29	234	18	228	no(k)	yes	yes	SPM_1 and/or SPM_2 data: timeshift?, suspicious mag.
Mar. 2010	25/03/2010	20/05/2010	56.1	56.1	~~56.1~~	56.1	29	234	18	228	yes	yes	no(h)	ADP velocity: suspicious mag., direction; timeshift?
May. 2010	20/05/2010	31/05/2010	-	11.1	11.1	11.1	29	234	18	228	-	yes	yes	
May. 2010	31/05/2010	23/07/2010	-	52.6	52.6	52.6	29	234	18	228	-	yes	yes	
Sep. 2010	06/09/2010	18/10/2010	-	41.9	~~41.9~~	41.9	29	234	18	228	-	yes	no(h)	ADP velocity: suspicious mag., dir. (v_{north} timeshift?)
Oct. 2010	18/10/2010	17/11/2010	21.4	21.4	29.9	21.4	29	234	18	228	yes	yes	yes	
Nov. 2010	17/11/2010	15/12/2010	28.2	28.2	28.2	28.2	29	234	18	228	yes	yes	yes	
Dec. 2010	15/12/2010	31/01/2011	-	23.8	16.3	~~23.8~~	29	234	18	228	-	no(l)	no(l)	
Jan. 2011	31/01/2011	21/03/2011	-	48.9	-	48.9	29	234	18	228	-	yes	-	
Mar. 2011	21/03/2011	24/03/2011	2.5	~~2.5~~	-	2.5	29	234	18	228	yes	no(g)	-	ADV velocity: suspicious direction, timeshift?

Tripod deployment			Data available [days]				Height of the sensors [cm]				Inclusion in combined ensemble?			Remarks
	Start	End	OBS	ADV	ADP	Depth/ Pressure	OBS_1	OBS_2	ADV	ADP	SPM (OBS)	Velocity (ADV)	Velocity (ADP)	
(1)	*(2)*	*(3)*	*(4)*	*(5)*	*(6)*	*(7)*	*(8)*	*(9)*	*10)*	*(11)*	*(12)*	*(13)*	*(14)*	*(15)*
Mar. 2011	24/03/2011	29/04/2011	24.4	24.4	-	24.4	29	234	18	228	yes	yes	-	
Apr. 2011	29/04/2011	23/05/2011	~~24.2~~	24.2	~~24.2~~	24.2	29	234	18	228	no(k)	yes	no(h)	OBS and ADP data: timeshift?
May. 2011	23/05/2011	11/07/2011	26.9	26.9	26.9	26.9	29	234	18	228	yes	yes	yes	
Jul. 2011	11/07/2011	18/08/2011	32.1	37.2	32.1	37.2	29	234	18	228	yes	yes	yes	
Aug. 2011	18/08/2011	09/09/2011	~~21.8~~	21.7	~~21.7~~	21.7	29	234	18	228	no(k)	yes	no(h)	ADP data: timeshift?; suspicious SPM_2 (OBS_2)
Sep. 2011	09/09/2011	12/10/2011	33.3	33.3	33.3	33.3	29	234	18	228	yes	yes	yes	
Oct. 2011	12/10/2011	24/11/2011	36.8	~~36.8~~	~~42.7~~	~~36.8~~	29	234	18	228	no(l)	no(g,l)	no(h,l)	ADV velocity: timeshift?; ADP vel.: suspicious direction
Nov. 2011	24/11/2011	03/02/2012	~~55.3~~	55.4	55.3	38.0	29	234	18	228	no(k)	yes	yes	SPM_1 (OBS_1) and/or SPM_2 (OBS_2): timeshift?; frequent SPM_2 >SPM_1
Feb. 2012	24/02/2012	19/03/2012	23.9	~~23.9~~	~~24.2~~	~~23.9~~	29	234	18	228	no(l)	no(g,l)	no(h,l)	ADP and ADV velocity: timeshift?
Mar. 2012	19/03/2012	25/04/2012	36.9	36.9	36.9	-	29	234	18	228	no(l)	no(l)	no(l)	
Jun. 2012	29/06/2012	23/08/2012	41.9	55.2	55.1	-	29	234	18	228	no(l)	no(l)	no(l)	
Dec. 2012	05/12/2012	01/01/2013	~~25.6~~	25.6	26.7	25.6	29	234	18	228	no(k)	yes	yes	high proposition of time SPM_2 (OBS_2) > SPM_1 (OBS_1)
Jan. 2013	24/01/2013	07/03/2013	41.8	41.8	41.8	-	29	234	18	228	no(l)	no(l)	no(l)	
Mar. 2013	07/03/2013	28/03/2013	~~21.2~~	21.2	21.2	21.2	29	234	18	228	no(k)	yes	yes	SPM_1 (OBS_1) and/or SPM_2 (OBS_2) data: timeshift?
Mar. 2013	28/03/2013	22/04/2013	24.8	24.8	24.8	24.8	29	234	18	228	yes	yes	yes	
Apr. 2013	22/04/2013	17/05/2013	24.8	24.8	24.8	-	29	234	18	228	no(l)	no(l)	no(l)	
May. 2013	17/05/2013	27/06/2013	41.2	41.2	41.2	-	29	234	18	228	no(l)	no(l)	no(l)	
Jun. 2013	27/06/2013	24/07/2013	26.9	26.9	26.9	-	29	234	18	228	no(l)	no(l)	no(l)	
Jul. 2013	24/07/2013	21/08/2013	28.2	28.2	28.2	-	29	234	18	228	no(l)	no(l)	no(l)	
Aug. 2013	21/08/2013	23/09/2013	26.8	26.8	32.8	26.8	29	234	18	228	yes	yes	yes	
Sep. 2013	23/09/2013	16/10/2013	23.0	23.0	23.0	-	29	234	18	228	no(l)	no(l)	no(l)	
Oct. 2013	16/10/2013	28/11/2013	27.0	27.0	42.9	27.0	29	234	18	228	yes	yes	yes	
Nov. 2013	28/11/2013	09/12/2013	7.0	11.1	11.1	-	29	234	18	228	no(l)	no(l)	no(l)	
Total measurement days:			**1153**	**1309**	**1290**									
Number of valid tidal cycles:			**1596**	**2314**	**1998**									

Remarks: f - OBS sensor position(s) out of range; g, h, k - doubtful ADV(g), ADP(h), OBS(k) measurements; l - no or doubtful depth data; j - only profile-averaged vel. available in VIMM data block

Table 3 - OD Nature deployments at WZbuoy: available data, valid data and data selected to construct combined ensembles

Tripod deployment			Data available [days]				Height of the sensors [cm]				Inclusion in combined ensemble?		
	Start	End	OBS	ADV	ADP	Depth / Pressure	OBS_1	OBS_2	ADV	ADP	SPM (OBS)	Velocity (ADV)	Velocity (ADP)
(1)	*(2)*	*(3)*	*(4)*	*(5)*	*(6)*	*(7)*	*(8)*	*(9)*	*10)*	*(11)*	*(12)*	*(13)*	*(14)*
Mar. 2013	28/03/2013	23/04/2013	25.9	25.9	25.9	25.9	29	234	18	228	yes	yes	yes
Apr. 2013	25/04/2013	14/05/2013	19.1	19.1	~~15.2~~	19.1	29	234	18	228	yes	yes	no(m)
Jun. 2013	10/06/2013	27/06/2013	17.2	17.3	-	17.2	29	234	18	-	yes	yes	-
Jun. 2013	28/06/2013	24/07/2013	26.1	26.1	26.1	26.1	29	234	18	228	yes	yes	yes
Jul. 2013	29/07/2013	21/08/2013	17.4	17.4	~~18.0~~	17.4	29	234	18	228	yes	yes	no(m)
Aug. 2013	23/08/2013	09/09/2013	17.1	17.1	-	17.1	29	234	18	-	yes	yes	-
Sep. 2013	12/09/2013	14/10/2013	13.4	32.4	32.4	32.4	29	234	18	228	yes	yes	yes
Oct. 2013	15/10/2013	13/11/2013	-	26.9	29.0	26.9	-	-	18	228	-	yes	yes
Nov. 2013	13/11/2013	26/11/2013	-	13.1	13.1	13.1	-	-	18	228	-	yes	yes
Nov. 2013	27/11/2013	10/12/2013	-	12.7	-	12.7	-	-	18	-	-	yes	-
Total measurement days:			**136**	**208**	**160**								
Number of valid tidal cycles:			**261**	**393**	**244**								

Remarks: m – suspicious ADP velocity direction

Table 4 - Overview of the available data and sensor heights for the OD Nature deployments near MOW0.
Remark: ADV was seriously damaged during deployment period: no OBS nor ADV data could be recuperated

Tripod deployment			Data available (days)				Height of the sensors (cm)			
	Start	End	OBS	ADV	ADP	Pressure	OBS_1	OBS_2	ADV	ADP
June 2008	23/06/2008	11/07/2008	-	-	18	-	26	228	19	227
Total measurement days:			-	-	18	-				
Number of valid tidal cycles (12h 25m):			-	-	20	-				

Table 5 - Overview of the available data and sensor heights for the OD Nature deployments at Blighbank.
Remark: no reports available at FHR. Confidential data

Tripod deployment			Data available [days]				Height of the sensors [cm]			
	Start	End	OBS	ADV	ADP	Pressure	OBS_1	OBS_2	ADV	ADP
June 2009	24/06/2009	14/07/2009	20.0	20.0	-	-	-	-	-	-
May 2010	5/05/2010	1/06/2010	26.9	26.9	-	-	-	-	-	-
Total measurement days:			**46.9**	**46.9**						
Number of valid tidal cycles (12h 25m):			**90**	**90**						

Table 6 - Overview of the available data and sensor heights for the OD Nature deployments at Gootebank.
Remark: no reports available at FHR. Confidential data

Tripod deployment			Data available [days]				Height of the sensors [cm]			
	Start	End	OBS	ADV	ADP	Pressure	OBS_1	OBS_2	ADV	ADP
Jun. 2009	23/06/2009	13/07/2009	19.8	19.8	-	-	-	-	-	-
Sep. 2009	19/10/2009	9/12/2009	50.7	50.7	-	-	-	-	-	-
Total measurement days:			**70.5**	**70.5**						
Number of valid tidal cycles (12h 25m):			**136**	**136**						

Appendix B Estimation of the major axis of the current velocity

Formulations

If the horizontal velocity components describe an ellipse, the axes X_1 and X_2 are called the major and minor axis of the ellipse. By definition the inclination is the angle between the east and the major axis. α in Figure 65 is then the direction of the major axis measured in degrees Azimuth.

Figure 65 - Coordinate transformation to major and minor axes

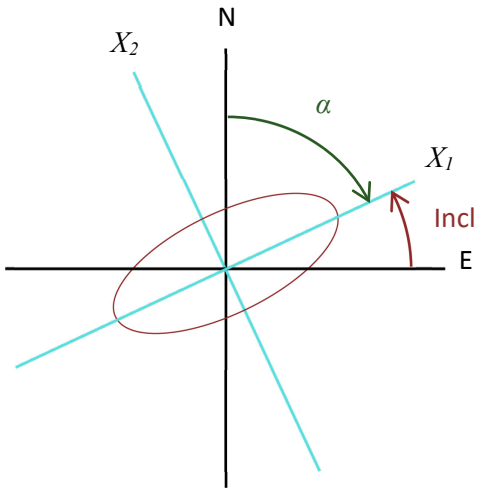

If u and v are the velocity components in the north and east direction, and u_1 and u_2 are the velocity components along the X_1 and X_2 axes, then:

One can now derive the direction α by minimizing u_2 in the L_2 norm:

with $\|u_2\|_{L2}^2 = \sum u_2(t)^2$

This constrained minimization is very straight forward to program within the Matlab environment:

```
u2    = @(alpha) norm( -cos(alpha)*u + sin(alpha)*v );
alpha = fminbnd(u2,0,pi);
```

Estimated major axis directions of the ADP and ADV velocity

Table 7 - Estimated major direction [°Azimuth]:
mean direction and standard deviation for the deployments at Blankenberge (ADP profile-averaged ~1.2mab; ADVOcean ~0.2mab)

Tripod deployment			ADP				ADVOcean			
			Major dir.		M2 ellipse		Major dir.		M2 ellipse	
	Start	End	mean	stdv	dir	95% CI	mean	stv	dir	95% CI
Nov. 2006	08/11/2006	15/12/2006	52	5.25	51	0.11	58	2.83	58	0.20
Dec. 2006	18/12/2006	07/02/2007	66	1.32	66	0.15	48	3.06	47	0.21
Jan. 2008	28/01/2008	25/02/2008	76	0.85	76	0.13	70	1.51	69	0.39
Mar. 2008	06/03/2008	10/04/2008	62	1.32	61	0.13	68	1.27	67	0.35
Apr. 2008	15/04/2008	05/06/2008	53	0.65	53	0.05	66	0.8	66	0.10
May 2009	04/05/2009	15/06/2009	69	2.49	69	0.20	64	2.3	63	0.35

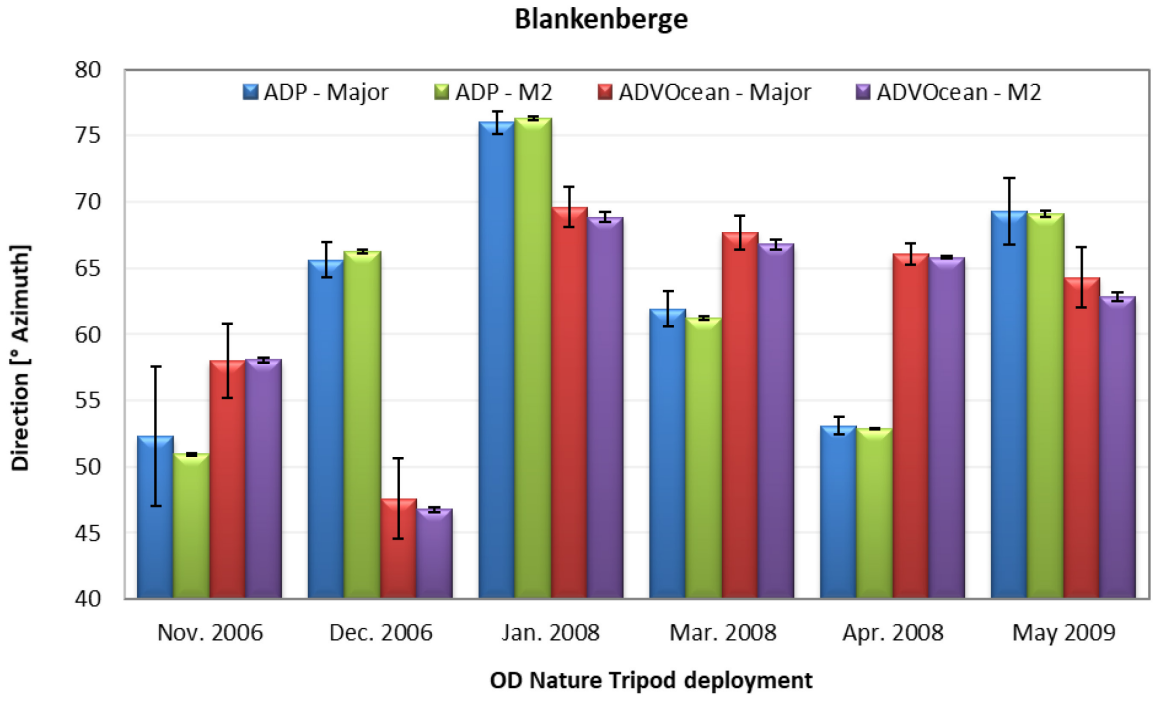

Table 8 - Estimated major direction [° Azimuth]:
mean direction and standard deviation for the deployments at MOW1 (ADP profile-averaged ~1.2mab; ADVOcean ~0.2mab)

Tripod deployment			ADP				ADVOcean			
			Major dir.		M2 ellipse		Major dir.		M2 ellipse	
	Start	End	mean	stdv	dir	95% CI	mean	stv	dir	95% CI
Feb. 2005	07/02/2005	08/02/2005	-	-	-	-	72	0.25	72	0.72
Apr. 2005	04/04/2005	15/04/2005	-	-	-	-	74	1.80	74	0.19
Jun. 2005	22/06/2005	11/07/2005	-	-	-	-	60	0.72	60	0.06
Nov. 2005	21/11/2005	05/12/2005	-	-	-	-	62	3.63	65	1.15
Feb. 2006	13/02/2006	27/02/2006	58	1.77	59	0.29	68	2.78	68	0.44
Mar. 2006	27/03/2006	18/04/2006	-	-	-	-	-	-	-	-
May 2006	15/05/2006	15/06/2006	69	1.80	70	0.09	-	-	-	-
Jul. 2007	10/07/2007	19/07/2007	51	0.42	51	0.12	55	0.97	55	0.57
Oct. 2007	23/10/2007	28/11/2007	62	0.94	62	0.12	65	2.94	64	0.39
Nov. 2008	17/11/2008	12/12/2008	81	1.40	81	0.19	-	-	-	-
Feb. 2009	09/02/2009	19/03/2009	64	1.57	64	0.30	51	1.75	51	0.41
Mar. 2009	26/03/2009	29/04/2009	72	0.44	72	0.24	60	0.65	60	0.36
Sep. 2009	10/09/2009	21/10/2009	60	0.75	60	0.23	64	0.44	63	0.58
Nov. 2009	06/11/2009	08/12/2009	73	0.62	75	0.26	60	2.50	63	0.34
Dec. 2009	11/12/2009	25/01/2010	57	1.00	58	0.20	52	1.31	53	0.23
Jan. 2010	25/01/2010	25/03/2010	73	1.15	72	0.26	55	2.63	51	0.38
Mar. 2010	25/03/2010	20/05/2010	-	-	-	-	58	4.00	60	0.34
May 2010	20/05/2010	31/05/2010	65	1.65	63	0.61	59	0.91	58	0.34
May 2010	31/05/2010	23/07/2010	64	1.37	65	0.37	73	2.68	72	0.29
Sep. 2010	06/09/2010	18/10/2010	-	-	-	-	48	0.54	48	0.18
Oct. 2010	18/10/2010	17/11/2010	58	1.00	58	0.40	62	3.16	62	0.54
Nov. 2010	17/11/2010	15/12/2010	62	0.97	61	0.35	57	1.95	57	0.33
Dec. 2010	15/12/2010	31/01/2011	64	0.81	64	0.37	55	1.17	55	0.37
Jan. 2011	31/01/2011	21/03/2011	-	-	-	-	50	5.72	52	0.32
Mar. 2011	21/03/2011	24/03/2011	-	-	-	-	-	-	-	-
Mar. 2011	24/03/2011	29/04/2011	-	-	-	-	67	1.14	69	0.52
Apr. 2011	29/04/2011	23/05/2011	-	-	-	-	69	1.41	68	0.31
May 2011	23/05/2011	11/07/2011	65	1.06	64	0.26	67	1.36	68	0.44
Jul. 2011	11/07/2011	18/08/2011	51	0.57	51	0.24	67	0.66	66	0.24
Aug. 2011	18/08/2011	09/09/2011	-	-	-	-	68	1.09	67	0.40
Sep. 2011	09/09/2011	12/10/2011	58	1.16	57	0.33	63	1.03	63	0.30
Oct. 2011	12/10/2011	24/11/2011	-	-	-	-	-	-	-	-
Nov. 2011	24/11/2011	03/02/2012	65	11.64	67	0.57	42	3.56	45	0.32
Feb. 2012	24/02/2012	19/03/2012	-	-	-	-	-	-	-	-
Mar. 2012	19/03/2012	25/04/2012	69	0.39	69	0.23	69	0.75	69	0.19
Jun. 2012	29/06/2012	23/08/2012	60	0.79	60	0.21	75	4.77	75	0.29
Dec. 2012	05/12/2012	01/01/2013	61	0.83	61	0.46	68	2.39	67	0.59
Jan. 2013	24/01/2013	07/03/2013	71	1.44	73	0.27	59	1.63	59	0.33
Mar. 2013	07/03/2013	28/03/2013	70	53.93	89	0.42	61	1.64	62	0.62
Mar. 2013	28/03/2013	22/04/2013	64	1.47	64	0.37	68	1.58	68	0.42
Apr. 2013	22/04/2013	17/05/2013	68	1.65	69	0.42	61	1.44	61	0.41
May 2013	17/05/2013	27/06/2013	65	1.00	65	0.22	68	2.86	66	0.28
Jun. 2013	27/06/2013	24/07/2013	85	1.76	83	0.43	57	1.21	55	0.32
Jul. 2013	24/07/2013	21/08/2013	59	0.52	59	0.31	64	1.40	64	0.30
Aug. 2013	21/08/2013	23/09/2013	73	0.74	72	0.28	64	1.94	62	0.36
Sep. 2013	23/09/2013	16/10/2013	66	1.21	65	0.39	70	0.81	70	0.36
Oct. 2013	16/10/2013	28/11/2013	68	0.75	68	0.30	57	4.04	57	0.61
Nov. 2013	28/11/2013	09/12/2013	65	0.66	64	0.69	60	0.70	60	0.61

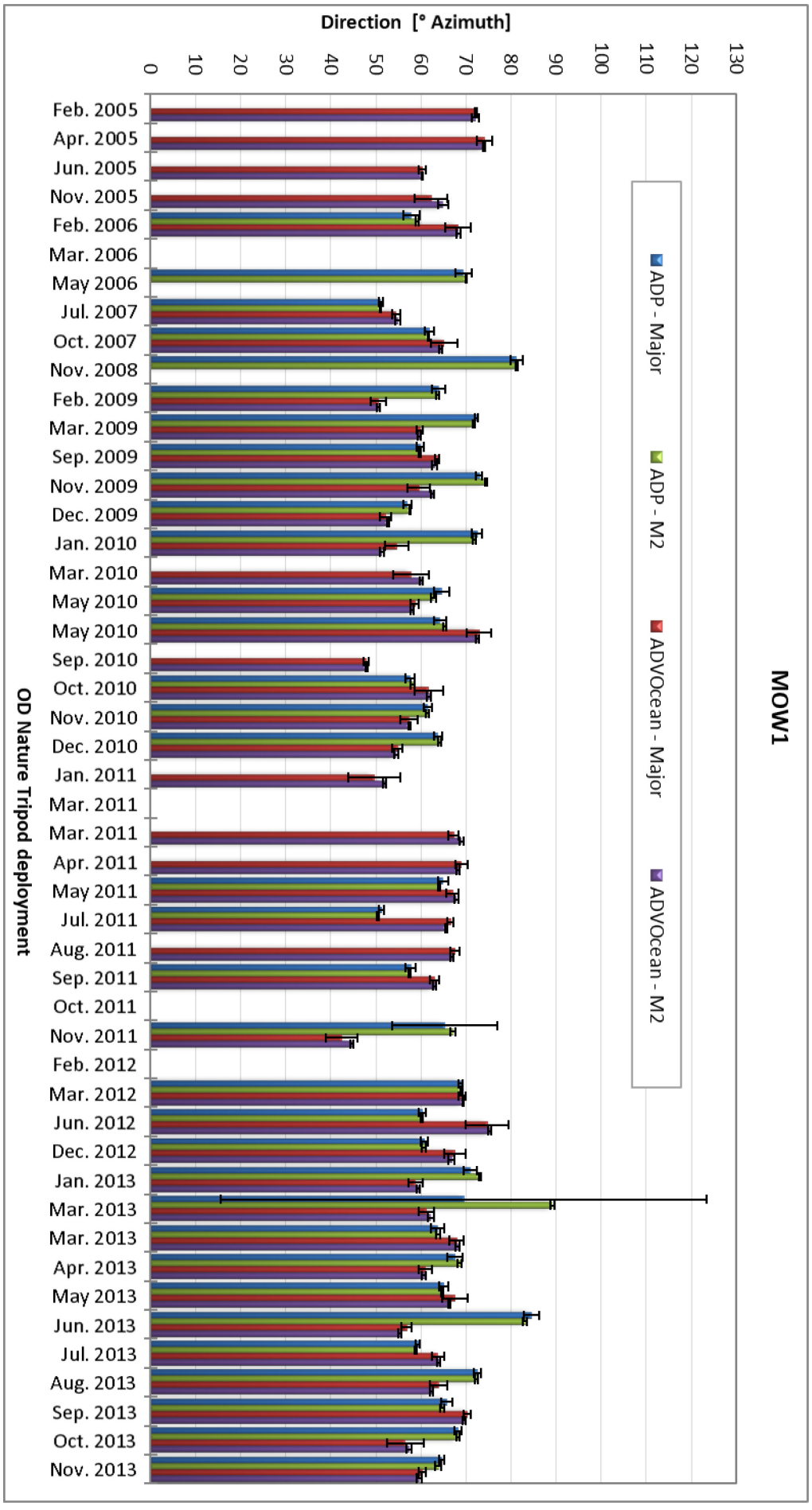
Direction [° Azimuth]
0
10
20
30
40
50
60
70
80
90
100
110
120
130
Feb. 2005
Apr. 2005
Jun. 2005
Nov. 2005
Feb. 2006
Mar. 2006
May 2006
Jul. 2007
Oct. 2007
Nov. 2008
Feb. 2009
Mar. 2009
Sep. 2009
Nov. 2009
Dec. 2009
Jan. 2010
Mar. 2010
May 2010
May 2010
Sep. 2010
Oct. 2010
Nov. 2010
Dec. 2010
Jan. 2011
Mar. 2011
Mar. 2011
Apr. 2011
May 2011
Jul. 2011
Aug. 2011
Sep. 2011
Oct. 2011
Nov. 2011
Feb. 2012
Mar. 2012
Jun. 2012
Dec. 2012
Jan. 2013
Mar. 2013
Mar. 2013
Apr. 2013
May 2013
Jun. 2013
Jul. 2013
Aug. 2013
Sep. 2013
Oct. 2013
Nov. 2013
OD Nature Tripod deployment
ADP - Major
ADP - M2
ADVOcean - Major
ADVOcean - M2
MOW1

Table 9 - Estimated major direction [° Azimuth]:
mean direction and standard deviation for the deployments at WZbuoy (ADP profile-averaged ~1.2mab; ADVOcean at ~0.2mab)

Tripod deployment			ADP				ADVOcean			
			Major dir.		M2 ellipse		Major dir.		M2 ellipse	
	Start	End	mean	stdv	dir	95% CI	mean	stv	dir	95% CI
Mar. 2013	28/03/2013	23/04/2013	80	1.61	80	0.41	74	2.18	69	0.88
Apr. 2013	25/04/2013	14/05/2013	-	-	-	-	65	1.00	68	0.84
Jun. 2013	10/06/2013	27/06/2013	-	-	-	-	75	1.46	76	0.60
Jun. 2013	28/06/2013	24/07/2013	58	1.04	59	0.35	63	0.70	63	0.39
Jul. 2013	29/07/2013	21/08/2013	-	-	-	-	66	0.89	66	0.44
Aug. 2013	23/08/2013	09/09/2013	-	-	-	-	72	0.78	72	0.46
Sep. 2013	12/09/2013	14/10/2013	48	1.61	49	0.39	65	1.54	64	0.38
Oct. 2013	15/10/2013	13/11/2013	77	1.16	78	0.51	67	1.36	68	0.55
Nov. 2013	13/11/2013	26/11/2013	51	1.13	52	0.98	71	1.36	70	0.92
Nov. 2013	27/11/2013	10/12/2013	-	-	-	-	71	2.74	72	0.69

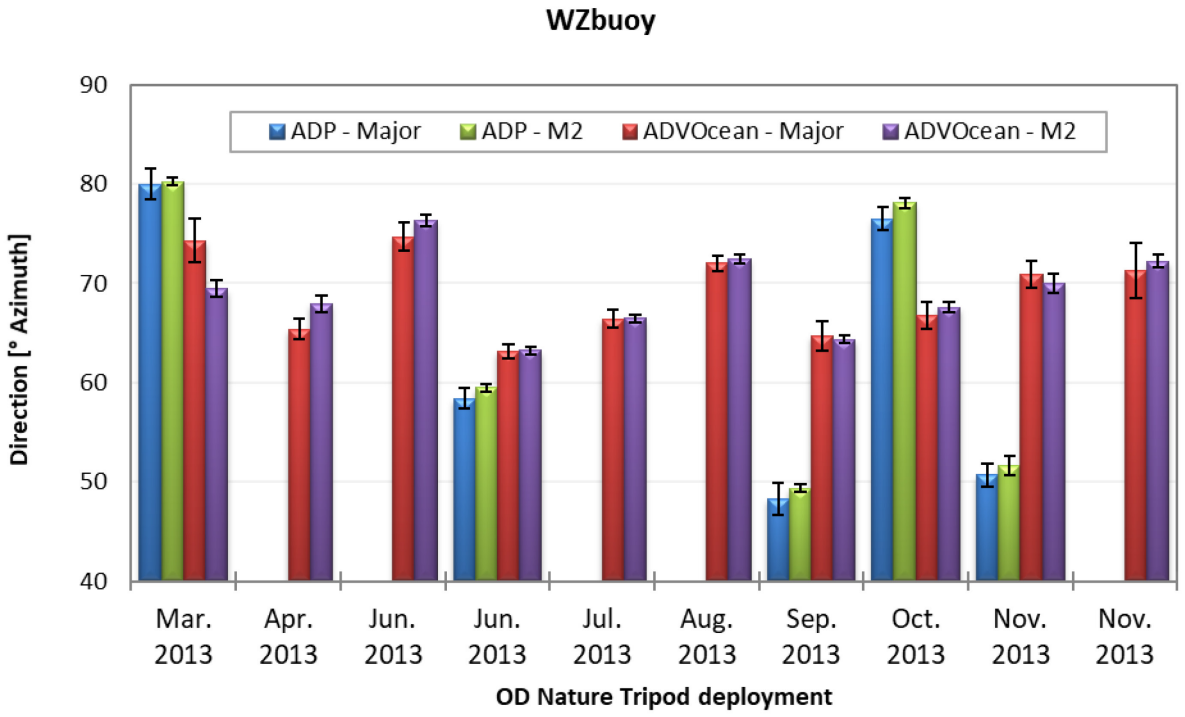

Table 10 - Estimated major direction [° Azimuth]:
mean direction and standard deviation for the deployments at MOW0 (ADP ≅ 1.2mab)

Tripod deployment		ADP				ADVOcean			
		Major dir.		M2 ellipse dir.		Major dir.		M2 ellipse	
Start	End	mean	stdv	M2	95% CI	mean	stv	dir	95% CI
23/06/2008	11/07/2008	66	1	68	0.29	-	-	-	-

Table 11 - Estimated major direction [° Azimuth]:
mean direction and standard deviation for the deployments at Blighbank (ADVOcean ≅0.2mab)

Tripod deployment			ADP				ADVOcean			
			Major dir.		M2 ellipse		Major dir.		M2 ellipse	
	Start	End	mean	stdv	dir	95% CI	mean	stv	dir	95% CI
Jun. 2009	24/06/2009	14/07/2009	-	-	-	-	55	1.06	53	0.21
May 2010	5/05/2010	1/06/2010	-	-	-	-	23	0.97	21	0.62

Table 12 - Estimated major direction [° Azimuth]:
mean direction and standard deviation for the deployments at the Gootebank
(ADP ≅ 1.2m above the bottom, ADVOcean ≅20cm above the bottom)

Tripod deployment			ADP				ADVOcean			
			Major dir.		M2 ellipse		Major dir.		M2 ellipse	
	Start	End	mean	stdv	dir	95% CI	mean	stv	dir	95% CI
Jun. 2009	23/06/2009	13/07/2009	-	-	-	-	35	16.04	38	1.47
Oct. 2009	19/10/2009	9/12/2009	-	-	-	-	42	0.92	41	0.3

Table 13 - Mean and standard deviation of the major and minor amplitude, tidal ellipse eccentricity, inclination and phase angle for the M2, S2 and M4 tidal constituents for the different OD Nature tripod deployment locations

	Tripod Deployment	Major Ampl. (m/s)		Minor Ampl. (m/s)		ECC (Maj./Min.)		Major dir. (°Az)		Phase (°)		Tidal excusion length	
		Mean	Stdv	Mean	Stdv	Mean	Stdv	Mean	Stdv	Mean	Stdv	Major ax.	Minor ax.
M2 (12h 25.24min)	MOW1 ADP	0.52	0.039	0.119	0.018	4.50	0.83	65.7	7.5	27.7	8.4	7.44	1.69
	MOW1 ADV	0.35	0.057	0.071	0.018	5.01	0.89	60.9	7.9	28.1	6.4	4.92	1.01
	Blankenberge ADP	0.50	0.034	0.039	0.005	12.86	1.51	62.0	8.5	27.7	3.4	7.11	0.56
	Blankenberge ADV	0.35	0.043	0.023	0.004	15.40	2.29	59.5	7.7	26.7	2.2	5.00	0.33
	WZbuoy ADP	0.53	0.017	0.136	0.017	3.99	0.64	64.6	13.2	22.5	3.5	7.58	1.94
	WZbuoy ADV	0.38	0.026	0.095	0.013	4.11	0.75	68.3	3.8	20.3	5.5	5.44	1.35
	MOW0 ADP	0.44	0.000	0.174	0.000	2.51	0.00	67.8	0.0	29.3	0.0	6.22	2.48
	Blighbank ADV	0.35	0.027	0.111	0.006	3.12	0.07	34.9	15.9	76.4	1.7	4.96	1.59
	Gootebank ADV	0.26	0.037	0.098	0.013	2.76	0.66	39.8	1.5	58.6	0.0	3.72	1.39
S2 (12 h)	MOW1 ADP	0.15	0.036	0.035	0.010	4.41	0.89	67.1	8.8	80.1	11.0	2.04	0.49
	MOW1 ADV	0.10	0.028	0.022	0.008	4.98	1.36	61.5	8.2	79.6	12.7	1.42	0.31
	Blankenberge ADP	0.14	0.030	0.009	0.007	12.65	2.95	62.3	8.9	79.1	13.5	1.93	0.13
	Blankenberge ADV	0.10	0.018	0.006	0.003	20.58	9.22	60.2	8.4	75.2	13.9	1.32	0.08
	WZbuoy ADP	0.17	0.024	0.044	0.011	4.02	0.56	66.1	12.6	74.7	5.1	2.34	0.62
	WZbuoy ADV	0.12	0.022	0.028	0.009	4.66	1.06	67.3	4.6	75.3	9.0	1.68	0.40
	MOW0 ADP	-	-	-	-	-	-	-	-	-	-	-	-
	Blighbank ADV	0.09	0.007	0.021	0.000	4.28	0.26	38.3	13.6	119.9	10.3	1.21	0.29
	Gootebank ADV	0.07	0.013	0.021	0.002	3.48	0.25	40.7	3.9	96.1	7.1	1.03	0.30
M4 (6h 12.62min)	MOW1 ADP	0.05	0.017	0.005	0.010	43.17	112.55	39.7	22.9	40.8	24.6	0.72	0.07
	MOW1 ADV	0.04	0.014	0.006	0.009	41.66	97.77	36.2	26.3	15.7	27.1	0.62	0.08
	Blankenberge ADP	0.07	0.015	0.007	0.005	38.58	58.86	59.8	7.8	41.9	12.8	0.99	0.10
	Blankenberge ADV	0.04	0.015	0.004	0.003	21.61	19.92	53.4	2.0	41.1	20.7	0.58	0.06
	WZbuoy ADP	0.06	0.012	0.014	0.008	5.44	3.07	26.5	55.4	9.8	93.9	0.83	0.20
	WZbuoy ADV	0.05	0.014	0.009	0.005	11.67	14.34	38.9	59.0	15.5	90.3	0.65	0.12
	MOW0 ADP	0.06	0.000	0.001	0.000	69.13	0.00	56.6	0.0	28.2	0.0	0.77	0.01
	Blighbank ADV	0.05	0.012	0.013	0.007	6.80	5.42	55.6	26.1	53.7	16.4	0.70	0.18
	Gootebank ADV	0.04	0.005	0.011	0.001	3.54	0.65	39.4	7.4	30.3	8.5	0.54	0.16

Appendix C Ensembles of current velocity and SPM concentrations

Blankenberge - Ensembles of ADP velocity

Figure 66 - Mean and standard deviation of the assembled ADP current magnitude (top) and direction (bottom) at ~1.9mab, Blankenberge. Left: neap tides, middle: normal tides, right: spring tides

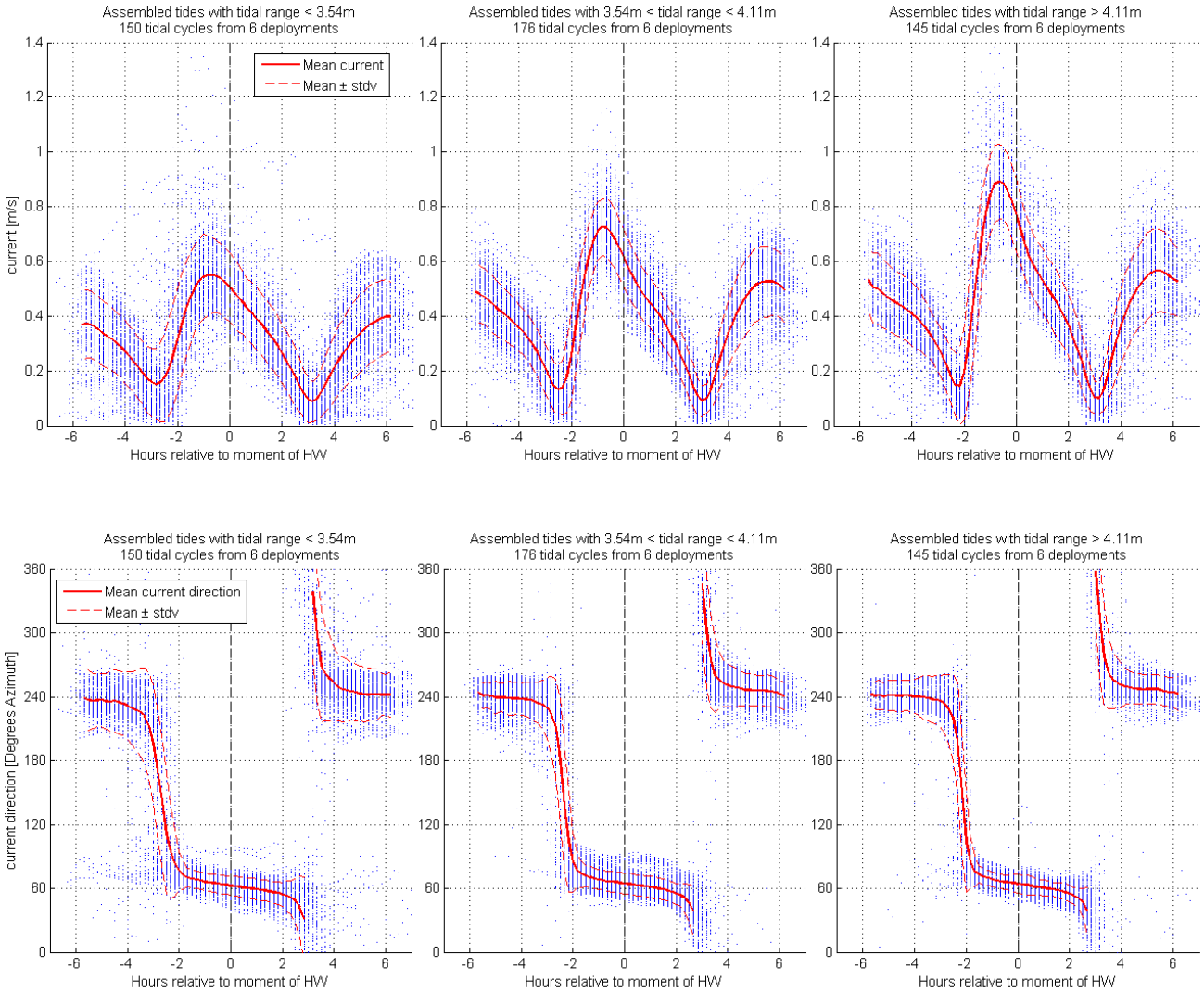

Blankenberge - Ensembles of ADV velocity

Figure 67 - Mean and standard deviation of the assembled ADV current magnitude (top) and direction (bottom) at ~0.2mab, Blankenberge. Left: neap tides, middle: normal tides, right: spring tides

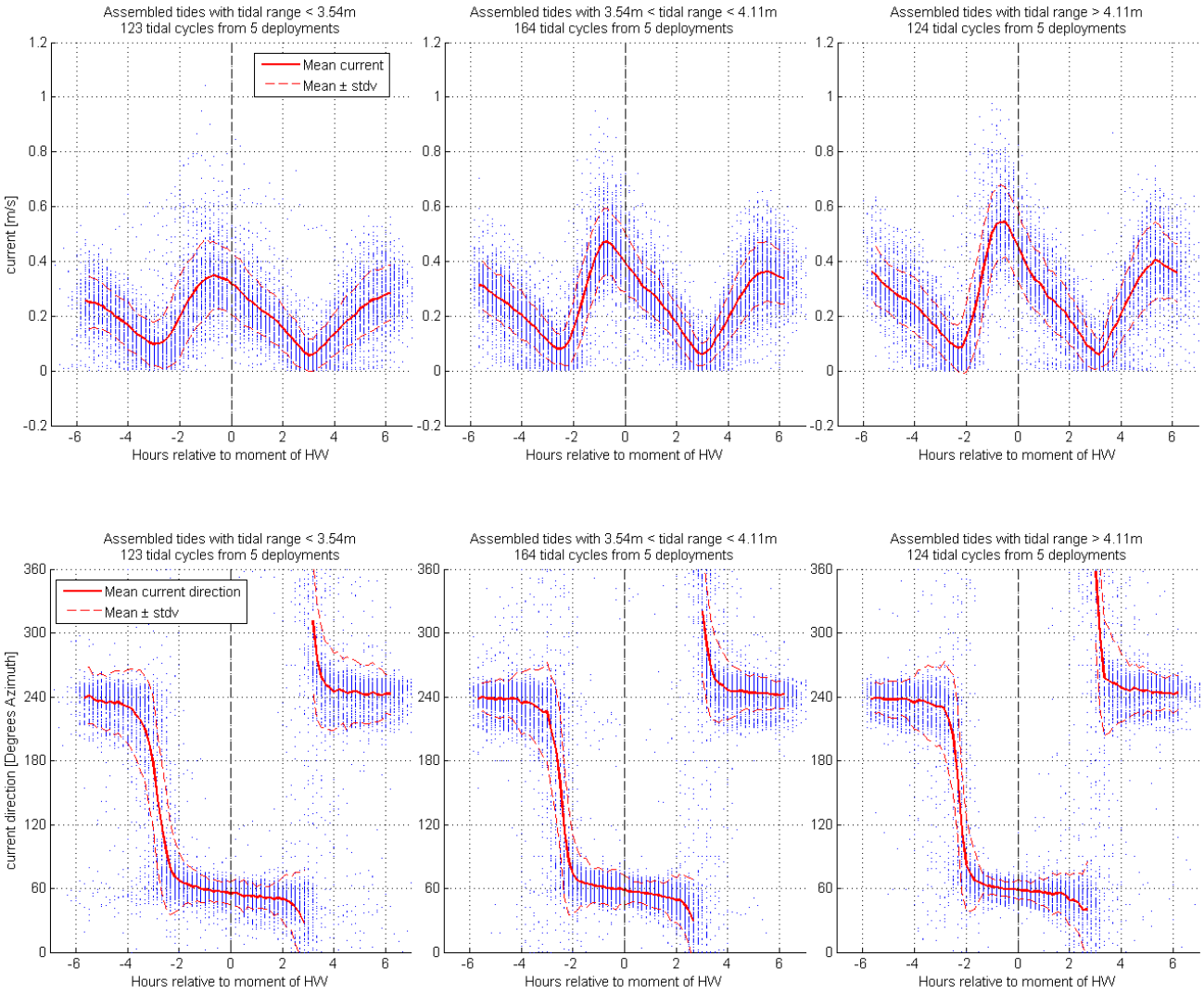

Blankenberge - Ensembles of SPM concentrations

Figure 68 - Median and 10th & 90th percentiles of the assembled SPM ~2.2mab (top), SPM ~0.2mab (middle) and Ro (bottom), Blankenberge. Left: neap tides, middle: normal tides, right: spring tides

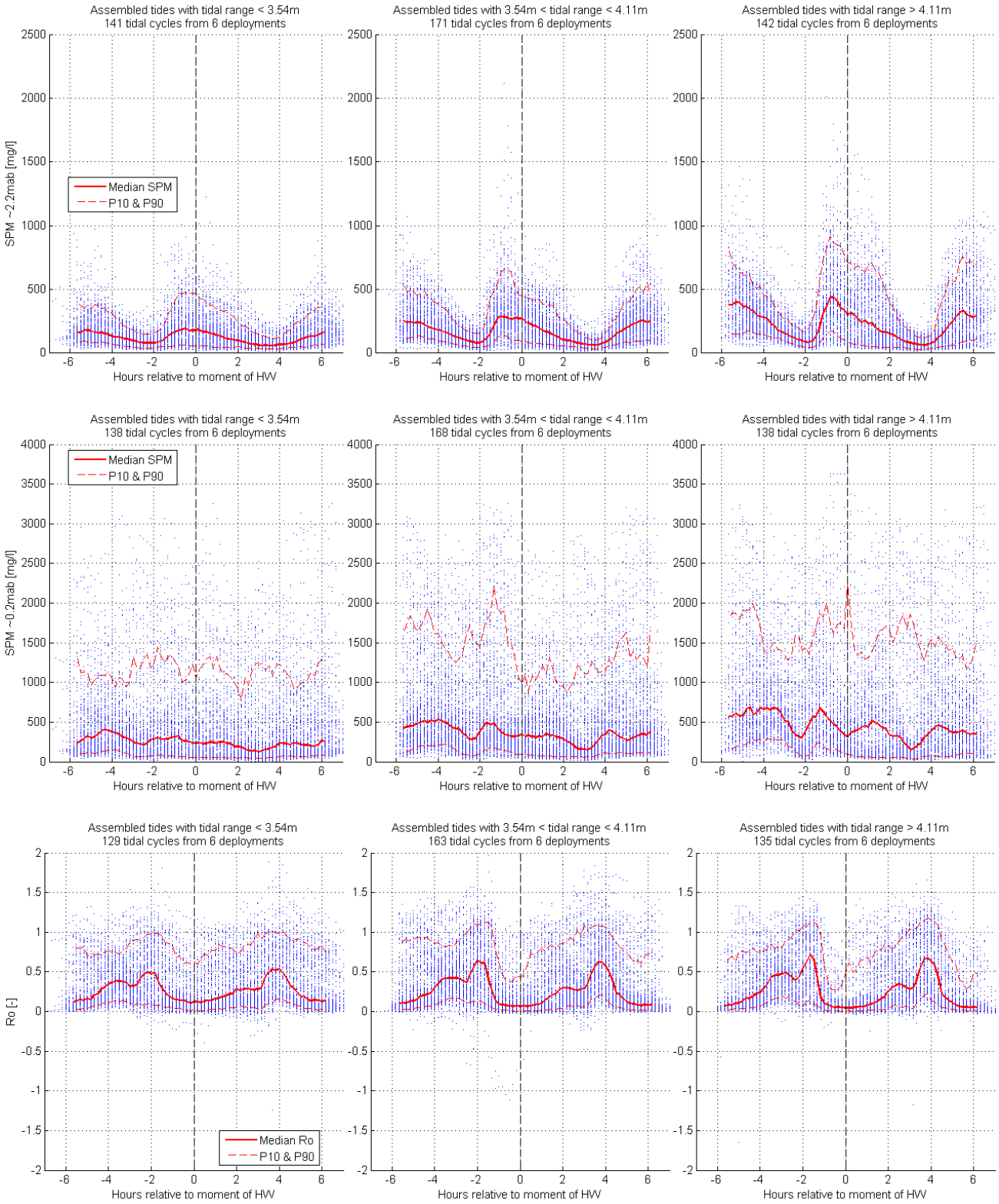

MOW1 - Ensembles of ADP velocity

Figure 69 - Mean and standard deviation of the assembled ADP current magnitude (top) and direction (bottom) at ~1.9mab, MOW1. Left: neap tides, middle: normal tides, right: spring tides

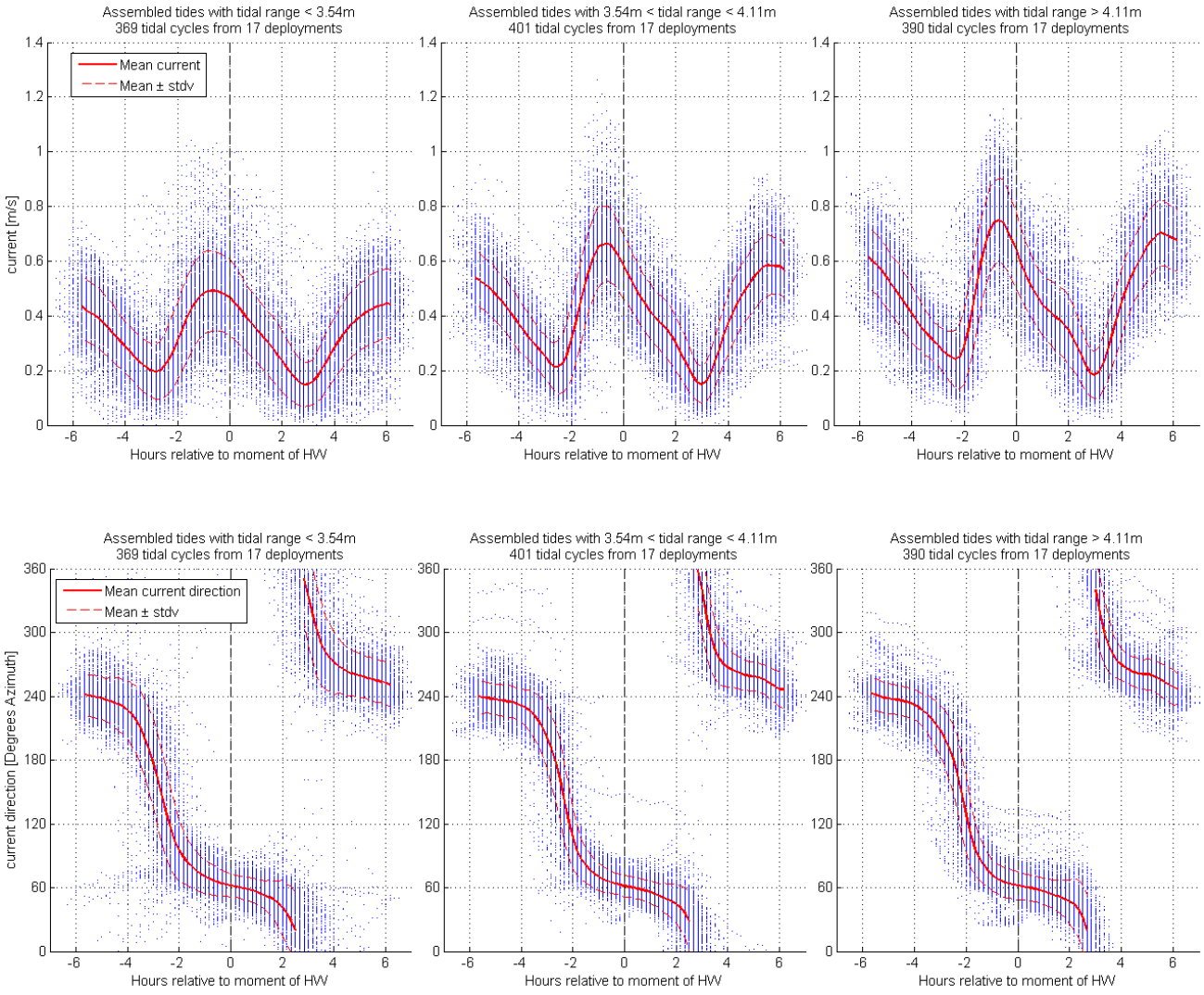

MOW1 - Ensembles of ADV velocity

Figure 70 - Mean and standard deviation of the assembled ADV current magnitude (top) and direction (bottom) at ~0.2mab, MOW1. Left: neap tides, middle: normal tides, right: spring tides

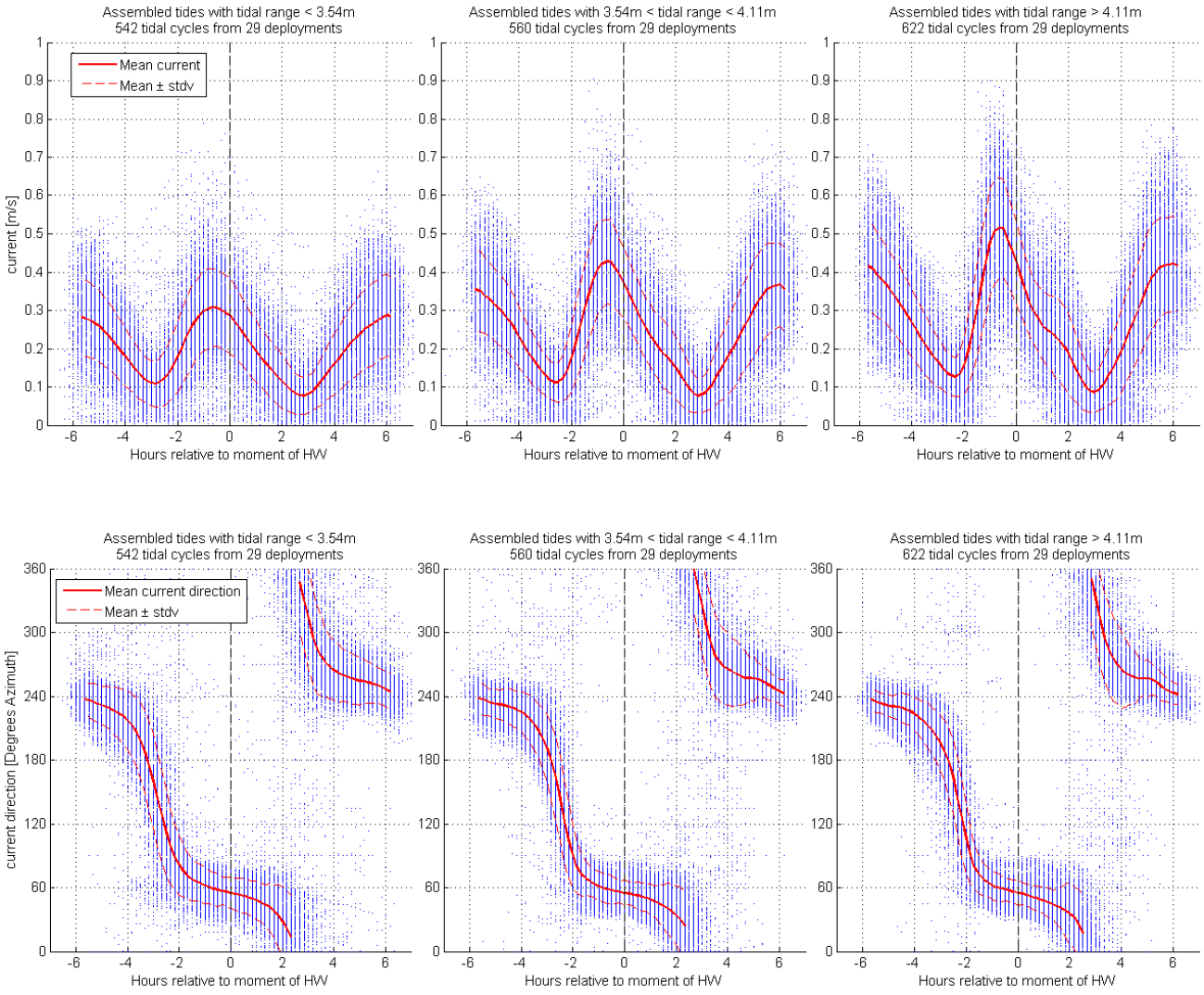

MOW1 - Ensembles of SPM concentrations

Figure 71 - Median and 10th & 90th percentiles of the assembled SPM ~2.3mab (top), SPM ~0.3mab (middle) and Ro (bottom), MOW1. Left: neap tides, middle: normal tides, right: spring tides

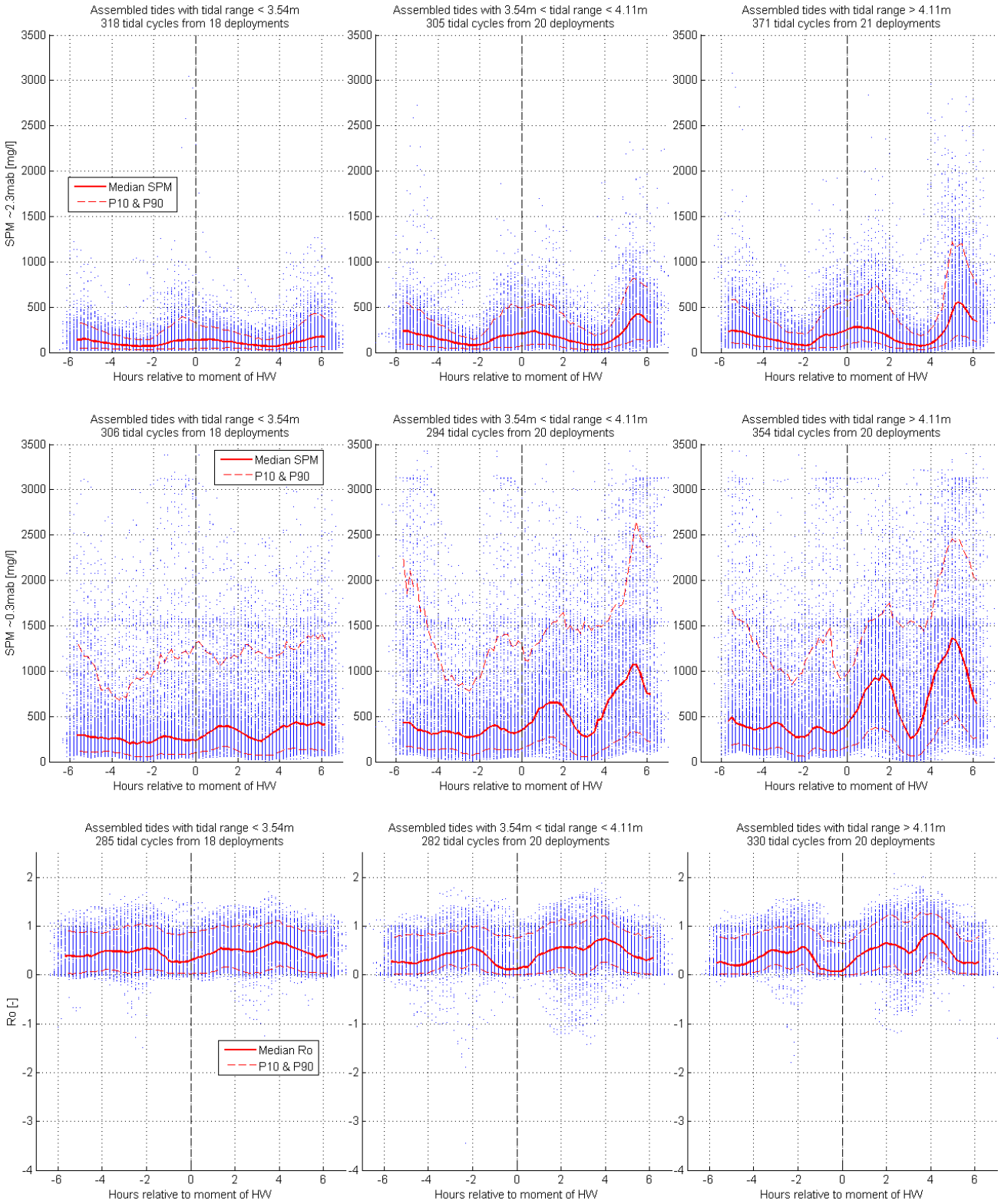

WZbuoy - Ensembles of ADP velocity

Figure 72 - Mean and standard deviation of the assembled ADP current magnitude (top) and direction (bottom) at ~1.9mab, WZbuoy. Left: neap tides, middle: normal tides, right: spring tides

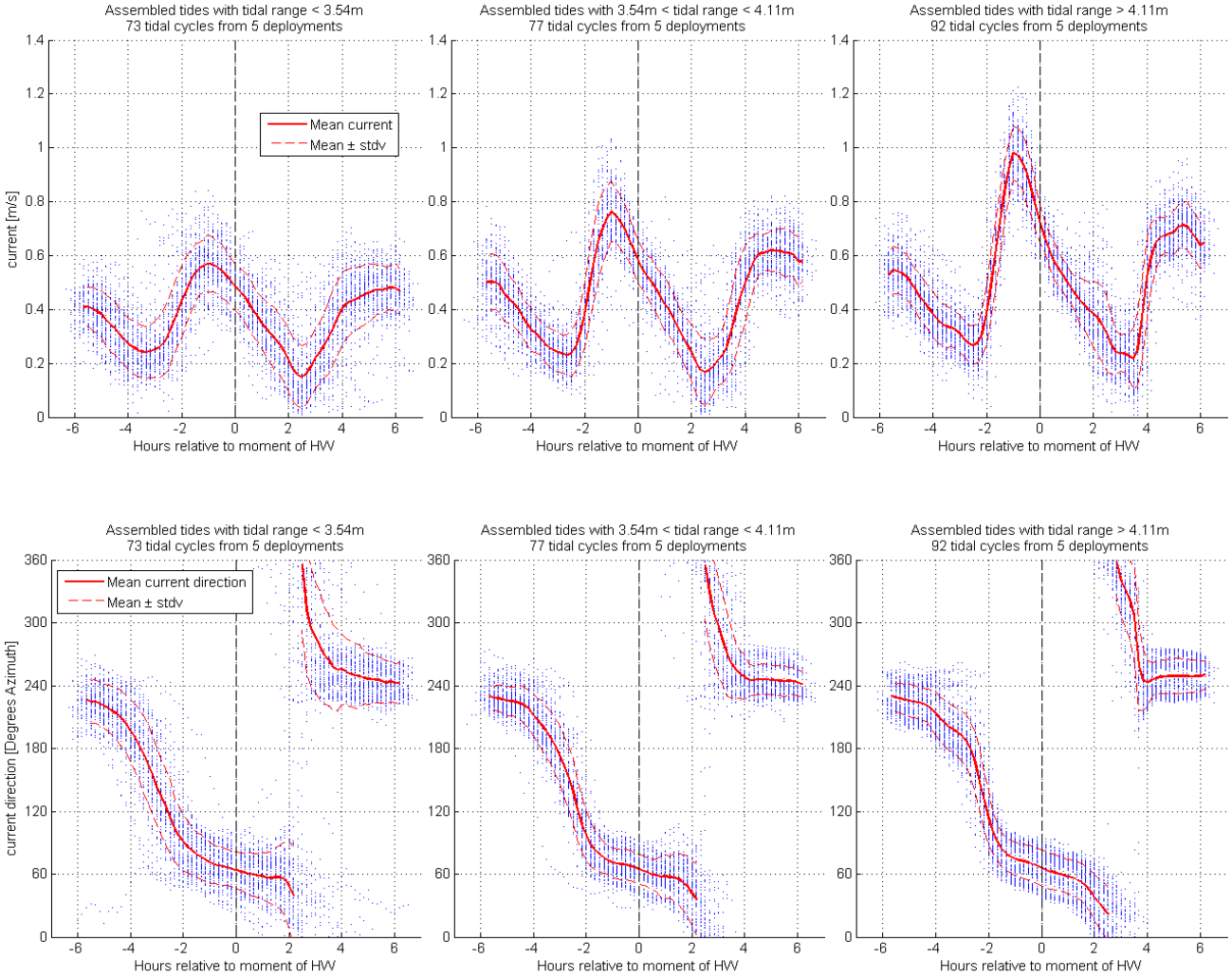

WZbuoy - Ensembles of ADV velocity

Figure 73 - Mean and standard deviation of the assembled ADV current magnitude (top) and direction (bottom) at ~0.2mab, WZbuoy. Left: neap tides, middle: normal tides, right: spring tides

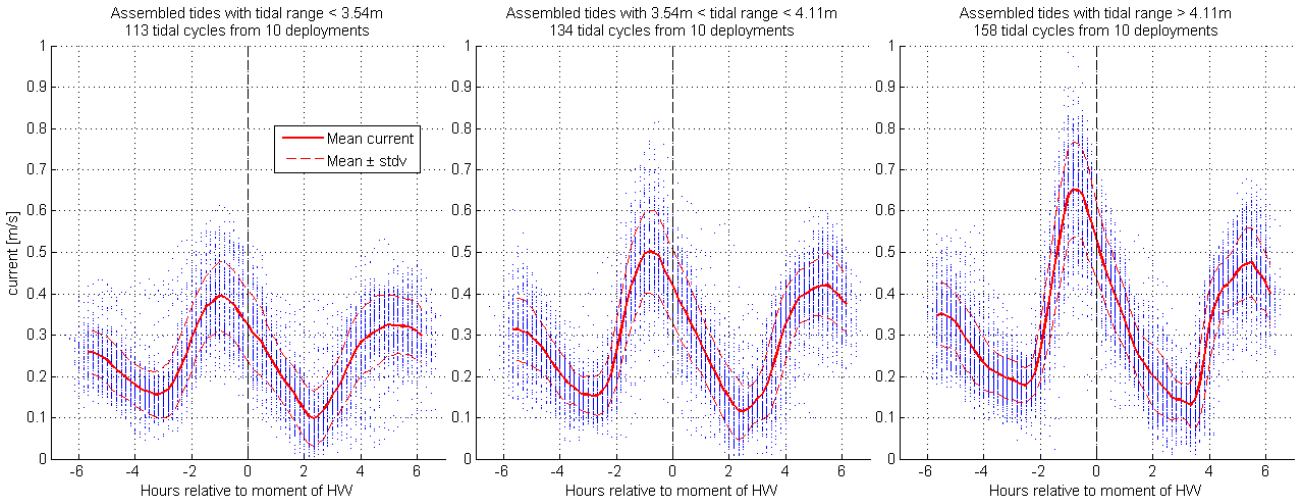

Figure 74 - Mean and standard deviation of the assembled ADV current direction ~0.2mab at WZbuoy. Left: neap tides, middle: normal tides, right: spring tides

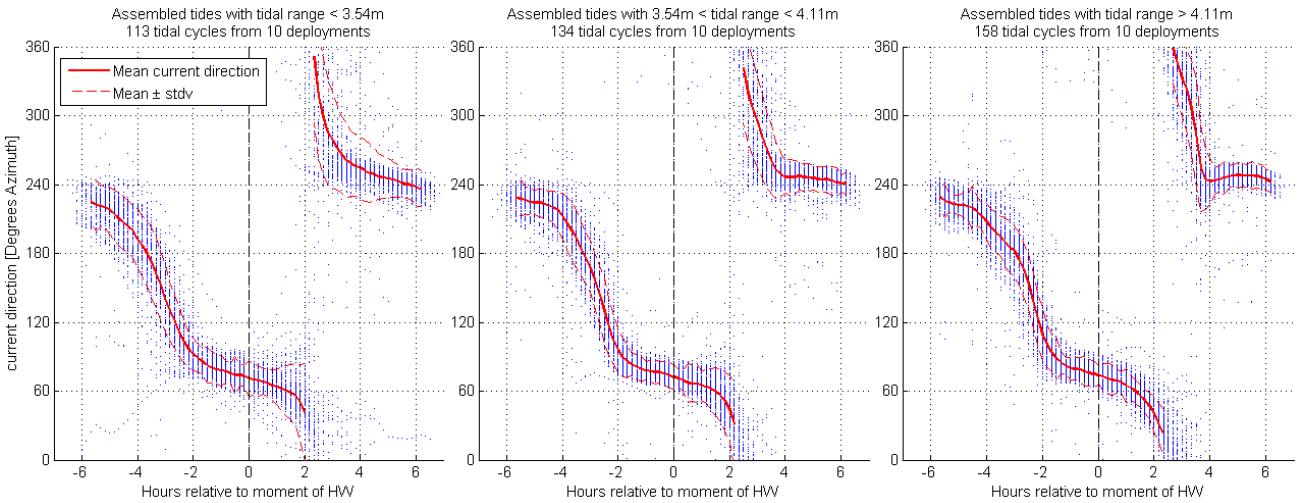

WZbuoy - Ensembles of SPM concentrations

Figure 75 - Median and 10th & 90th percentiles of the assembled SPM ~2.3mab (top), SPM ~0.3mab (middle) and Ro (bottom), WZbuoy. Left: neap tides, middle: normal tides, right: spring tides

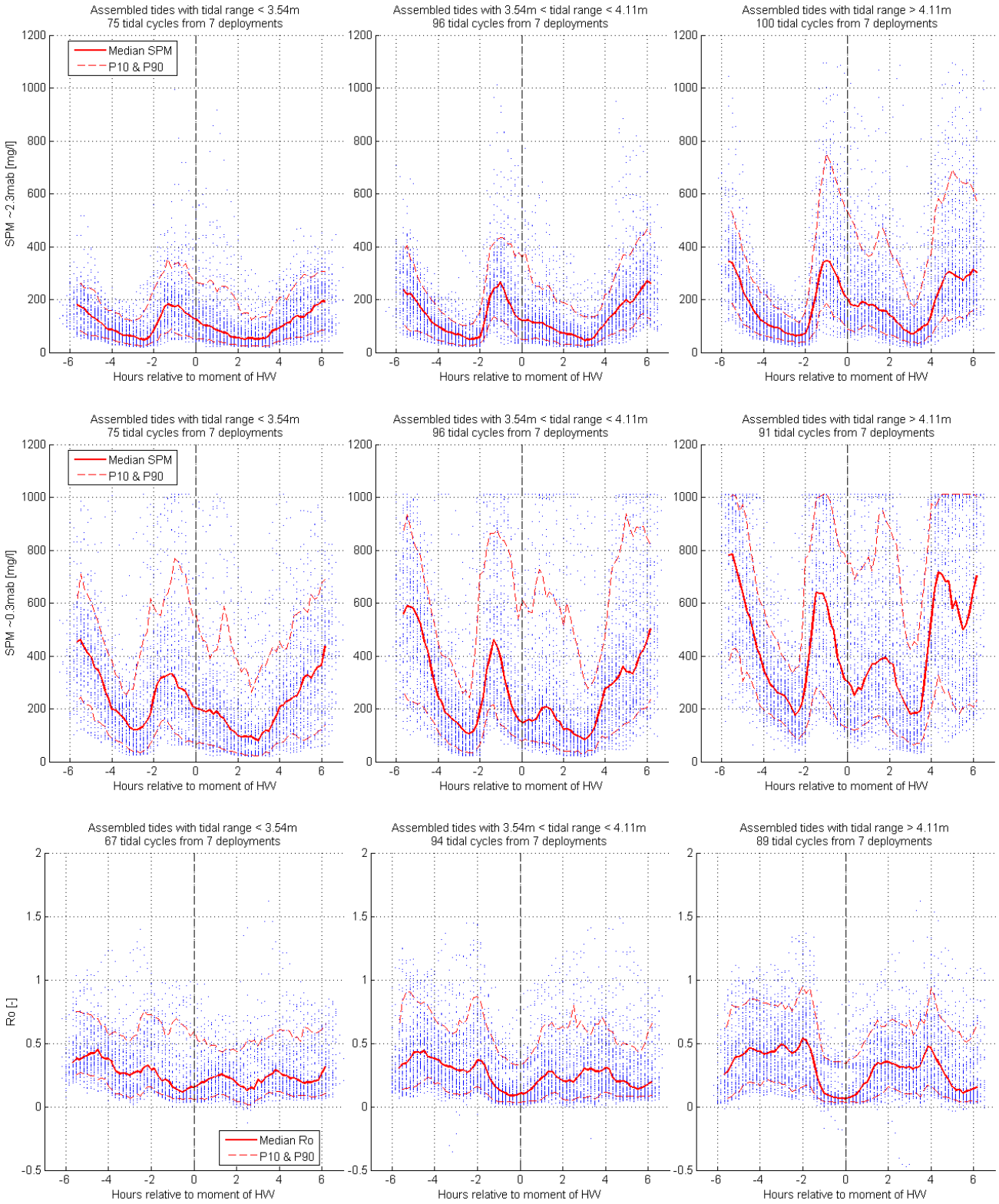

Blighbank - Ensembles of ADV velocity

Figure 76 - Mean and standard deviation of the assembled ADV current magnitude (top) and direction (bottom) at ~0.2mab, Blighbank. Left: neap tides, middle: normal tides, right: spring tides

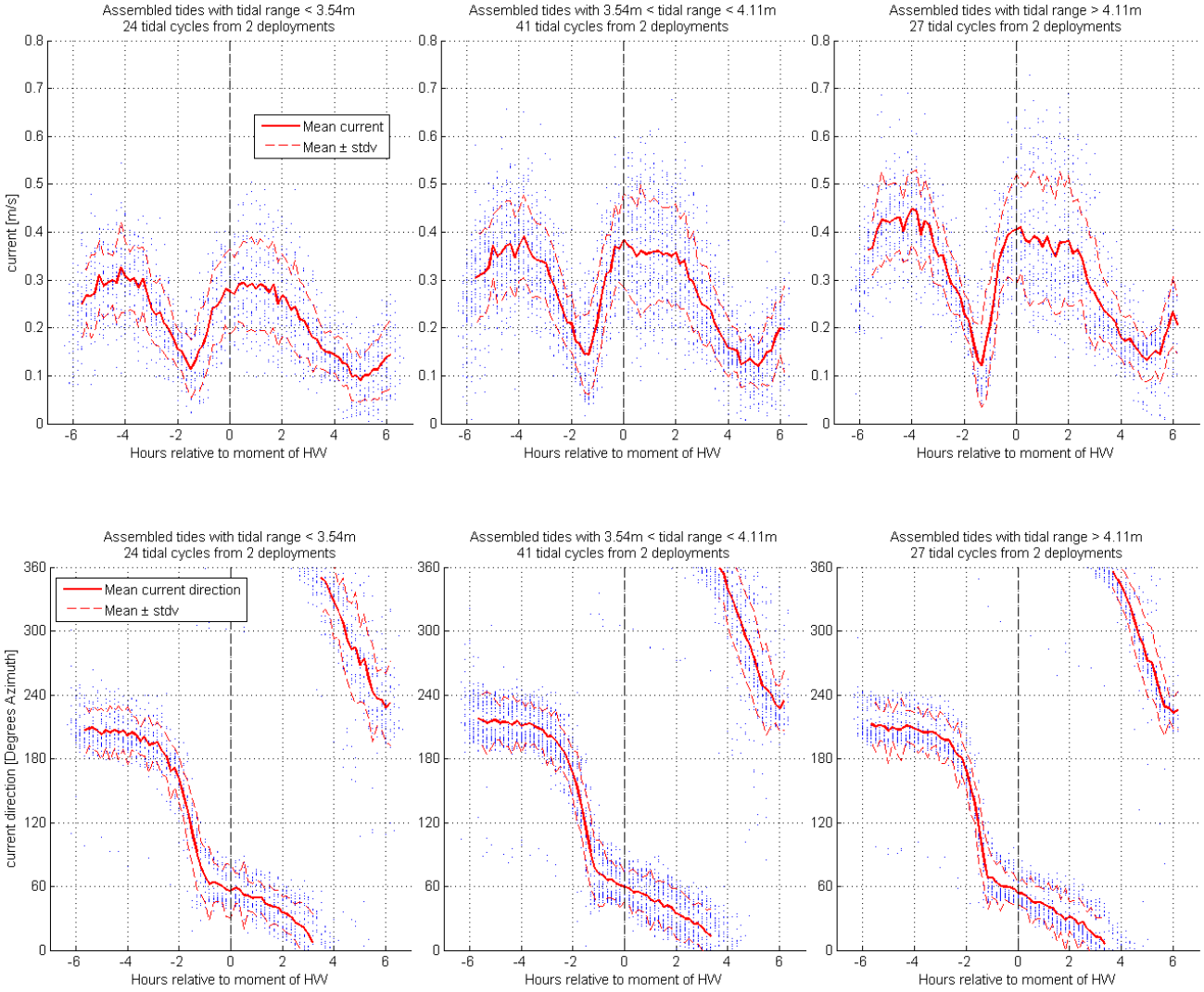

Gootebank - Ensembles of ADV velocity

Figure 77 - Mean and standard deviation of the assembled ADV current magnitude (top) and direction (bottom) at ~0.2mab, Gootebank. Left: neap tides, middle: normal tides, right: spring tides

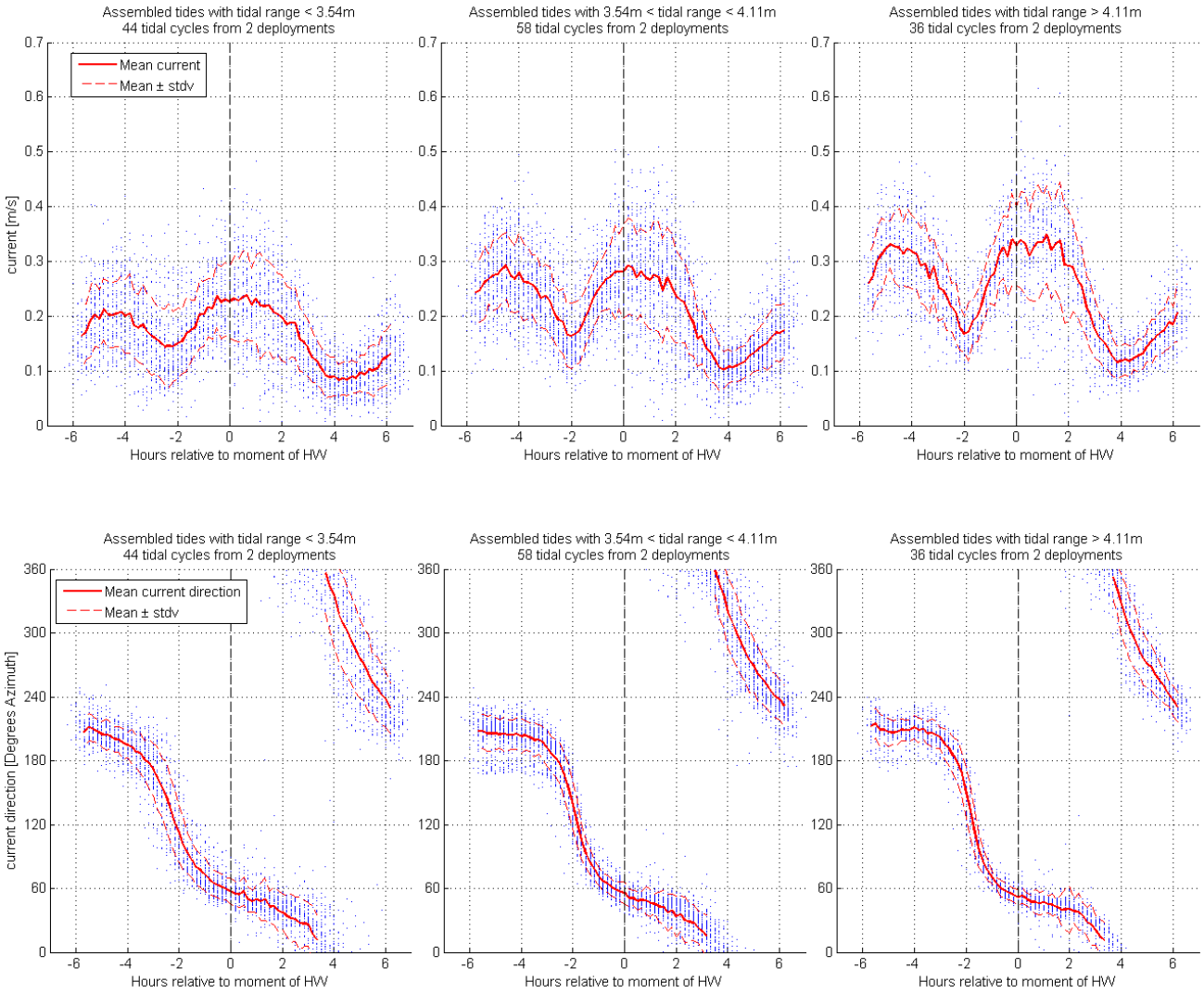

Appendix D SPM concentration probability density

Blankenberge - SPM concentration probability density

Figure 78 - Time dependent probability density of the assembled SPM ~2.3mab (top) and SPM ~0.3mab (bottom), Blankenberge. Left: neap tides, middle: normal tides, right: spring tides

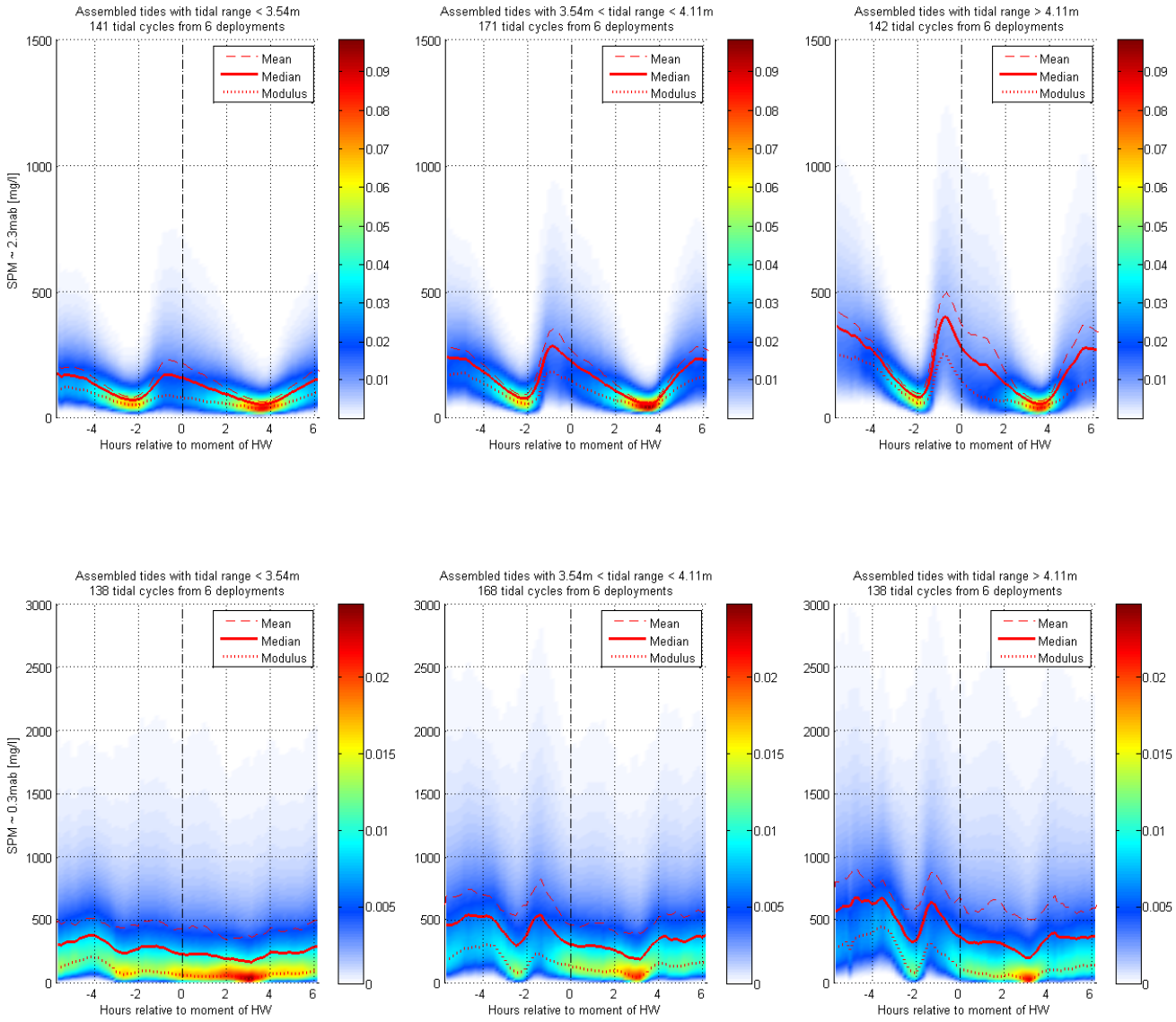

MOW1 - SPM concentration probability density

Figure 79 - Time dependent probability density of the assembled SPM ~2.3mab(top) and SPM ~0.3mab (bottom), MOW1. Left: neap tides, middle: normal tides, right: spring tides

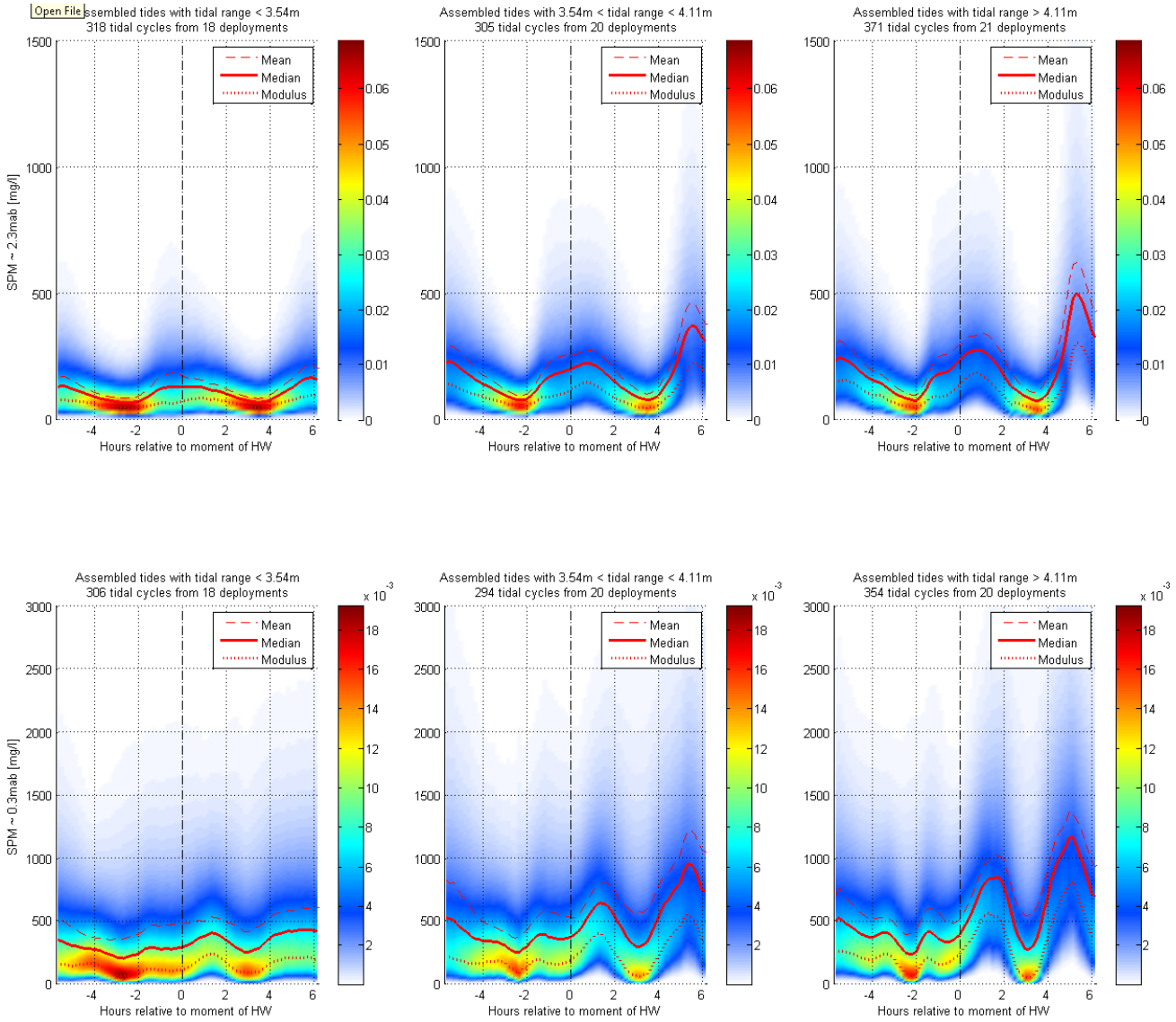

WZbuoy - SPM concentration probability density

Figure 80 - Time dependent probability density of the assembled SPM ~2.3mab (top) and SPM ~0.3mab (bottom), WZbuoy. Left: neap tides, middle: normal tides, right: spring tides

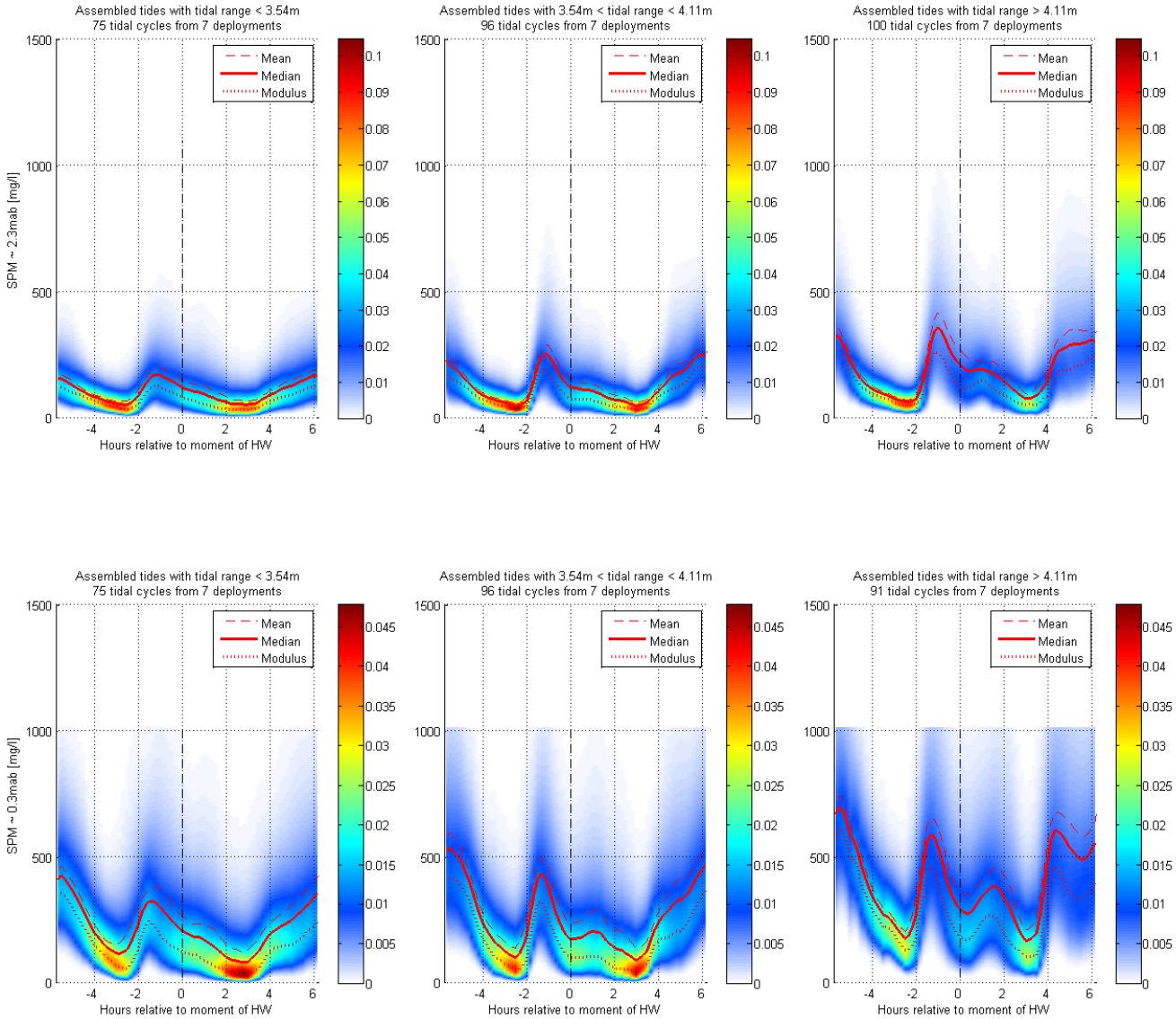

Appendix E Tidal ellipses with colour scale for mean SPM and Rouse number

Blankenberge - Tidal ellipses

Figure 81 - Tidal ellipse with colour scale for mean SPM ~2.3mab, ADP velocity ~1.9mab at Blankenberge.
Left: neap tides, middle: normal tides, right: spring tides

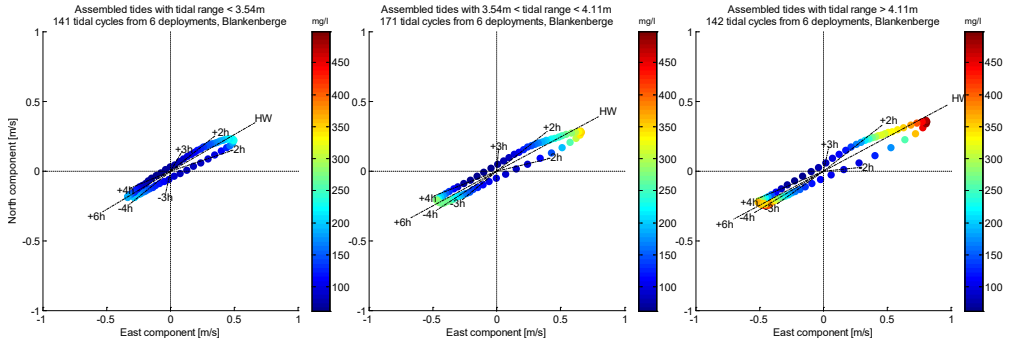

Figure 82 - Tidal ellipse with colour scale for mean SPM ~0.2mab, ADV velocity ~0.2mab, Blankenberge.
Left: neap tides, middle: normal tides, right: spring tides

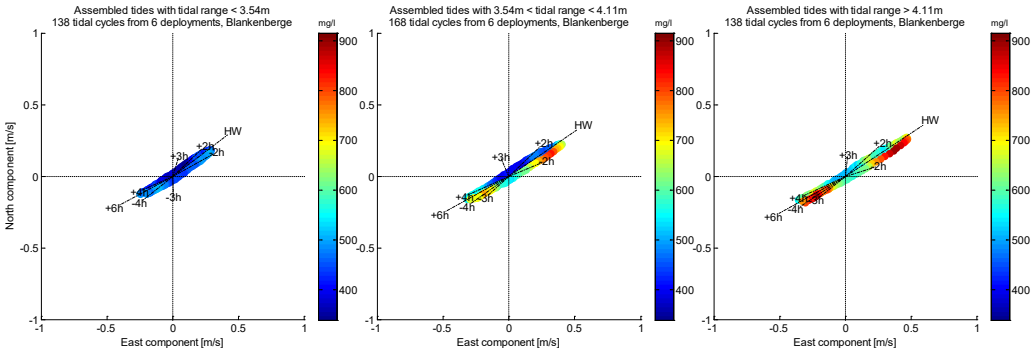

Figure 83 - Tidal ellipse with colour scale for mean Ro, ADP velocity ~1.9mab at Blankenberge.
Left: neap tides, middle: normal tides, right: spring tides

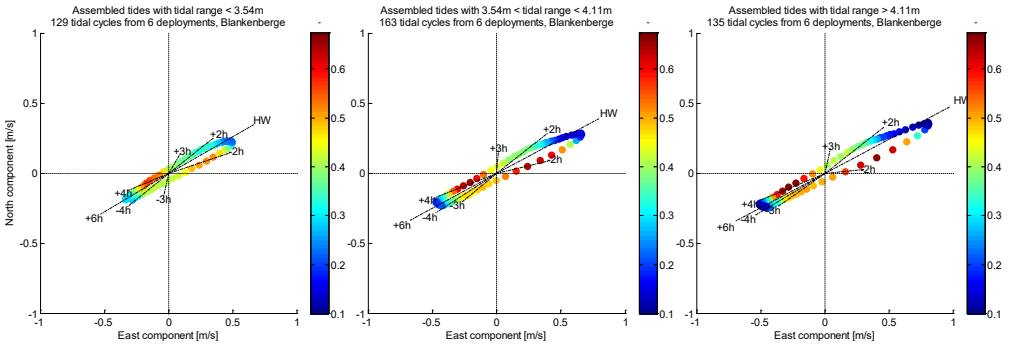

MOW1 - Tidal ellipses

Figure 84 - Tidal ellipse with colour scale for mean SPM ~2.3mab, ADP velocity ~1.9mab at MOW1.
Left: neap tides, middle: normal tides, right: spring tides

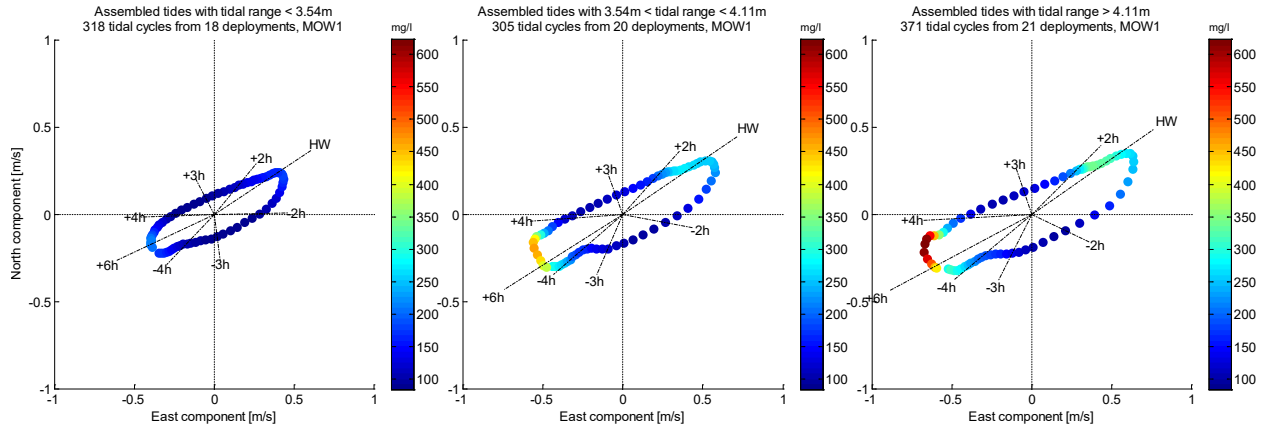

Figure 85 - Tidal ellipse with colour scale for mean SPM ~0.3mab, ADV velocity ~0.2mab at MOW1.
Left: neap tides, middle: normal tides, right: spring tides

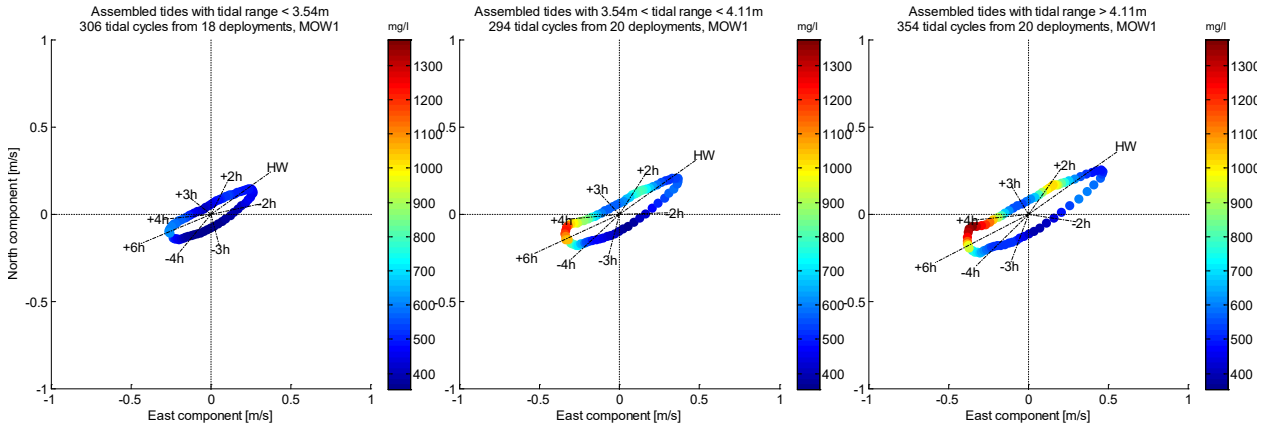

Figure 86 -Tidal ellipse with colour scale for mean Ro, ADP velocity ~1.9mab at MOW1.
Left: neap tides, middle: normal tides, right: spring tides

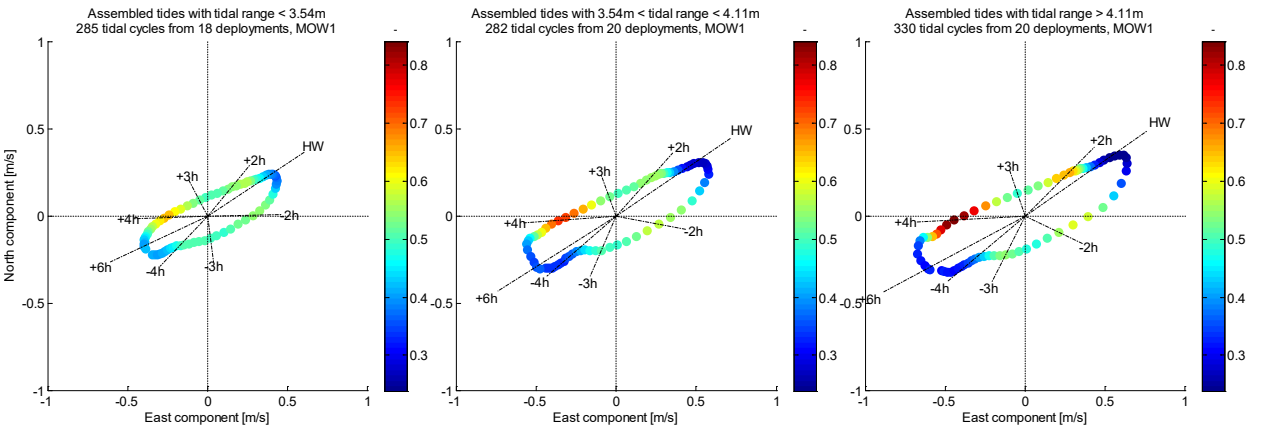

WZbuoy - Tidal ellipses

Figure 87 - Tidal ellipse with colour scale for mean SPM ~2.3mab, ADP velocity ~1.9mab at WZbuoy.
Left: neap tides, middle: normal tides, right: spring tides

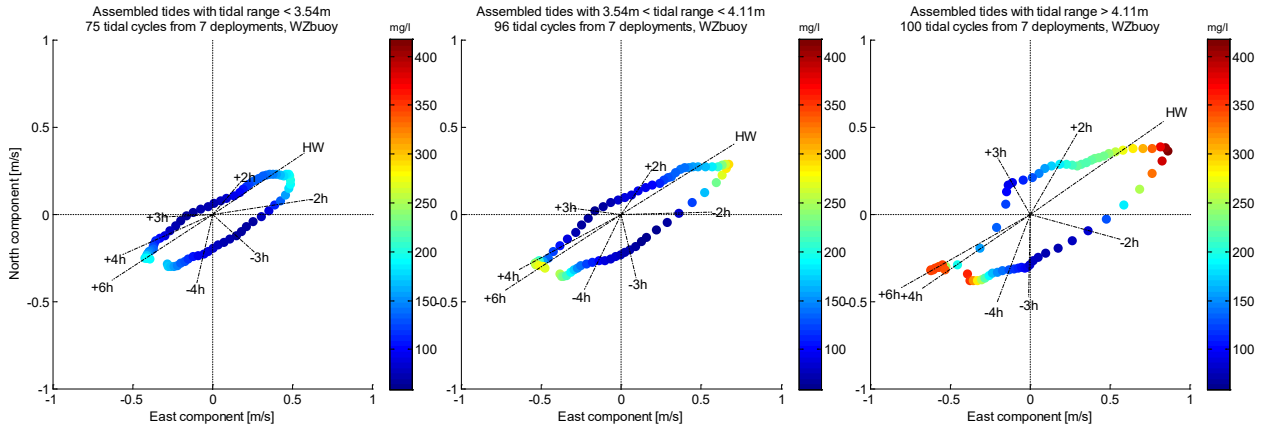

Figure 88 - Tidal ellipse with colour scale for mean SPM ~0.3mab, ADV velocity ~0.2mab at WZbuoy.
Left: neap tides, middle: normal tides, right: spring tides

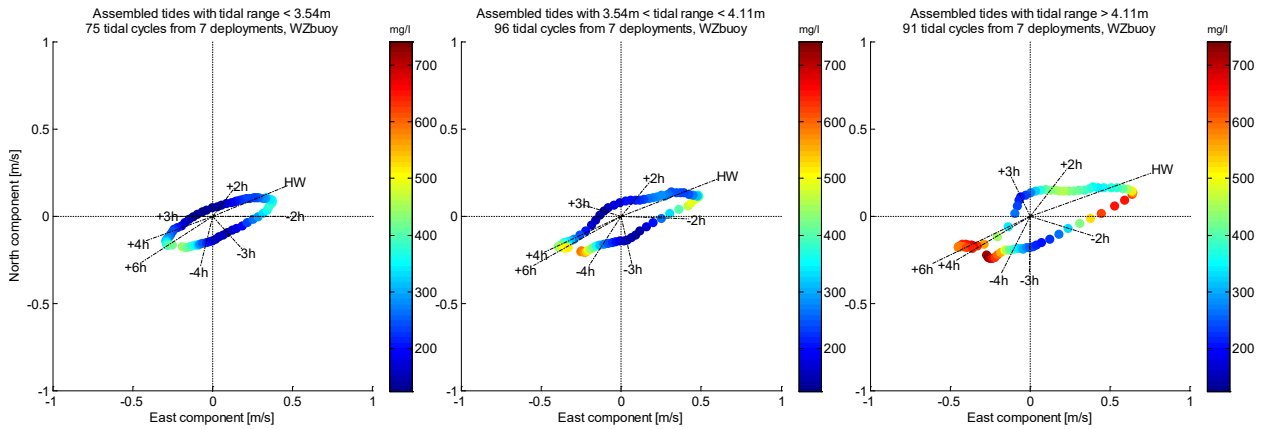

Figure 89 - Tidal ellipse with colour scale for mean Ro, ADP velocity ~1.9mab at WZbuoy.
Left: neap tides, middle: normal tides, right: spring tides

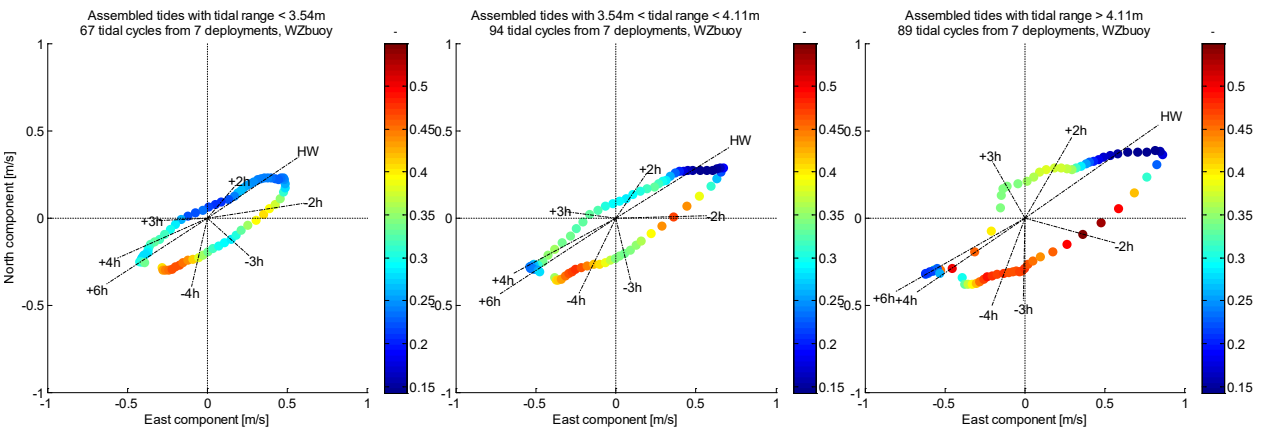

DEPARTMENT **MOBILITY & PUBLIC WORKS**
Flanders hydraulics Research

Berchemlei 115, 2140 Antwerp
T +32 (0)3 224 60 35
F +32 (0)3 224 60 36
waterbouwkundiglabo@vlaanderen.be
www.flandershydraulicsresearch.be